
THE UNIVERSITY
*of* EDINBURGH

# Direct personnel hazard in wave overtopping flows at seadikes

*Claudio Sandoval*


THE UNIVERSITY *of* EDINBURGH

*Master of Philosophy*

THE UNIVERSITY OF EDINBURGH

2015

# Abstract

All the human activities at the coastal line are exposed to the wrath of the ocean, the action of waves being one of the most important. Every year in the UK alone, three or four people die due to wave overtopping flows, often including children among the casualties. Currently the design methods of the coastal defences restrict the wave overtopping discharge to a pre-defined level. The methods to calculate the overtopping discharge are well known and widely validated; on the other hand the definition of that admissible discharge is much less studied. This thesis is focused to explore the relation between wave overtopping flow and admissible levels for people at the crest of seadikes.

The research is divided in two main areas. The first one is related with the human stability and the identification of the overtopping flow's parameters responsible to generate a critical situation. Secondly is the link back between this critical flow parameters and the wave condition which can generate them on a seadike. These two main areas are treated separately, based on an exhaustive literature review for each topic, to then combine their results generating a risk prediction for overtopping flows.

For the first topic few studies were found which have explored the human stability in overtopping flows, being necessary to extend the research to projects related with fluvial floods. In addition, and due to a lack of data from real overtopping flows a thorough analysis of video records of real overtopping accidents is conducted, yielding a new data of the flow condition that a person could be exposed in an actual overtopping flow. With this information two methods to estimate the critical flow condition which can produce instability on a person are improved and validated for nonviolent overtopping flows. More information was found regarding the prediction of the overtopping flow's parameters. These finding are used to develop two methods which allow estimating the velocity and depth of the most hazardous flow for a wave condition and seadike geometry.

With all this information a series of risk matrices and envelopes are derived, with which it is possible to predict if a certain wave condition will generate overtopping

flows capable to unbalance a person at the crest of seadikes. The admissible overtopping for people calculated here are compared with present guidelines and a much more optimistic prediction is found, being the pedestrian prediction generated here more alike to a “trained personal”. Also a significant dependence of the overtopping limits to the seadike geometry is found, aspect which is not considered in the present recommendations. In addition, a great influence of the person characteristics, weight and height, on the tolerable overtoppings is detected.

Due to a wide view of the process is considered in this thesis the area which are needed to explore deeper are detected and further work are proposed.

# Acknowledgements

Firstly, I would like to thank my supervisor, Dr Tom Bruce, who helped me to develop my research, for his continuous support and advice.

To my wife, Camila, who supported me during these two years of studies and in every aspect of my life, thank you for your patient and love.

Also I would like to thank to William Allsop for his wise words and assertive recommendations.

# Declaration

I declare that this thesis was composed by myself, that the work contained herein is my own except where explicitly stated otherwise in the text, and that this work has not been submitted for any other degree or professional qualification except as specified.

Claudio Sandoval

# Contents

# List of Figures

# List of Tables

# Nomenclature

| | | |
|---|---|---|
| $A_n$ | = projected area against the flow | [$m^2$] |
| $B$ | = average body width exposed normal to the flow | [m] |
| $C_d$ | = drag coefficient | [-] |
| $c_d$ | = coefficient for the run-up depth | [-] |
| $c_{dc}$ | = coefficient for the overtopping depth at the seadike crest | [-] |
| $c_u$ | = coefficient for the run-up velocity | [-] |
| $c_{uc}$ | = coefficient for the overtopping velocity at the seadike crest | [-] |
| $d$ | = flow depth | [m] |
| $d_{max}$ | = maximum overtopping flow depth | [m] |
| $d_{cr}$ | = critical flow depth which unbalance a person | [m] |
| $d_c(x_c)$ | = overtopping flow depth on the crest at $x_c$ | [m] |
| $d(z)$ | = run-up flow depth on the seaward slope at z | [m] |
| $d_1$ | = rotational distance from pivot point to the person´s centre of gravity | [m] |
| $f$ | = friction factor (=0.01 for smooth structures) | [-] |
| $F_b$ | = buoyancy force | [N] |
| $F_f$ | = drag force of the flow ($=C_d \cdot \frac{\rho}{2} \cdot u^2 \cdot A$) | [N] |
| $F_r$ | = friction resistance | [N] |
| $g$ | = gravitational acceleration = 9.81 | [$m/s^2$] |
| $h_p$ | = person height | [m] |
| $H_{m0}$ | = significant wave height from spectral analysis ($=4 \cdot \sqrt{m_0}$) | [m] |
| $H_s$ | = significant wave height | [m] |

| | | |
|---|---|---|
| $L_f$ | = width between the feet | [m] |
| $m$ | = subject mass | [kg] |
| $M_f$ | = moment generated by the flow | [N·m] |
| $M_r$ | = restoring moment of the subject | [N·m] |
| $n$ | = seaward slope = $1/\tan\alpha$ | [-] |
| $N_{ow}$ | = number of overtopping waves | [-] |
| $N_w$ | = number of incident waves | [-] |
| $P_{ov}$ | = probability of overtopping per wave = $\frac{N_{ow}}{N_w}$ | [-] |
| $P.N.$ | = product number calculate in Abt *et al.* (1989) | [-] |
| $q$ | = mean overtopping discharge | [$m^3$/s/m] |
| $R_c$ | = crest freeboard of the coastal defence | [m] |
| $R_{u\,2\%}$ | = run-up exceeded by 2% of incident waves | [m] |
| $t$ | = storm duration | [s] |
| $T_m$ | = average wave period | [s] |
| $T_{m-1,0}$ | = average wave period from spectral analysis (= $m_{-1}/m_0$ ) | [s] |
| $u$ | = flow velocity<br>The real interpretation of this parameter is the speed of the flow, but in order to maintain the same notation of the previous studies it will be called velocity. | [m/s] |
| $u_{max}$ | = maximum overtopping flow velocity | [m/s] |
| $u_{cr}$ | = critical flow velocity which unbalance a person | [m/s] |
| $u_c(x_c)$ | = velocity of the overtopping flow on the crest at $x_c$ | [m/s] |
| $u(z)$ | = velocity of the the run-up flow on the seaward slope at $z$ | [m/s] |
| $V_o$ | = total volume of the subject | [m] |
| $V_{\max}$ | = maximum overtopping volume per wave | [$m^3$/m] |

| | | |
|---|---|---|
| $V_d$ | = submerged volume of the body | [$m^3$] |
| $\alpha$ | = seaward angle | [°] |
| $\gamma_\beta$ | = reduction factor due to angled wave attack | [-] |
| $\gamma_f$ | = reduction factor due to roughness of the surface | [-] |
| $\gamma_v$ | = correction factor due to vertical wall on the slope | [-] |
| $\rho$ | = water density | [$kg/m^3$] |
| $\rho_o$ | = density of the human body (=1,062) | [ $kg/m^3$] |
| $\xi_0$ | =breaker parameter based on $s_0$ ($= \tan\alpha / \sqrt{s_0}$) | [-] |
| $\mu$ | = coefficient of friction between shoe sole and ground | [-] |
| $\theta$ | = angle of the person against the current | [°] |

# Chapter 1
# Introduction

## 1.1 Introduction

Very many human activities happen at the coast, from residential, industrial to recreational, and all of them are in proximity to the action of the sea, which has the potential to modify the coast line, damage houses, roads or railways and generate hazardous situation for persons. One of the most common and major risks for people happens when the waves crash against the coastal defences and a flow is generated at the top of the structures, called it wave overtopping, which can have enough energy to knock over and injure a person, or even carry them into the sea. An average of 2-3 people drowns per year in the UK coast due to overtopping. To prevent or reduce these consequences, coastal defences are built, with the most common being seadikes, vertical walls and armoured sloped. At the present, the design of the crest level of these structures is usually carried out by limiting the mean discharge ($q$) that will overtop the defence. The prediction of this discharge has been extensively studied and clear methods to calculate it have been elaborated and validated for a wide range of wave condition and type of defences, especially seadikes which have the more extensive literature available. On the other hand the determination of the admissible discharge has been less studied and the currently tolerable levels are based upon judgment and evidence from a small number of documented studies. In particular, the prediction of hazard levels of overtopping for people is one of the less developed and therefore is full of uncertainties and remains today as a “black box” in the current coastal manuals. This study´s aim is to explore, in terms of detailed physical processes, the relation between wave overtopping flows and hazard for personnel at the crest of a seadike. Only seadikes are considered in the present study due to the availability of literature on overtopping flows, but that this need not restrict later development of methods to apply to other classes of structure

## 1.2 Research objectives

The main purpose of this research is to study hazard for people that an overtopping wave could generate at the crest of a seadike, in order to offer a physically rational basis for discussion of the present design guidelines, and to orient future research. In order to achieve this, the following specific objectives were defined:

- Study the whole wave overtopping process in order to identify the key elements involved;
- identify the critical overtopping parameters which produce the hazard for a person;
- generate the link back from the critical overtopping parameters to the wave conditions and the seawall geometry that could rise to these conditions;
- developed a methodology to predict whether a wave condition could generate hazardous flows for people at a given structure, and;
- analyse the influence of the critical parameters and their associated uncertainties.

## 1.3 Thesis structure

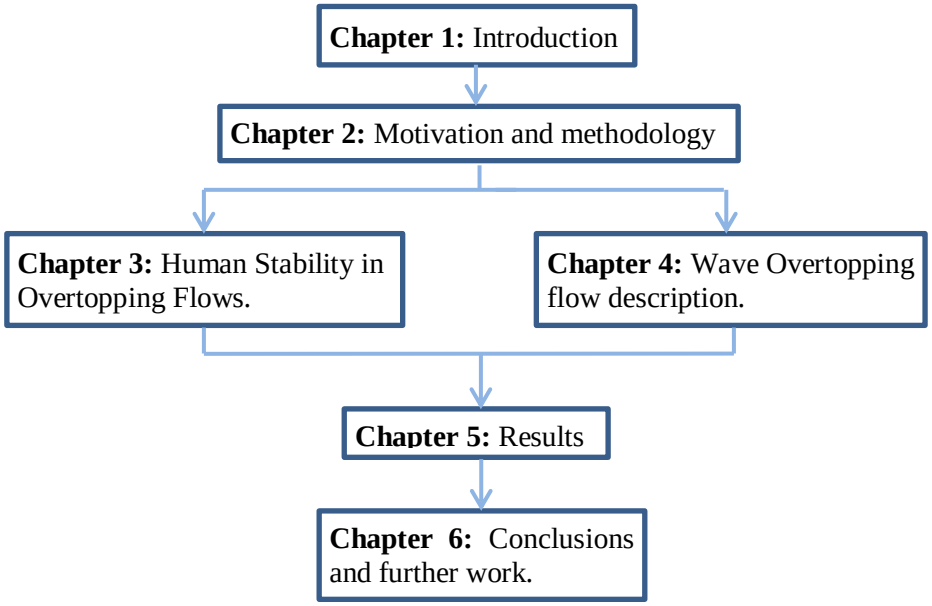


**Figure 1.1:** Thesis structure.

Figure 1.1 shows the structure of the present thesis. This thesis is divided in four main areas. First, in Chapter 2, the current guidelines of admissible discharge for personnel are presented. In Chapter 3, the human stability under overtopping flow is analysed leading to the determination of critical instability curves. In Chapter 4, the link between the overtopping flow characteristics and the wave condition are analysed and two methods to calculate the most dangerous flow at the crest of a seadike are proposed. In the last part of the study—Chapter 5—the work of Chapter 3 and 4 is brought together, and a series of hazard predictions are derived. In addition the sensitivity of the prediction to the main assumptions, parameters, and their associated uncertainties is explored.

**Chapter 2. Motivation and methodology:** Here an analysis of the overtopping process is conducted and the consequences that overtopping flows can generate are analysed.

**Chapter 3. Human stability in overtopping flows:** Four studies related to human stability in running waters are analysed, and the applicability of their results to wave overtopping flows discussed. An exhaustive internet search of video records of real overtopping accidents was conducted, yielding a unique database of estimated velocities and depths of the flows that caused the video subjects to lose balance and fall in to the flow. A satisfactory agreement was found between both data even though it clear that the flows generate during the previous experiment did not recreated all the possible situations that a person could be exposed during an overtopping event. At the end of this chapter, two instability mechanisms are proposed to be used to determinate the critical flow velocity and speed which generated a critical condition for a person.

**Chapter 4. Wave overtopping flow description:** Here a review of the literature related to the prediction of the physical characteristics of an overtopping flow is presented. Few studies were found and these only applicable to seadikes. The velocity ($u$) and depth ($d$) of the overtopping flow have been the parameters most studied. On the other hand there is a paucity of literature on the duration of the

overtopping flow. With the available information, two methods to estimate the main parameters of a overtopping flow were developed which are functions of the wave conditions and seadike geometric characteristics.

**Chapter 5. Risk predictions:** In this chapter, the models proposed in Chapter 3 and 4 are brought together and a methodology to predict whether a certain wave condition will produce hazardous flows for pedestrians on the crest of a seadikes is developed. A series of hazard matrices and hazard envelopes are derived and presented for different seadike slopes and freeboards. In addition, a sensitivity analysis of the results with respect of the main assumptions, and uncertainty is made which suggest the areas where is necessary to focus the future works in order to improve the hazard predictions developed here.

**Chapter 6. Conclusions:** Here a review of the principal findings and the main contributions of this research are presented. Future lines of study to improve this area are suggested.

# Chapter 2

# Motivation and methodology

## 2.1 Wave overtopping process

All coastal defences are designed to resist the forces produces by the ocean waves and to prevent flooding at their back. But, as in all type of structures it is not realistic to build one that will work in all types of conditions. Instead, they are designed for a certain design lifetime and wave return period, which should result in acceptable performance under those extreme conditions. Some damage or flooding can occur, but all the time, the security of the protected area is ensured, and the failure of the defence is prevented.

After a wave hits the sea wall of the coastal defence, two processes occur. The first one is call run-up which consist the water running up on the surface of the seaward face of the coastal defence. When that flow has enough energy to reach the crown of the defence and pass to the protected area, it is called wave overtopping.

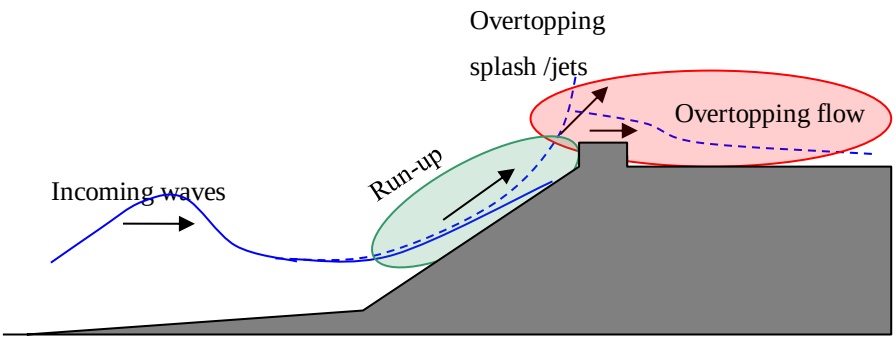


**Figure 2.1:** General representation of wave run-up and wave overtopping.

Wave overtopping events occur when the crest height of the structure it is not enough to prevent the pass of the water over its crown (Figure 2.1). This process can be very

turbulent, violent and irregular and not all waves during a sea condition will overtop the coastal defence.

Wave overtopping can have very different physical forms: a smooth flow "green water" event, a highly turbulent flow "white water", splash or a combination in a single event - see Figure 2.2. The type of the wave overtopping depends upon the wave characteristics, the bathymetry near the defence and more important the type of coastal defence. In general for sloped coastal defences, such as seadikes, more homogeneous overtopping flows are expected than at very steep defences, such as vertical walls. This is because in the latter case, the waves will be stopped abruptly by the defence producing violent and turbulent overtopping flows.

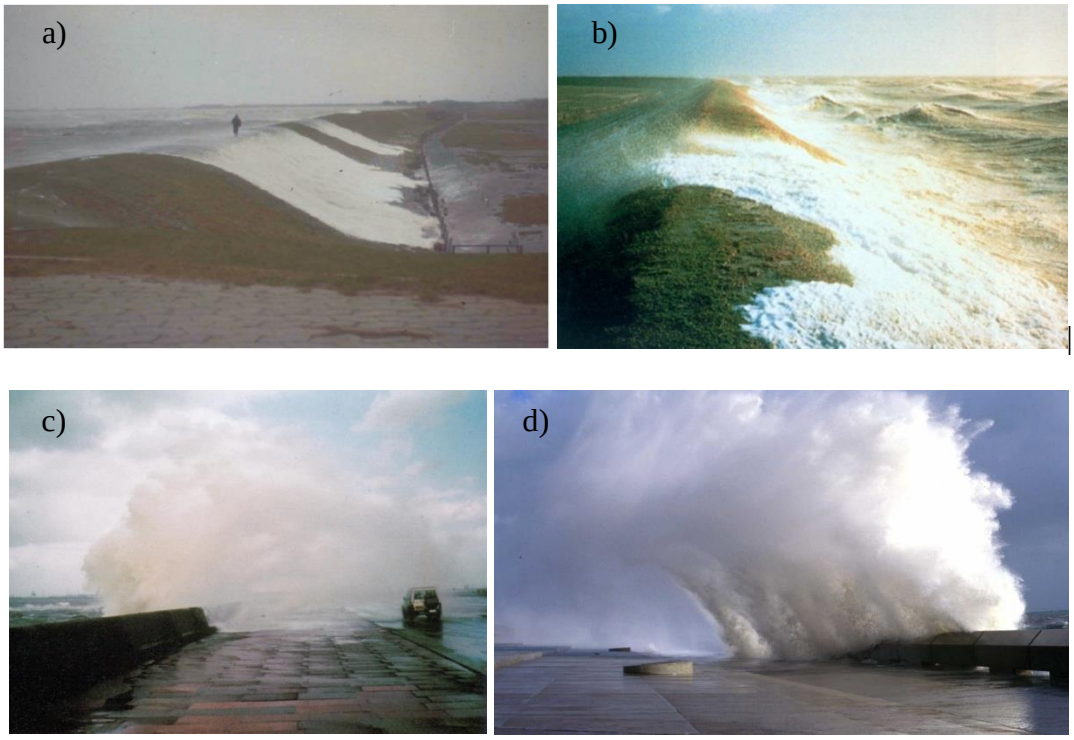


**Figure 2.2:** Wave overtopping examples. a) Green water (photo: EurOtop, 2007) b) White water (photo: http://www.floodsite.net) c) Spray (photo: http://www.kennisbank-waterbouw.nl) d) Splash/jets (photo: EurOtop 2007).

Once the overtopping flow passes the crest of the defence, it will progress across the width of the crest but also may spread out along a length of the crest. This spread of the flow produce a loss of velocity and depth of the flow, helped by the roughness of the surface and in case of permeable ground, infiltration of water into the structure.

The description of this overtopping flow is less studied, existing methodologies to describe it only applicable to seadikes.

## 2.2 Wave overtopping consequences

Wave overtopping flows can be extremely dangerous for people and they can also cause serious damage to the structures exposed to them.

The accidents along the coast related with overtopping flows are not as unusual as public perception of hazard might suggest, and the consequences can be from an unwanted soaking to drowning. In Figure 2.3 it is shows a massive overtopping at the Chinese coast which produced several accident and damage. In average 2-3 people per year die along the UK coast due to wave overtopping (CLASH Work Package 6, 2004). Moreover the UK's Royal National Lifeboat Institution (RNLI) report on the 2014 that 167 deaths occur along the UK's coast during the year 2013, a four year high, with 39 deaths and more than 1,000 rescued in the Scotland's coast with 21% the most common cause of the accident is people falling while are walking or running along the coast (BBC, 24/07/2014), accidents which can be related wave overtopping accidents.

**Figure 2.3:** Screen shots from video of wave overtopping accident China's Hangzhou Bay. (Source: National Geographic, http://www.nationalgeographic.com/)

The coastal construction field is another potential hazardous zone for workers. If the safety measures are not appropriates and the predictions are not accurate workers can be exposed to overtopping flows and be washed into the sea.

Wave overtopping flows also can cause damage to structures protected by the defence such as: buildings, roads and railways, and in the coastal defence itself. The erosion of the crest and the landward slope is one of the most important consequences of overtopping and one of the major concerns in the design of sloped defences. Furthermore wave overtopping flows can produce significant pressures against secondary defences and building walls (Figure 2.4). In CLASH Work Package 6 (2004), Appendix J, a series of tested in real wave overtopping situation were conducted and recorded forces up to 8,800 N wave overtopping flow velocities of 14 m/s, proof of the big damage potential that a wave overtopping can has.

In addition, sea level rise and, perhaps more importantly, apparent increased storminess, been making the wave overtopping event more frequent and bigger, causing more hazardous situations and increasing the damage due to freak waves. For instance the UK´s authorities are already evaluating future actions due to it is estimated that around 7,000 houses will be lost in the next 100 years to rising sea and more frequent and more intense storms (BBC, 29/12/2014),.

Coastal roads and railways can be easily damaged by erosion due to overtopping flows, causing expensive repairs and affecting the connections and the transport of a country. Figure 2.5 shows damage in railway and road at the coast of Dawlish, UK, destroyed by a storm in winter of 2014, its reconstruction had cost of £35m.

Vehicles can also be affected by wave overtopping. They may be severely damaged in accidents on coast roads caused by the flow that managed to pass the coastal defence. Beside the loads of the flow against the cars or trucks the reduction of visibility and wet road (leading to possible “aqua-planing”– total loss of road-to-tyre friction) increase the hazards for drivers at the coast line during storms.

Thus, it is apparent that the risk existing at the coastline, taken together with the pressures for use and development, e.g.: marinas and coastal paths are greater than ever, producing and increasing the potential hazard areas for people and structures. This in turn demands better methodologies to predict the consequences due to wave overtopping loads. This work aims to make a contribution to this.


**Figure 2.4:** Wave overtopping over buildings at the UK´s coast (photo: http://www.bbc.co.uk)

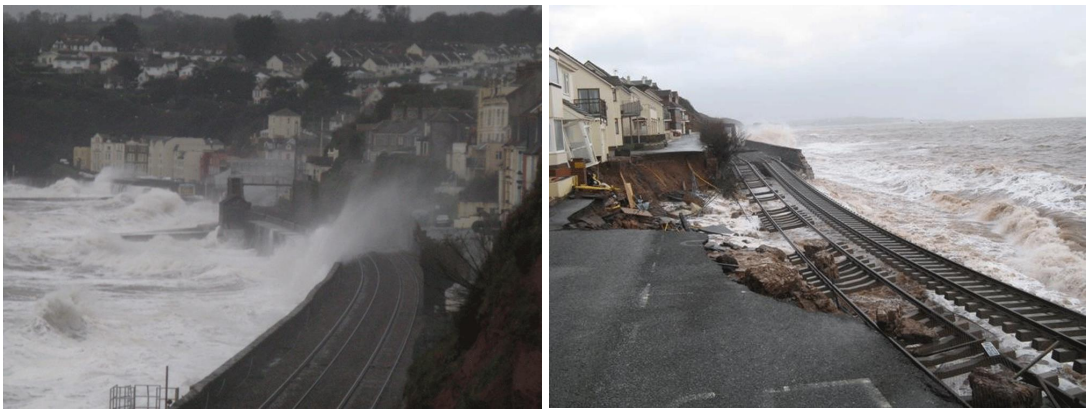

**Figure 2.5:** Wave overtopping damage in railway, road and coastal defence, Dawlish UK (photo: http://www.networkrail.co.uk/).

## 2.3 Overtopping hazard for pedestrians

Due to the diversity of the physical nature of wave overtopping and the resulting flows, it have been very difficult to establish comprehensive guidance to define when a certain wave condition acting on a specific coastal defence may cause hazard for pedestrians behind the coastal defence.

Hazard is defining as any source of potential harm or adverse health effects on someone exposed to it. Every overtopping flow could be considered as a source of hazard because can produce a negative consequence to a person, from just fall due to the flow with no adverse health effect, to be drag by the flow and drowning. The probability that a hazard will affect a person producing a specific consequence is

known as risk. This risk is related to the dimension of the event, a smaller overtopping will have a lower risk than a large overtopping. A larger overtopping event will have more chance to generate negative consequences. The earliest guidelines have used the mean discharge of overtopping to define the risk of it (table 2.3) predicting different consequences depending on the overtopping discharge.

**Table 2.1:** Critical overtopping discharge Franco et al. (1994).

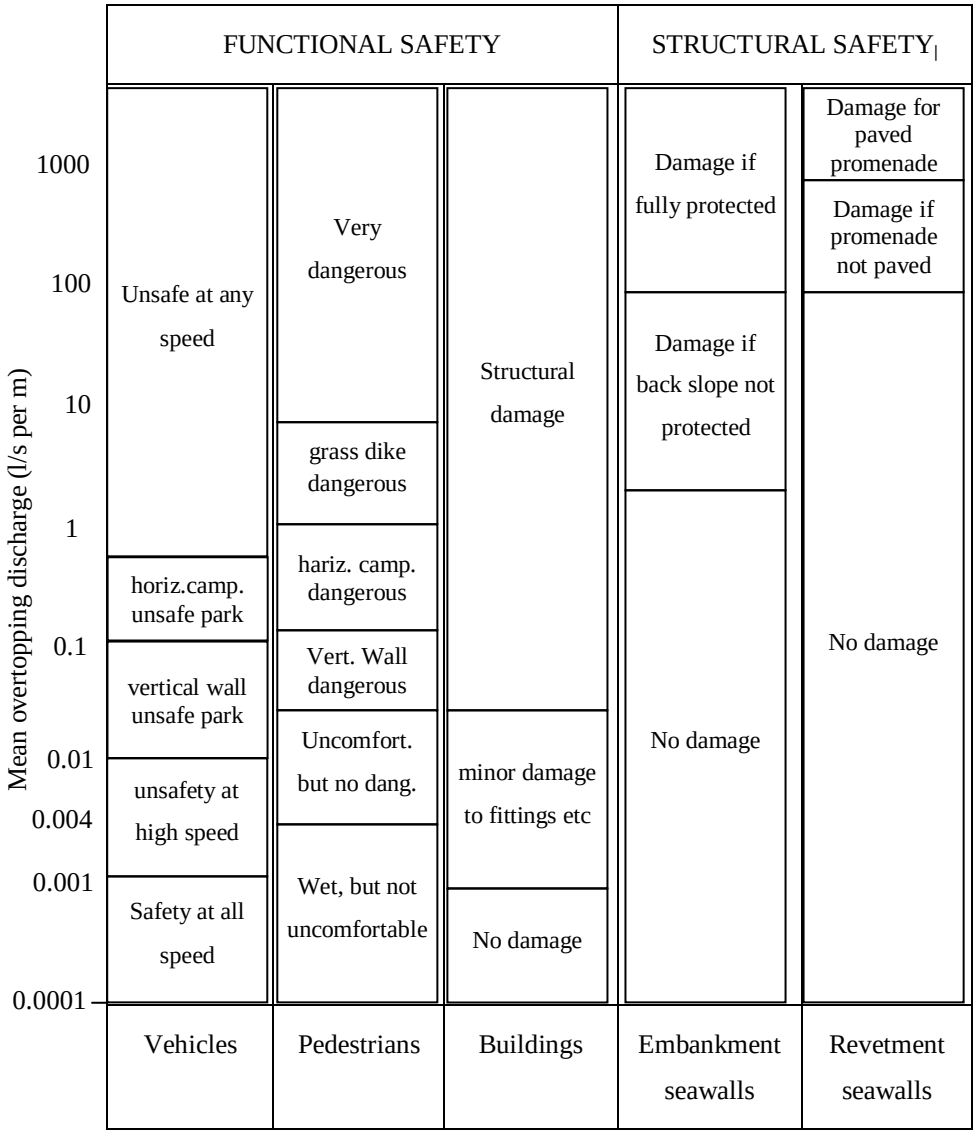


Recent studies have identified that the mean discharge is not the most appropriate parameter to predict risk, and that the maximum individual event volume (Franco *et al.* 1994) is more useful, as wave conditions with the same mean discharge can

deliver very different individual overtopping volumes, depending on the wave conditions and the structure type.

In De Rouck (2009) an extensive review of these previous guidance and others was conducted and considering more recent measurements and observations, an update of the limit overtopping discharges and maximum individual volumes was suggested for pedestrians, table 2.4. These results are the basis for the recommendations of the EurOtop (2007, chapter 3.2).

**Table 2.2**: Risk for pedestrians and its related overtopping discharge.(EurOtop, 2007)

| **Risk type for pedestrian** | $q$ | $V_{max}$ |
|---|---|---|
| Unaware pedestrians, no clear view of the sea, relatively easily upset or frightened, narrow walkway or close proximity to edge. | 0.03 | 2-5 |
| Aware pedestrians, clear view of the sea, not easily upset or frightened, able to tolerate getting wet, wider walkway. | 0.1 | 20-50 |
| Trained staff, well shod and protected, expecting to get wet, overtopping flow at lower levels only, no falling jet, low danger of fall from walkway. | 1-10 | 500 |

It can be seen from table 2.4 that the tolerance to overtopping volumes depends upon several characteristics of the pedestrian who is receiving the flow, such as their attitude and experience, their sightline to the sea and the features of the walkway can influence whether or not a certain event can be dangerous. However, no link to the characteristic of the person, as height and weight are given, and also the first two limits are not related to a consequence either.

Franco (1994) established that the safe limit of overtopping will also vary with the type of the coast defence, this is not mentioned in table 2.4. The same wave conditions could generate different overtopping depending of the coastal defence type, thus the risk will be different.

As previously asserted, the mean discharge $q$ is not a good parameter to predict hazard levels; therefore table 2.4 also gives representative values of $V_{max}$. However, this parameter is still not fully sufficient to predict direct hazard, in view of different combinations of wave conditions and coastal defences can produce different overtopping flows depth and velocity. It is clear, therefore, that it is these actual flow parameters that determine if certain situations can be hazardous for pedestrians or not. No information exists to relate the wave overtopping flow condition with hazard for pedestrian.

## 2.4 Methodology

Two main areas for study have been identified. The first concerns the stability of a person exposed to overtopping flows, *i.e.* "when will a wave overtopping flow generate a hazardous condition for pedestrians?" To answer this it is necessary to identify the mechanisms that can lead to a person losing its stability, and which critical hydraulic parameters of the flow are responsible for this loss of stability. The second area to study is the way to predict these parameters knowing a wave condition and a coastal defence. Being able to define the critical overtopping flows and which wave conditions could generate them it will be possible to develop a overtopping risk prediction for people.

These two areas of study were treated separately due to them have very different physical background and literature. For each topic a complete search of relevant literature was conducted, finding important investigations for both of them. The hazard for person due to overtopping flows is the less studied, being necessary to extend the search to fluvial studies.

The whole process of overtopping and hazard for people involve many things, such as the person´s characteristics, the reaction of the person, clothing, type of structure, and the hydraulics flow parameters. Each one of them has an effect on the consequence of the overtopping, but there is no study which identifies how they influence the level of hazard. One of the objectives of this project is to a have a wide view of the process in order to identify the key elements. In order to explore in

extensive the relation between overtopping flows and their risk for people within the time available for the present study (two years) it is not possible go too deep in each aspect, being necessary to work with data from literature, leaving off the table the developed of CFD and physical models. Having a wider view of the process will generate a good base for future work.

To generate a database of overtopping flows which were able to produce hazardous conditions for people, an analysis of overtopping accident recorded in video was conducted. These videos are an important source of information because they recorded people being catch by real overtopping flows and from them it is possible to estimate the flow characteristics and the consequences in the persons. The velocity and the depth of the flows were estimated. In addition this analysis gives information of the consequences, being able to identify which real wave overtopping flow could unbalance a person. This new data added to the data collected from the literature was used to improve a methodology to calculate the critical flow which could knock over a person.

With all the information gathered a series of risk matrices and envelopes were elaborated. These predictions classified the wave condition as hazardous or not hazardous depending on whether they could generate an overtopping flow with characteristics to unbalance a person

## 2.5 Chapter conclusions

In this chapter, the principal aspects of the wave overtopping process and the consequences that its flow can produce on people, buildings and vehicles have been explored and reviewed.

Several studies have determined that the mean wave overtopping discharge, $q$, is not the most appropriate measure to estimate hazard, pointing to the individual overtopping volume as a better indicator. Even this measure, however, does not give information about the flow that it will be generated behind the defence, which can be very different for the same volume but generated by different wave conditions or acting in different type of coastal defences. Thus, it is asserted that the best way to predict hazard will be via the prediction of the overtopping flow on the crest of the

structure, where the people will interact with it. Sadly this post-overtopping flow is the aspect less studied with only methods applicable to seadikes, but other types of structures are need to be studied in further works.

The study of hazard and risk for people has been conducted mainly from synthesis of a collection of observations in the field, leading to the establishment of a relationship between the mean discharge and the maximum individual event volume and the consequences for people. These estimations were compiled in De Rouck (2009) and a general table with admissible limits of overtopping for given hazard types was developed. These guidelines are very general and they do not specified for the type of person that are valid and the consequences which can be expected are not given. Moreover the limits of $q$ and $V$ are not linked to a type of costal defence.

The methodology was also explained in this Chapter. The research was divided in two areas; first the human stability in overtopping flows, and secondly the prediction of the overtopping flows. For each one an exhaustive literature review was conducted, and a video analyse is conducted in order to generated actual data of overtopping accident, and developed a methodology to defined when a flow could knock over a person.

In the following chapters, the study of these two main areas is presented. An extensive review of previous studies from coastal and fluvial communities is conducted and together with new results a novel approach to defined critical condition for pedestrians is elaborated.

Chapter 3

# Human stability in overtopping flows

## 3.1 Introduction

The literature on the stability of people under the effect of wave overtopping flows is limited to a modest number of studies. More extended is the literature on human stability under flows related with fluvial floods. In this area several studies have tested human subjects in controlled flows which have generated a quantification of the critical flows parameters and mechanisms that can lead to a person lose stability and fall into the flow.

This chapter presents an extended review of studies related with human stability under different types of flows, and a novel analysis of real overtopping accidents. The chapter then proceeds to appraise the applicability of the results found in the fluvial literature to wave overtopping hazard for pedestrians. The principal hydraulic parameters and mechanism of human instability are identified and quantified with this new information.

## 3.2 Previous studies

The earliest study found which looked the critical flow characteristics on human stability was Abt *et al*. (1989), and its aim was to found a general criteria to define a high flood hazard zone for human. At that time, safety agencies used a variety of methods to define hazardous flood for the population, but none of these were based upon fundamental consideration of a human's ability to stay stable under running waters. The parameters studied in this work were the combinations of flow velocity and depth that will lead a person lose its stability. A series of tests were carried out in a recirculating flume of 61 m. long, 2.44 m. width and 1.22 m. depth at the Engineering Research Center of Colorado State University. The flume floor were prepared with different material in order to study a range of bed

conditions/roughnesses: turf, smooth concrete, steel, and chip were all tested. Moreover the ability to change the slope of the flume gave the option to study the effects of inclined floor, with slopes of 0.5% and 1.5% used.

The first phase of the Abt *et al.* (1989) were carried out using a rigid body monolith, Figure 3.1. Results were then used to verify the theoretical envelope for the rotational instability as follows: The rotational instability results from the balance of moment around the point A in figure 3.1, being the main force acting over the body are: the monolith weight (W), the buoyancy (B), and the hydrodynamic force (P).

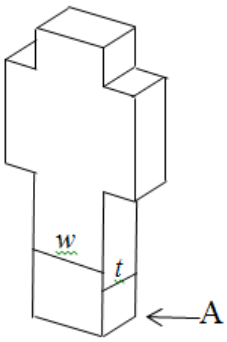


**Figure 3.1:** Rigid monolith used in Abt *et al*. 1989 research no information of *w* and *t* is given.

$$\sum M_A = [(W - B)\cdot(0.5\cdot t)] - [P\cdot(0.5\cdot d)] = 0 \qquad (3.1)$$

with: $B = t \cdot w \cdot d \cdot \gamma_w$

$\gamma_w$ =unit weight of water

$P = C_d\, \rho \frac{u^2}{2} A_n$

$C_d$ = coefficient of drag

$\rho$ = water density [kg/m$^3$]

$u$ = flow speed [m/s]

$A_n$ = projected area against the flow [m$^2$]

Assuming a uniform velocity in the cross section of the flow, equation (3.1) was solved by the author to give a toppling envelope for the rigid monolith (figure 3.2). This curve delineates the conditions where the body will stay stable (under the curve), and the conditions where the monolith will be knocked over by the flow (over the curve). The experimental results for critical flow depths and velocities at the point of toppling were in good agreement with the predicted envelope.

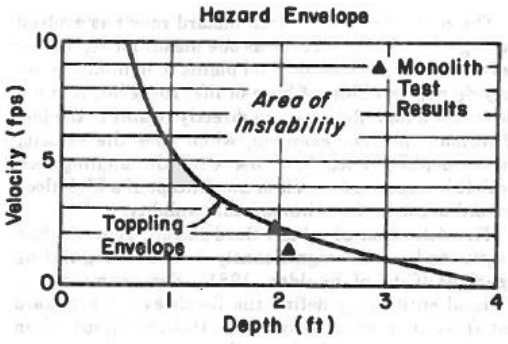


**Figure 3.2:** Toppling envelope for rigid body monolith Abt *et al*. 1989. Source: Human Stability in a High Flood Hazard Zone, Abt *et al*. 1989.

As part of Abt *et al.* (1989) study twenty human subjects were tested under a controlled flow: two females and 18 males; weight between 40.9 kg., and 91.4 kg.; height from 1.52m. to 1.90m. For a fuller description, see table B.1 Appendix B. All subjects wore similar clothing, jeans or slacks; pull over shirts and tennis shoes, sandals or light boots. In addition for safety reasons all subjects wore a helmet and a harness, connected to a beam over the flume. Figure 3.3 shows the general set up of the test and the instant when one subject is unbalance by the flow.

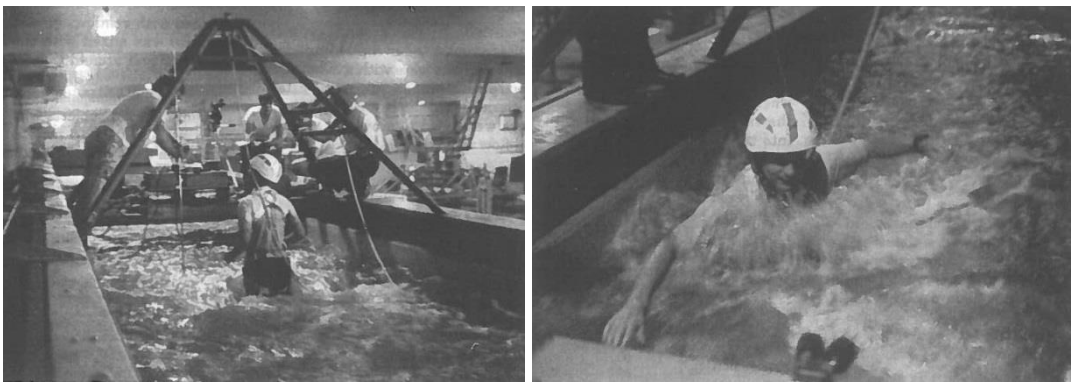

**Figure 3.3:** Experimental setup carried out by Abt *et al.* 1989. Source: Human Stability in a High Flood Hazard Zone, Abt *et al*. 1989.

At the beginning of each test, the subject took position in the test section of the flume and was exposed to a pre-test, gentle flow condition. All the subjects were allowed to accustom to the situation, giving her/him the chance to feel safe in the flow. Then the flow was slowly increased in order to avoid the generation of waves. During the test, the subject was asked to move in three directions: against the flow; with the flow, and across the flow. The test continued until it was impossible for the subject remain stable standing or walking, at which point the critical average velocity ($u_{cr}$) and the critical depth of the flow ($d_{cr}$) was recorded. Moreover it was calculated a product number ("P.N.") $u_{cr}$ x $d_{cr}$ as an indicator of resistance for each test.

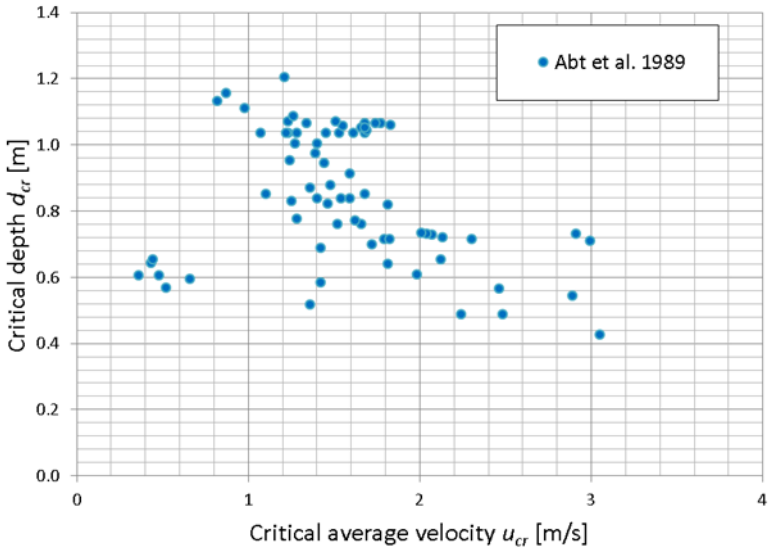


**Figure 3.4:** Critical speed and depth from Abt *et al.* 1989 experiment.

71 tests were conducted, the results of which are shown in Figure 3.4. It was concluded by the authors that the monolith results are very conservative *(i.e.* safe), as its PN was significantly smaller than the found for the human subjects, but they represented a useful starting point for further work. A wide range of results for the human subjects were found, explained due to each person having to inform the team when they could no longer stay stable. In the absence of an actual fall, this is a subjective evaluation likely to be influenced by each person's characteristics: their height and weight, and also their particular skills, confidence and perception of risk.

The ability of each person to react and adapt to the flow, through *e.g.* changing the position of the feet; leaning into the flow, or using arms for balance, was a very important factor in determining each subject's ability to withstand the flow for longer. For the conditions tested, it was found that stability was not affected by the type of surface used, and no clear effect of the floor's slope was found. With the results, a methodology to predict the P.N. which could cause instability of a person was proposed based upon a semi-logarithmic curve, and as a function of the person's weight and height. A more extensive analysis of this methodology is presented in section 3.4.

$$P.N. = \exp\left(m \cdot h_p \, {}^{0.222}\!/_{1000} + 1.088\right) \tag{3.2}$$

with: $P.N.$ = Product number [$fp^2/s$]
$m$ = person's mass [pounds]
$h_p$ = person's height [inches]

Abt *et al.* (1989) identified the following bias:

- the use of safety equipment could made the subject accept more risk than in a real situation,
- the subjects learned how to resist the flow,
- the subjects were tested more than once and the latest results may reflect fatigue,
- the tests did not model other, perhaps critical factors such as bad visibility, debris flows, and water with low temperature
- the subjects did not carry additional loads, and
- all subjects were in good health.

Under the European Commission project "Development of Rescue Action Based on Dam-Break Flood Analysis (RESCDAM) 2001", co-ordinated by the Finnish Environment Institute, more tests of human stability under controlled flow were

conducted. The experiments were carried out in a model basin 130 m. long, 11 m. wide and 5.5 m. deep, at the Helsinki University of Technology's Ship Laboratory. Different flow conditions were recreated by using a mobile platform installed on a towing carriage, which could move along the basin with a velocity up to 8 m/s. Additionally, the platform's height could be adjusted, so different flow depths were reproduced. The subjects stood on the steel grating of the platform.

Seven human subjects were tested: 5 males and 2 females; weights between 48-100 kg; heights 1.6-1.95, and ages 17-60 years, see table B.1 Appendix B. Two of the male subjects were in fact professional rescuers In terms of clothing, all subjects wore Gore-Tex survival suits and in addition, three were tested wearing waders. As in Abt *et al.*'s (1989) study, the subjects were equipped with safety helmet and a safety rope.

Each subject was tested individually and allows to familiarize with the equipment before run the test. At first it was generated a flow were the subjects could stand without problems for an initial depth. It was asked to the subjects to walk across the flow and downstream, if the subjects were able to remain stable the velocity was gradually increased until the stability was lost and the critical velocity ($u_{cr}$) for that specifically depth ($d_{cr}$) was recorder. The same methodology was used for at least different depths per person. Figure 3.5 it can be seen the general set-up a critical moment.

As in Abt *et al*, 1989, wide scatter was found in the results due to the different characteristics of the subjects (mass and height) and the different reactions of each person. The results, ($u_{cr}$, $d_{cr}$), for each subject are shown in figure 3.6. The authors compared these results with the ones from Abt *et al*(1989), see Figure 3.9, and it was found that they had a smaller P.N., differences which were attributed to the use of different clothing and a more slippery surface used in RESCDAM experiment. The use of different clothing could had change the area against the flow increasing the drag force and also could increase the buoyancy force which would decrease the resistance of the subjects.

**Figure 3.5:** Experimental setup carried out under RESCDAM project, 2001. Source: Appendix 2, RESCDAM (2001).

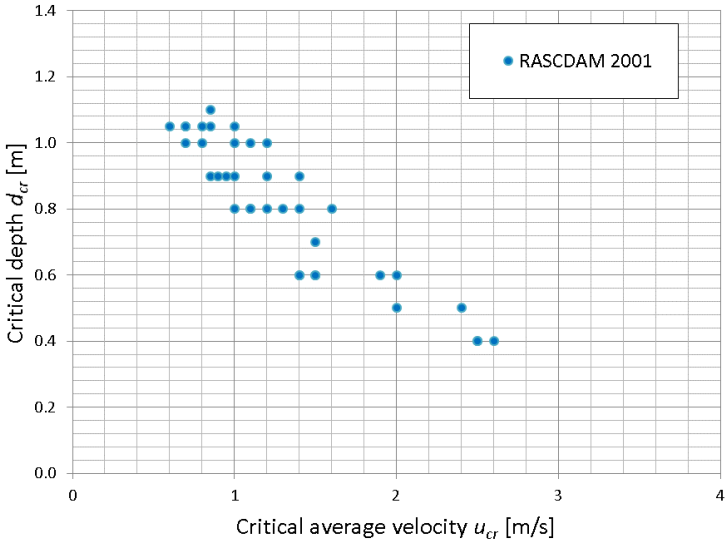


**Figure 3.6**: Critical speed and depth from RESCDAM project, 2001.

In an attempt to reproduce more realistic conditions, the Flood Hazard Research Centre (FHRC) carried out a series of tests in a real flow, reported in Jonkman and Penning-Rowsell (2008). The experiments were conducted in a flood relief channel of the river Lea, designed to control the level of the river in case of flooding by the used of sluices gates. One male professional stuntman subject, 1.7 m. tall and

weighing 68.25 kg., was tested on different flow situations, depending on how much the sluice gates were opened and the position in the channel that the tests were conducted. The test area was located around 75 m from the gates on a concrete bed with a foreshore slope of approximately 1%. The subject wore a dry-suit with rubber soled shoes. By contrast with the previous studies analysed in this work the subject didn´t use any safety equipment as helmet, or safety rope. Instead, after fall, the subject was rescued by a special team downstream. The experiments were carried out during daylight and with a water temperature no more than 10°C. Near the subject, the water depth ($d_{cr}$) and the water velocity ($u_{cr}$) were recorded using a Starflow Ultrasonic Doppler instrument attached to the channel bed. The subject was tested in three scenarios: the first one standing while the sluice gates were opening; the second, walking across flow to deeper and faster water in the centre of the flow; and finally walking rapidly towards the sluices into faster waters. The subject was given the freedom to react how he considered be the best way to resist the flow.

It was reported that for the standing position, the subject could maintain stability with a depth up to 0.35 m. and a flow velocity of 2.6 m/s or 2.4 m/s, after this the subject fell. For the walking test across the flow the unstable condition start with a depth of 0.26 m. and a velocity of 3.1 m/s. When the subject walked against the flow the results give a critical depth also of 0.26 m. and a flow´s velocity of 3.0 m/s, see Figure 3.8. The subject report that standing still in the flow was much easier remain stable than walking in the flow.

Only one study was found in this literature search whose aim was specifically to study the human stability in wave overtopping flows, reporting on an initiative carried out the 1995 by the Japanese Port and Harbour Research Institute (PHRI), with results reported in Endoh and Takahashi (1995). This study was focussed on wave overtopping on promenade breakwaters, which have dual objectives to protect the harbour from storm waves and also provide public areas for recreation (see Figure 3.7). Three human subjects, with heights 1.64 m to 1.83 m and weights 64 kg to 73 kg, were tested in a large current basin, 50 m. long and 20 m width, but only the results of two subjects were reported in Endoh and Takahashi (1995). As in Abt *et al.* (1989) study, a flow in a flume was generated and increased until the person

lost his balance, at which point the critical depth ($d_{cr}$) and velocity ($u_{cr}$) of the flow was recorded. In addition, the forces due to the flow against the subject were measured with load cells. The influence of different alignments of the persons against the flow and different leg separations was included in this study. Moreover, the study of the frictional coefficient between two types of shoe soles (leather and rubber) and the different floors (smooth concrete, rough concrete, concrete covered with alga and concrete covered with seaweed) was also included, see Appendix B for full results.

**Figure 3.7:** Promenade breakwater with recreation use, Whitby Harbour, UK. Copyright John Harding and licensed for reuse under this Creative Commons Licence.

From the results, Figure 3.8, Endoh and Takahashi (1995) studied two models of human instability: "slipping" and "tumbling". The first one occurs when the flow´s force against the body ($F_f$) is bigger than the maximum available friction resistance of the subject ($F_r$). It is anticipated that for fall due to this mechanism, the person will tend to fall with legs pointing downstream. The second mechanism models the falling process rising when the moment produced by the flow around the feet of the subject is bigger than the restoring moment produced by the weight of the person. In this scenario, it is anticipated that the person will fall with head downstream. A good agreement was reported between the models proposed and its experimental results. A more extensive analysis of these models is presented further in section 3.4.

Figure 3.8 (b) reproduces the results from one of the subjects, height 1.83 and weight 73 kg., who was used to study the influence of changing position, from standing just in front of the flow (blue points) to standing with both legs parallels to the flow (red points), but as it can be seen in the graph no significant influence was found.

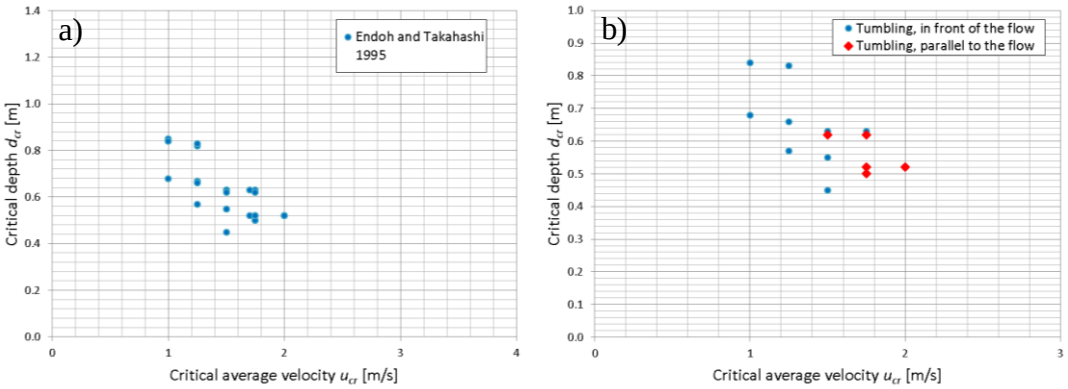


**Figure 3.8**: Critical speed and depth from Endoh and Takahashi, 1995. (a) General results (b) Results of the subject B.

Table 3.1 present a summary of the most important parameters and experiment configurations for the studies reviewed in detail in this chapter. Additionally, the results from the four projects are plotted together in Figure 3.9.

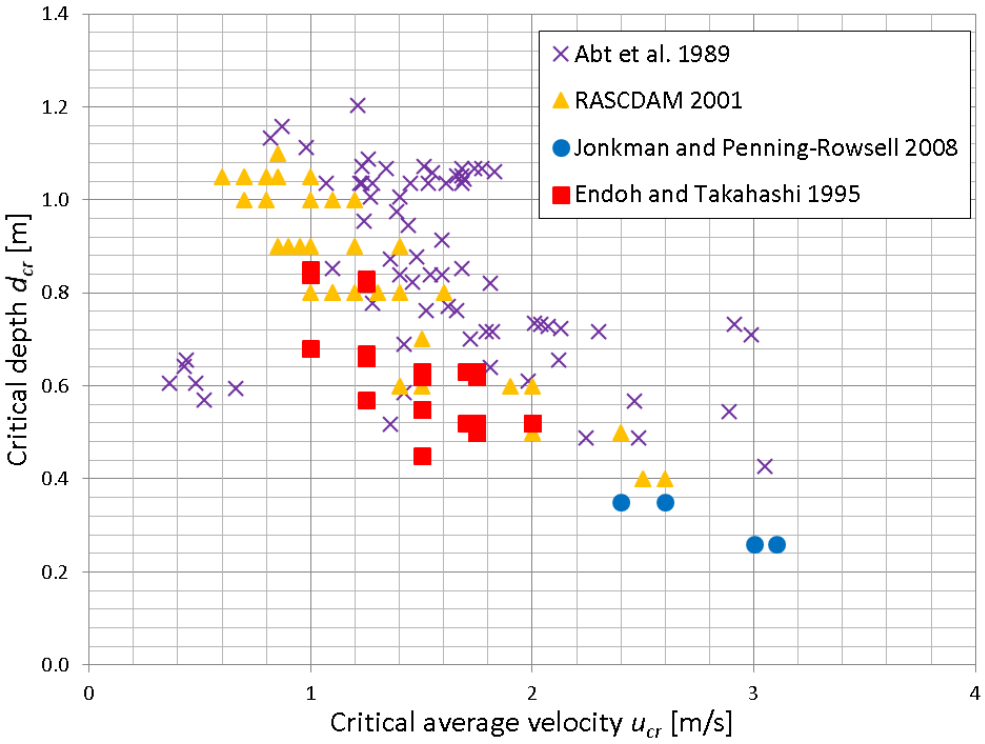


**Figure 3.9:** Critical speed and depth from previous studies, Abt et al, 1989; Endoh and Takahashi, 1995; RESCDAM, 2001; Jonkman and Penning-Rowsell, 2008, plotted together.

**Table 3.1**: Summary of the setup and results of previous studies (Abt et al, 1989; Endoh and Takahashi, 1995; RESCDAM, 2001; Jonkman and Penning-Rowsell, 2008).

| Study | Facilities | Surface | Slope | Subjects | Clothing | Subjects experience | Pre-acclimatisation | Range of critical parameters |
|---|---|---|---|---|---|---|---|---|
| Abt *et al.* 1989 | Current flume | Simulation of turf, smooth concrete, steel, and chip. | 0.5% and 1.5% | 2 females and 18 males H=[1.52-1.9]m W=[40-90]kg | Jeans, slacks, pull over shirts and light shoes | None | Yes | $u_{cr}$=[0.36-3.50] m/s $d_{cr}$=[0.43-1.2] m |
| Endoh and Takahashi, 1995 | Current flume | Smooth concrete, rough concrete, concrete covered with alga and concrete with seaweed. | No information | 2 male H=[1.64-1.83] m W= [65-80] kg | Rubber and leather shoe soles. | None | Yes | $u_{cr}$ =[1-2] m/s $d_{cr}$ =[0.45-0.85] m |
| RESCDAM, 2001 | Basin and mobile platform | Steel grating | 0% | 2 females and 5 males H=[1.6-1.95]m W=[48-100]kg | Gore-tex survival suits | Included two professional rescuers | Yes | $u_{cr}$ =[0.6-2.6] m/s $d_{cr}$ =[0.4-1.1] m |
| Jonkman and Penning-Rowsell, 2008 | Relief channel | Concrete | 1% | 1 male H=1.7 m W= 68 kg | Dry-suits with rubber shoes | Professional stuntman | No | $u_{cr}$ =[2.4-3.1] m/s $d_{cr}$ =[0.26-0.35] m |

From figure 3.9, a wide scatter in the results is evident, but a trend between the critical depth at loss of stability ($u_{cr}$) and the critical velocity of the flow ($d_{cr}$) is however evident, even though the subjects used had different characteristics and different flow tolerance to be unstable. RASCDAM and Endoh and Takahashi (1995) results are in the same range of $u_{cr}$ and $d_{cr}$; Abt *et al.*(1989) give a bigger resistance of the subject to fall due to the flow – differences that may be explained by different test conditions and protocols. It is also important to notice that the experiment conducted under more "realistic" conditions, Jonkman and Penning-Rowsell (2008), gives the more pessimistic results into influence of the depth although the subject was a professional stuntman, he still could not remain stable in any flow depth greater than 0.35 m. This is a depth much smaller than the maximum ($d_{cr}$=0.7m) reported in Abt *et al.* (1989), for similar $u_{cr}$, but in line with the trend of RESCDAM and Endoh and Takahashi results. This could be due to these being the only experiments that did not give the opportunity to the subjects to get used to a pre-test condition. Getting familiar to a pre-flow means that the subjects knew roughly what to expect when the flow increases, and thus be more prepared to remain stable. Additionally, the perceived safer conditions in a laboratory setting could mean that the subjects were more prepared to take bigger risks, and therefore remain longer in the controlled flow than in a real situation.

No studies were found during this research which had conducted tests in flows more similar to wave overtopping flows which are anticipated to be violent and very turbulent. It is therefore not possible to assume that the results of the studies presented are a true representation of human stability under wave overtopping flows.

With the ubiquitous availability of video recording facility on smart phones, and posting to sites like youtube, it is now possible to get estimations of the characteristics of depth ($d$) and velocity ($u$) during and overtopping flow and its consequences for people. Such a search and study has been conducted for the first time, which, its asserted, leads in to a better understanding of the conditions that a person could be exposed under wave overtopping flows, and therefore give strong evidence to support, or otherwise, the applicability of Figure 3.9 for wave overtopping flows.

## 3.3 New video analysis

With the current evidence base, it is very difficult to assess the extent to which the results found from the previous studies can be applied to wave overtopping and direct hazard, because it is not known the extent to which the conditions of flow used during those experiments are representative of a wave overtopping flow. In order to determine the extent to which they can be useful, it is necessary to know the general characteristics of wave overtopping flows and, in particular, the ranges of velocity ($u$) and depth ($d$) that can be expected, and also whether there are any other influencing factors not considered in the previous studies.

The literature shows a complete absence of quantified data on human accidents under wave overtopping flows. In this study, for the first time, advantage is taken of an alternative source of information which was not available until quite recently – data from videos of actual events, made possible by (i) the ubiquitous mobile phone camera and (ii) sites such as YouTube where videos are made readily available. Thus, an extensive internet search was conducted in this work, gathering video evidence from real situations which show pedestrians being exposed to real wave overtopping flows. From these, it was possible to analyse the different ways in which the water interacted with the persons and how they reacted to it.

Several videos where found, table 3.2, but not all of them had the minimum quality to make an analysis of the flow characteristics. They have moving shots, bad resolution, not clear view of the accident, or they do not offer a strong reference to estimate the distance. Only three videos were found that offered the opportunity to do a quantitative analysis, video 1, 2 and 3.

**Table 3.2:** List of wave overtopping accidents.

| Video | Name | Source | Comments |
|---|---|---|---|
| 1 | *Annual Wave* | National Geographic | Good quality |
| 2 | *Dangerous Storm Surge Waves on Lake Michigan!!! Best Footage!!!* | Youtube | Good quality |
| 3 | *Massive rogue wave injures crowd at the Maverick's Surf contest on 2/13/10* | Youtube | Good quality |
| 4 | *Chinese TV Journalist Gets Drenched by 70-Foot-High Wave* | Youtube | No distance references |
| 5 | *Large Rogue Wave Accident at Mavericks Surf Contest 02/13/10 Feb 13, 2010* | Youtube | No distance references |
| 6 | *Mavericks Wave Slams Spectators pt2* | Youtube | Slow-motion, unknow factor |
| 7 | *Mavericks Wave Slams Spectators pt3* | Youtube | No clear view of accidents |
| 8 | *Mavericks Wave Slams Spectators pt4* | Youtube | No clear view of accidents |
| 9 | *Mavericks Wave Slams Spectators pt1* | Youtube | Moving shot and no clear view of the accidents |
| 10 | *Dramatic footage of woman running from massive wave in Tramore Co Waterford* | Youtube | No distance references |

- Video 1, "*Annual Wave"* : A wave overtopping event produced by a tidal wave in the Qiantang river, China.

**Figure 3.10**: Screenshots video 1. Source: National Geographic, http://video.nationalgeographic.com/video/annual-wave?source=relatedvideo.

- Video 2, "*Dangerous Storm Surge Waves on Lake Michigan!!! Best Footage!!!"* (2011): A wave overtoppings on a promenade on Lake Michigan, United States. Video made by a local news.


**Figure 3.11**: Screenshots video 2. Source: https://www.youtube.com/watch?v=T9HUwAIFSEo, myfoxchicago.com.

- Video 3 "*Massive rogue wave injures crowd at the Maverick's Surf contest on 2/13/10*" (2010): A wave overtopping accident during a surf competition on Maverick Coast, United States, amateur video.

**Figure 3.12**: Screenshots video 3. Source https://www.youtube.com/watch?v=jV7KhSdUQPU.

Of course, none of these videos were recorded with the objectives to being used as a source for a quantitative study, so they don´t have the resolution or clear measurements units that a proper experimental video would have, but they have a satisfactory quality to get very useful, quantified information about the general conditions to which pedestrians can be exposed during a wave overtopping event and therefore they can help to identify facets of hazardous wave overtopping flow.

The following parameters were estimated in each video: the average speed of the front of the flow ($u_f$) in the section were the person was hit the maximum flow depth ($d$) that the person received or the depth at the moment of loss of stability, and the

duration ($T_{ov}$) of the overtopping event. For each parameter, the general methodology of calculation was the following:

- for $u_f$ it was necessary to define a reference distance, and then determine the time taken it by the water to cover this distance. The average speed could then be calculated.
- for $d$, an average height for the persons in the video was assumed, based upon statistical data for the average height for a male or female in the country where the video was recorded. Then, from the videos, it was possible to estimate the depth to which each subject became submerged based upon the relative depth to the assumed human height.
- the duration $T_{ov}$ was obtained directly from the video timing.

The videos found not just included records of persons being knout over by the flow, but they also include people able to resist the flow and not fell. In the next section a full analysis of the videos and its founding are presented individually.

### 3.3.1 Video 1: Qiantang river, China

This video show the arrival of a tidal wave in the Qiantang river, China. This event occurs yearly at the end of the summer and it is a popular attraction that hundreds of tourists go to see. Several coastal defences exist along the shore of the river to prevent serious damage in the closest structures and also keep safe the habitant of the city, but even thought this is a very predictable event, because of the fascination that the waves crashing against the coastal defences produce in people, several accidents occur every year due to the unnecessary risks that the curious take to have a good view of the surge. This video provides an overview of this phenomenon, and also provides a record of a massive accident due to the overtopping (between 35s and 45s on the video). It is true that this event is not originated by a wind wave- the main focus of this research but the overtopping flow produced bears a lot of similarity with an overtopped flow on a promenade resulting from “normal” waves. It is therefore taken as a valid case study for this thesis.

Several people were completely washed out by the flow, demonstrating that the drag force of the flow was much bigger the minimum necessary to just unbalance a person, but not all those washed out are in sufficiently clear view to be analysed. Even though the big number of potential subjects to study, only four persons are close enough to the camera to offer us the possibility to estimate the average speed ($u_f$) and the depth ($d$) of the flow that lead to the person being wash out. The persons analysed were labelled as it shown in Figure 3.14.

The specific place where the accident occurred is not identified in the video, but that is not relevant information for this study being more important the local geometry and the characteristic of the wave overtopping flow, both aspects can be obtained from the video. As it can be seen in Figure 3.13, the cross section where the accident take place is formed by a defence, type unknown, which seems to have a small crown wall, protecting a concrete promenade of around 8m width, which ends at the land side with a cut of around 2m. to make way for the natural topography, see Figure 3.13.

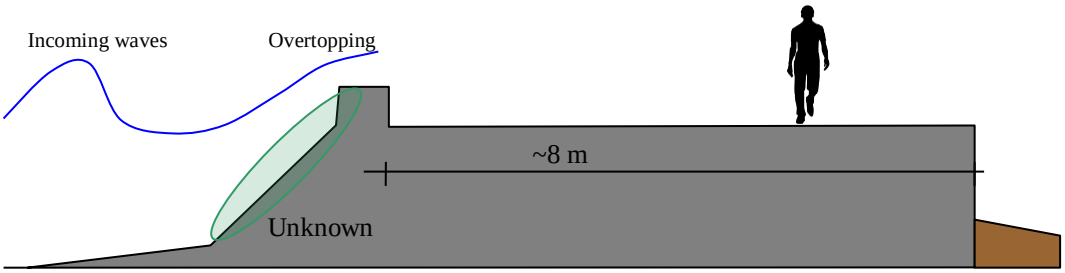


**Figure 3.13**: Approximation of the cross section where the overtopping accidents take place in video 1. No scale.

It can be seen that the flow did not generate a big jet/splash at the moment of overtopping the defence, so it can be assumed that the defence is a slope of some description (unless the wave hit the defence with a significant angle). Another important characteristic of note that could influence on the level of hazard is that the water is charged with sediments - inferred due to the colour of the water. Thus, its density and therefore consequent drag forces may be elevated.. No large debris can be seen in the water.

The coastal defence has a crest wall which makes a big influence in the way the flow behaves. At the crest of the wall, a zone with very aerated water can be seen, which then increases its velocity due to the small fall after the crest wall. Following this, the flow runs over the concrete promenade, impacting the people before running down again on the cut at the opposite (down-wave) side of the platform. Moreover it was noted that the maximum discharge doesn't occur at the beginning of the flow but more close to the mid-time of the overtopping duration. Another interesting aspect noticed was that the farther the flow was from the defence more smooth the flow seems to be and more gradual, or less violent, is the increasing of depth.

In order to identify a distance for reference the width and length of the cars were used based on similar dimensions for cars like the ones shown the video . The full methodology used for the estimation of the parameters is presented in Appendix A.

The person´s height used for the estimation of the depth was 1.70m., which corresponds to the height of the average Chinese adult male (Yang *et al.* 2005). Because of the limited resolution of the video were assumed that all the subjects were adult men.

In general, all the people (15 to 20 persons) chose to run once they saw the approach of water that overtopped the defence, but only a few of them managed to escape (4 persons), due to a late reaction and also because the geometry of the platform meant that people could not run ahead of the flow, but instead they had to run perpendicular to the flow and were quickly reached by the water.

It can be seen in Figure 3.14 that the subjects A and B were not reached by the flow, being successful in their escape. Person C is only reached by a thin layer and together with person D they were able to resist the flow and not fall. On the other hand, persons E and Q were reached by the flow and were completely washed out and carried by the flow down to the natural topography. The average speed and depth estimated are presented in table 3.3.

Despite the big volume of water overtopped and the number of persons carried by the flow, the depths generated were not great. None of the persons analysed received a flow deeper than knee height before fall. Very fast waters were however estimated,

which in combination with the depth were able to produce a discharge strong enough to sweep away every person who received the developed flow.

**Table 3.3**: Speed ($u_f$), depth ($d$), and overtopping duration ($T_{ovt}$) estimated from video 1.

| Subject | Sex | Age | Height* [m] | Surface | $u_f$ [m/s] | $d$ [m] | $T_{ovt}$ [s] | Consequence | Observation |
|---|---|---|---|---|---|---|---|---|---|
| *E* | male | adult | 1,7 | concrete | 3,45 | 0,43 | > 10 | Wash out | Running |
| *F* | male | adult | 1,7 | concrete | 3,45 | 0,43 | > 10 | Wash out | Running |
| *C* | male | adult | 1,7 | concrete | 4,96 | 0,11 | > 10 | No | Running |
| *D* | male | adult | 1,7 | concrete | 3,52 | 0,21 | > 10 | No | Running |

Note: * Assumed according to national averages; not estimated from video.

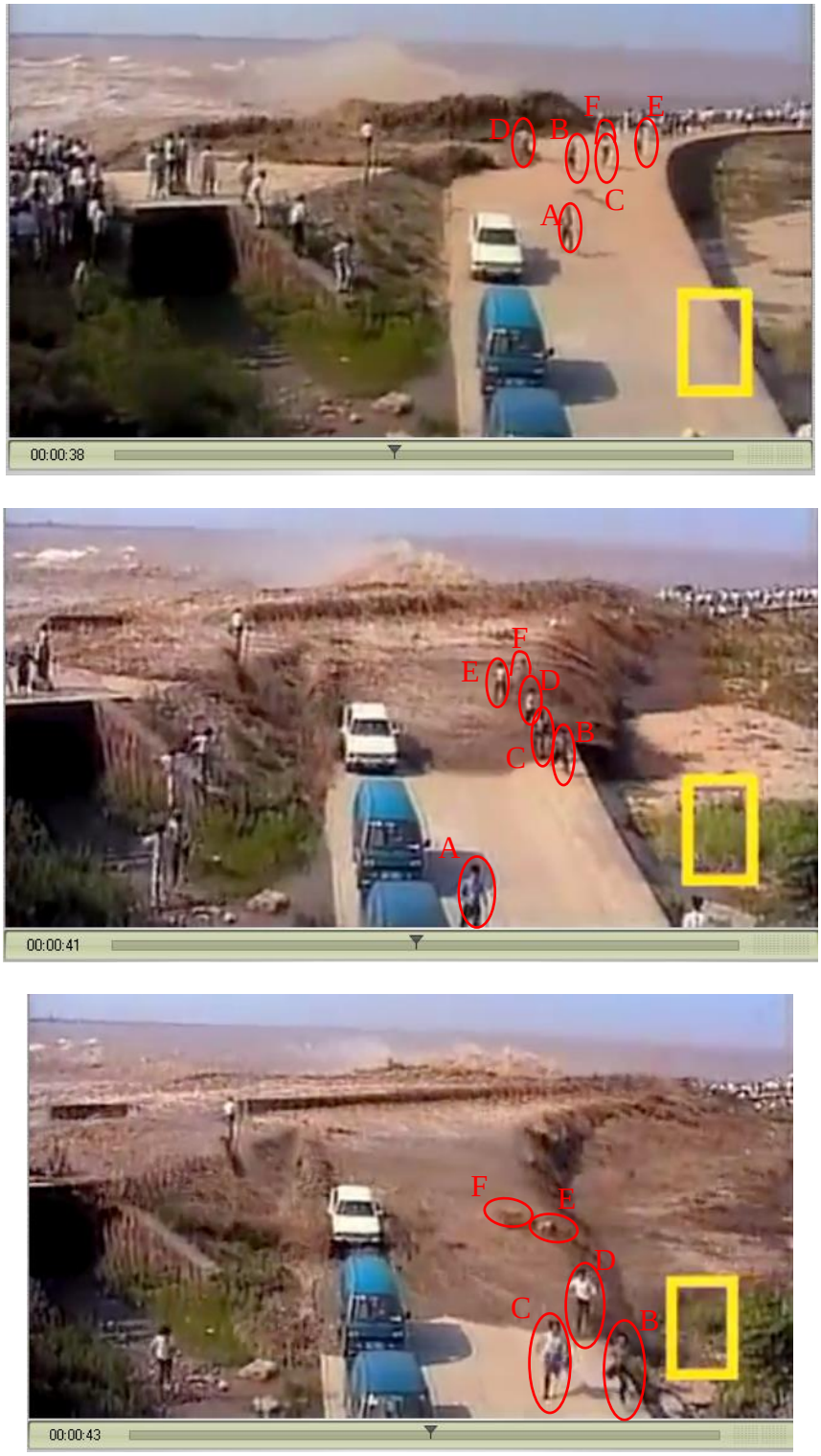


**Figure 3.14**: Screenshots video 3 and labels of subjects analysed. Source: National Geographic.

### 3.3.2 Video 2: Lake Michigan, United States.

The second video analysed provides a record of a storm on Lake Michigan, United States, which wave of 3.6m. to 4.8m at Chicago´s coast. A local news show captured the waves crashing against a coastal defence which offer protection to a road and generated a platform which is used as promenade. The waves generated a significant number of wave overtopping events, with discharge flowing across the promenade before being reflected at the second wall by the road, as is shown in Figure 3.15.

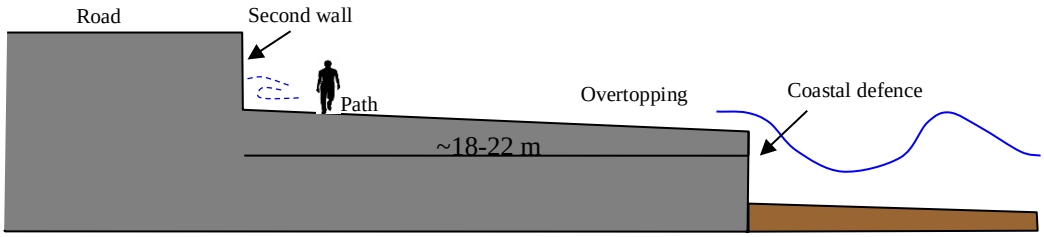


**Figure 3.15:** Sketch of the cross section where the overtopping accidents take place in video 2. Not to scale.

With the coastal defence´s crest level being lower than the eye level of the pedestrians, the people had a clear view of the lake and could anticipate a potential dangerous situation due to the big waves breaking along the defence line. Despite this, some persons took the risk anyway to proceed along the most dangerous section of the path where several wave overtopping events had already been occurring.

Pedestrians and cyclists were reached by different sizes of wave overtopping events, generating several consequences: people who held their balance and did not fall, others who just could not walk anymore, and others who lost stability and were swept by the flow.

In addition, this video gave the opportunity to analyse the influence of the geometry of the exposed setting and how this can affect the possible consequences in case of accidents. In this case, the path is between the primary coastal defence and a secondary wall enclosing the road foundations. Also, it was noticed that the promenade has a gentle slope to the lake, which is good in order to reduce the wave overtopping height, but it works in favour of the flows when it get reflected by the second wall. It can be said that two flows were generated in a big wave overtopping

event: the first one is the one normally expected which came from lakeside, after the waves break, to the land side, and secondly is the less anticipated flow which is the first one after reflection by the secondary wall. In most cases, it was this second flow took people by surprise.

Incidents affecting seven persons are recorded with at least the minimum video quality to be analysed – one pedestrian and six cyclists. Three persons received both the original overtopping flow and the reflected flow – a situations that were also included in the analysis. Under these circumstances, it is necessary to considerer whether the subjects could be already unbalanced by the first flow or, on the contrary, be more prepared to receive the second flow. Although , therefore the response of the subject to the second flow is therefore likely to be influenced by the previous experience, these do correspond to a real situation and the information obtained is considered relevant for this research. The results of the analysis are presented in table 3.4.


**Figure 3.16**: Subject being washed out, 1m:30s-1m:41s. Source: myfoxchicago.com

A satellite image of the area where the event took place was used in order to get the reference distances to calculate de average speed of the front of the flow, $u_f$.

The person height used for the estimation of the depth was 1.77m for males and 1.63m for females, which corresponds to the United States average heights (Mcdowell *et al.* 2008). Secondly and because of most of the cases analysed here correspond to cyclists, the diameter of a standard bicycle wheel (0.66m) was used as an additional reference. More information and the full procedure of estimation is presented in Appendix A.

As in video 1, the flows in the present video are faster and shallower than most of the flows recreated in previous experiments in the literature. It is however apparent that, flows with very low depth were able to unbalance the pedestrians and cyclists. Smaller volumes of overtopping were recorded in video 2 compared with video 1, but they were able to produce a hazardous situation too.

**Table 3.4:** Speed ($u_f$), depth ($d$), and overtopping duration ($T_{ovt}$) estimated from video 2.

| Subject | Sex | Age | Height* [m] | Surface | *uf* [m/s] | *d* [m] | $T_{ovt}$ [s] | Consequence | Observation |
|---|---|---|---|---|---|---|---|---|---|
| B ch | Male (B) | Adult | 1.77 | concrete | 3.77 | 0.22 | 4 | Stop | Could no longer ride bicycle. |
| | Male (B) | Adult | 1.77 | concrete | 6.73 | 0.17 | -- | Wash out | Fall due to the reflected flow. See figure 3.15 |
| | Male (B) | Adult | 1.77 | concrete | 3.77 | 0.22 | 5 | No | Now walking; resisted new overtopping flow. Used bicycle as a third point |
| E ch | Female (P) | Adult | 1.63 | concrete | 1.56 | 0.1 | 4 | No | |
| F ch | Male (B) | Adult | 1.77 | concrete | 7 | 0.14 | 4 | Stop | Could no longer ride bicycle. |
| G ch | Male (B) | Adult | 1.77 | concrete | 4.19 | 0.11 | -- | Stop | Could no longer ride bicycle. |
| | Male (B) | Adult | 1.77 | concrete | 3.05 | 0.33 | -- | Fall | Fall due to the reflected flow |
| | Male (B) | Adult | 1.77 | concrete | 5.15 | 0.3 | -- | No | Now used the bike as a "walking stick". Is aware of the hazard. |
| H ch | Male (B) | Adult | 1.77 | concrete | 2.5 | 0.08 | -- | No | |
| I ch | Male (B) | Adult | 1.77 | concrete | 4.56 | 0.16 | -- | Stop | Stop due to the flow crashing against second wall |
| | Male (B) | Adult | 1.77 | concrete | 3.5 | 0.08 | -- | No | |
| K ch | Male (B) | Adult | 1.77 | concrete | 3.89 | 0.11 | -- | Stop | Stop due to the flow crashing against second wall |

Note: (B) = Biker, (P) = pedestrian, * = Assumed according to national averages; not estimated from video. $T_{ovt}$ = duration of the overtopping flow at the spot were the subject was reached by the flow.

### 3.3.3 Video 3: Maverick´s coast, United States

The third video analysed shows wave overtopping at a beach at Pillar Point, Mavericks´s coast, United States. One of the most important surfing competitions takes place here, giving an indication of a significant wave climate. Thousands of people attend the event to watch the best surfers of the world. No formal structures exist to receive the audience, so spectators watch the contest from the beach and a nearby hill. This video was recorded by a spectator standing on the hill, and shows how a massive run-up event overtops, or overflows a low seawall before reaching the

place where several persons are and swept away, causing several injuries. This event could be consider between a wave overtopping and overflowing, but in either case, the flow parameters and direct consequence can be linked well, and its results can be incorporated into a wave overtopping study.

Figure 3.17 shows an approximation of the section where the accidents took place. The surface is the natural sand beach (in contrast to videos 1 and 2). A seawall, which is part of the coastal defence of the Pillar Point harbour, has generated a region of sediment deposition, to the right-hand side, and an region of erosion, producing different topography levels. This height difference generated an increase of the flow speed after breaking against the wall and also reduced the people's visibility of the sea from the lower level, so they did not have a clear view and could easily be taken by surprise.

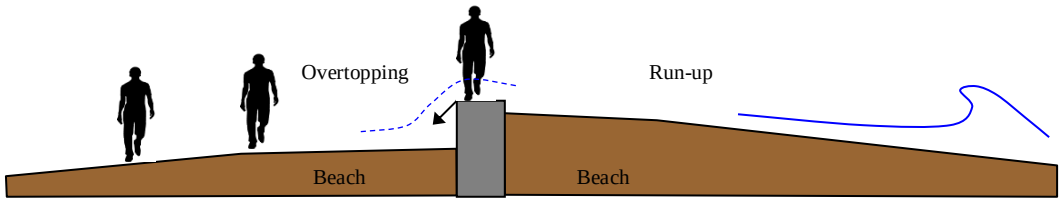


**Figure 3.17**: Approximation of the cross section where the overtopping accidents take place in video 3. No scale.

To estimate the velocity of the flow a satellite image of the sector was used, more detail in Appendix A.

The person heights used for the estimation were as those used in the analysis of video 2, the United States average heights of 1.77m and 1.63m for males and females respectively (Mcdowell *et al.* 2008).

Ten persons can be easily identified in the video as being reached by the flow. Among these, four were completely washed out by the water, two just fell, and the other four managed to resist the flow and remained standing due to they received just a thin layer of water. Sadly, not all of the subjects identified offer the minimum image quality to be analysed, and only for five cases could the average speed of the

front of the flow, $u_f$, and the depth, $d$, be estimated. The results are presented in table 3.5.

All the people decided to run from the flow, so the flow reached the persons in motion, and not with two feet on the ground.

**Table 3.5:** Speed ($u_f$), depth ($d$), and overtopping duration ($T_{ovt}$) estimated from video 3.

| Subject | Sex | Age | Height* [m] | Surface | *uf* [m/s] | *d* [m] | $T_{ovt}$ [s] | Consequence | Observation |
|---|---|---|---|---|---|---|---|---|---|
| Am | Male | Adult | 1.77 | Sand | 5.19 | 0.44 | 5 to 10 | Wash out | Beaten by the flow |
| Bm | Male | Adult | 1.77 | Sand | 5.19 | 0.44 | | Wash out | Beaten by the flow |
| Dm | Male | Adult | 1.77 | Sand | 3.99 | 0.3 | | Wash out | |
| Gm | Male | Adult | 1.77 | Sand | 3.62 | 0.3 | | Fall | |
| Fm | Female | Adult | 1.63 | Sand | 3.99 | 0.14 | | No | |


**Figure 3.18**: Screenshot video 3. Source: https://www.youtube.com/watch?v=jV7KhSdUQPU

As in the previous videos, the combination of fast water and low depth was able to produce a very hazardous situation for the people. In this video, also observed were several subjects who were beaten by a jet of water which was produced when the flow crashed into the seawall. This situation occurred very close to the seawall and

the people who were standing there were washed out by the flow immediately with no visible resistance.

### 3.3.4 Analysis of video evidence - discussion

Three videos of real wave overtopping accidents were found during and exhaustive research, conducted in this research, which have a sufficient quality to permit the analysis of the characteristics of a real wave overtopping flow, without scale effects, and the quantification of critical flow speed and depth parameters, $u_f$ and $d$, which caused to a person fell into the flow or be washed out by it. Figures 3.19 and 3.20 show the results identified by video and by consequences.

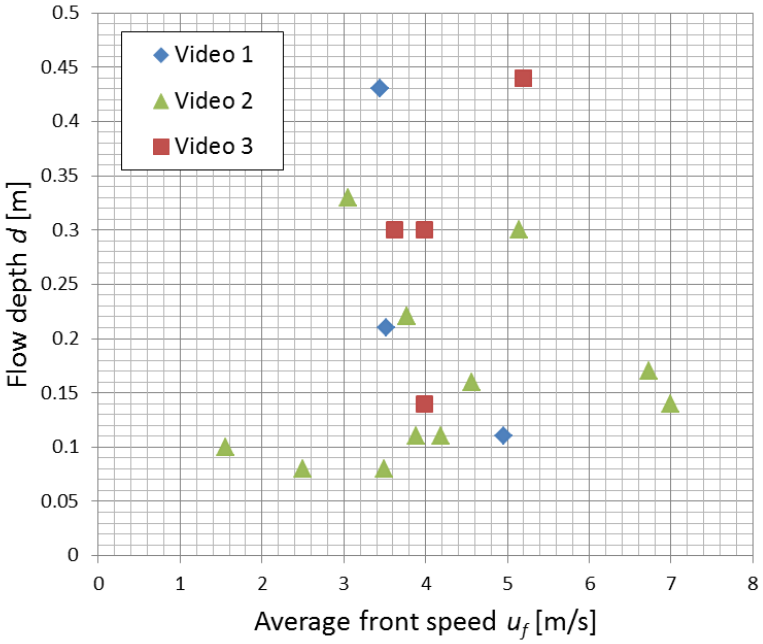


**Figure 3.19**: Results from video analysis. Distribution of flow speeds and depths in analysed data set.

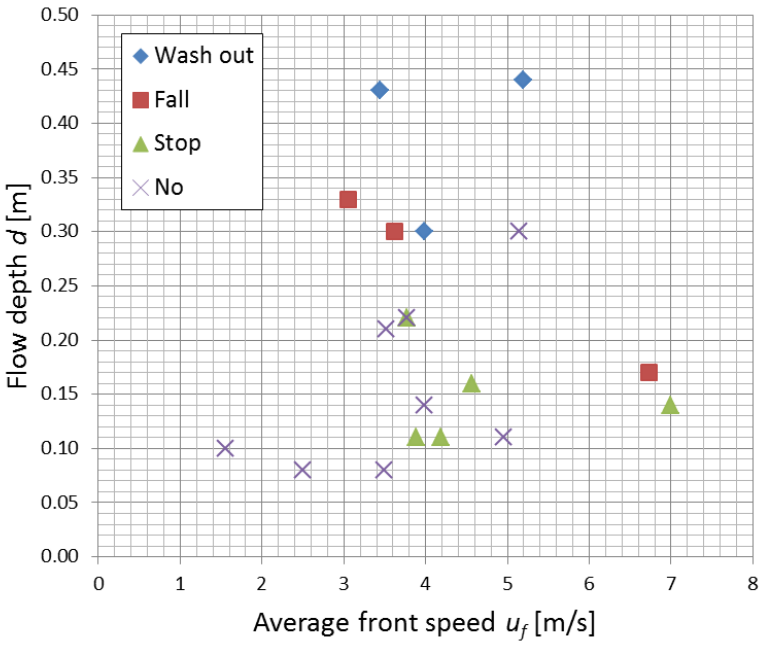


**Figure 3.20**: Results from video analysis. Consequence of each event again plotted as flow depth vs speed.

It can be seen that video 2 gave the widest range of flows due to several wave overtopping events being recorded and analysed, whereas in video 1 and 3, just one massive event is available. Due to the size of the events of video 1 and 3, it is possible to have different dimension of $u_f$ and $d$, depending of the location of the subject (person) being analysed. It should also be noted that each person can have a different tolerance, resulting in different consequences for the same event.

Several conclusions can be made from the video analysis:

- The wave overtopping events analysed had relatively low depths - there was no situation with a depth higher than the knees of the subjects. Neverthless, these conditions resulted in enough drag to destabilise a person.
- Fast wave overtopping flow were observed, with 3 – 4 m/s being typical, and up to 7 m/s measured. These speeds were a key factor in the hazard potential of the flow.
- Wave overtopping events are very violent flows, characterised by rapidly changing water depth and velocity.

- People close to the defence line can be exposed to jet of water (video 3). They can hit a person in a point higher than its feet and have the sufficient energy to knock over. It can be seen in the videos that all the people, around 14 persons, which received the main flow in a point higher than the feet level were easily washed out and dragged by the flow. On the other hand the people who received the same flow but at the feet level were able to resist in a better way and not all of them were dragged by the flow, 5 of 9.
- The geometry of the cross section of where the events occur has a crucial factor in the behaviour of the flow and in the level of consequences that could generate. In the cases studied a significant effect of crown or secondary walls was observed in video 1 and 2, also the slope of the promenade in video 2 and the abruptly cut of the promenade in video 1 with no hand rail or protection of any kind generate extra sources of hazard.
- The way in which individuals react to the flow is very diverse and appears to affect the individual's resistance to be knocked over by small and medium sized overtopping. For massive overtopping it seems that the reaction (standing or running) of the person has less influence, being more important the flow parameters, u and d, to define consequences (video 1). In video 3 is possible to observe different reactions for the same event and it can be seen that the persons who run with the flow, 3, were able to resist, no one of them were knock over by the flow, on the other hand the 2 persons which did not move or move slowly were knock over and dragged by the flow.

These new results have an important value because they are estimation from real events, with no scale effects where it was possible to watch the real reaction of people, not wearing safety equipment, not having the opportunity to get used to a pre-test condition and being free to react instinctively.

## 3.4 Comparison of literature results and video analysis

Figure 3.21 presents a comparison between the hazardous conditions identified in the videos analysis conducted here, with the results of the studies in the literature. It is immediately apparent that the flow conditions identified as hazardous in the previous studies correspond to deeper and slower flows than those estimated from the video analysis. It is clear from the video that no situation occurs where the water was 1m deep. The Jonkman and Penning-Rowsell (2008), study which was conducted in a "natural channel" under semi-realistic conditions, has the most similar results to the video analysis, with low depth and fast waters also identified as critical situations for human stability. There are several reasons for the differences between the present study and the other studies in the literature:

i. The capabilities of the flumes used may have limited the opportunity to explore faster waters, so it turned out to be a significant depth that was needed to destabilize the subjects;
ii. the controlled environment of the laboratory generated a sense of security in the persons tested, so they may have been more willing to take risks than in a real situation;
iii. the opportunity to get used to a pre-test flow prepared the persons and may have assisted them in resisting being destabilised for longer;
iv. the flows were increased gradually, so the subjects had enough time to adjust their position to maintain their stability;
v. in general, all the persons on the video ran from the flow – a situation which was not considered in the previous studies.
vi. Despite these factors a clear trend can be seen in Figure 3.20 which gives a stronger basis, than ever before, for analysis of the mechanism(s) for human stability under overtopping flow conditions.

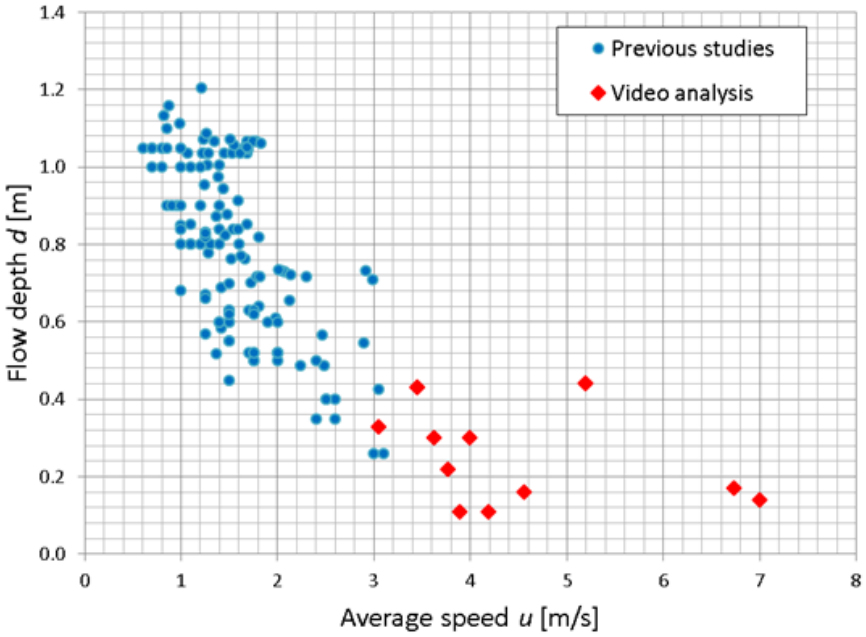


**Figure 3.21:** Flow speed and depth data from the video analysis of actual events, plotted together with results of studies from literature (Abt et al, 1989; Endoh and Takahashi, 1995; RESCDAM, 2001; Jonkman and Penning-Rowsell, 2008). Note that for the video analysis, the speed is taken to be the average speed of the front of the flow, $u_f$, whereas in the previous studies, it is the instantaneous flow measured at the moment of instability of the subject.

## 3.5 Mechanism of human instability

The synthesis of the results of the studies found in the literature and the new video analysis show a clear pattern linking the flow´s velocity, *u*, the flow´s depth, *d*, and the stability of people under those condition. It seems to be plausible to find a prediction of the line separating the stable and unstable regions on the graph *u* v/s *d* (Figure 3.22).

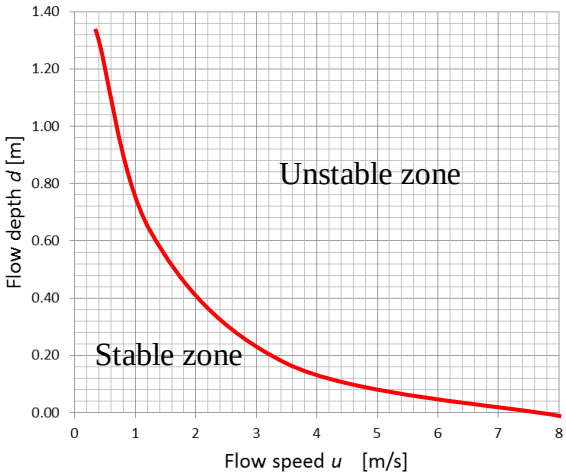


**Figure 3.22**: Schematic graph of hazard zone and instability curve.

The first attempt found to derive an analytical prediction method for hazardous flows for people was conducted in Abt *et al*. (1989). These authors used the results of their tests to define a *product number*, P.N., according to equation (3.2), to predict the discharge, *u·d*, that will generate an unstable condition for a person. The model proposed was a function of the weight and the height of the subject and was independent of the type of surface and slope.

Translating equation 3.2 to S.I. units, the equation becomes:

$$P.N. = 0.305^2 \cdot \exp\left[19.272 \cdot \left(m \cdot h_p / 1000\right) + 1.088\right] \qquad (3.3)$$

where: P.N. *product number* [m$^2$s]; $m$ is the person's mass [kg], and $h_p$ is the person's height [m]

Figure 3.23 presents the prediction of the P.N. calculated with the methodology proposed by Abt *et al*. (1989) compared with the results of the previous studies. The data from the video analysis is not included due to the weight of each subject being unknown. There is not a good agreement between the prediction and the data. The prediction increases exponentially with the height and weight but the human resistance does not appear to increase at such a rate. It is important to note that this P.N. methodology was calibrated under the test conditions of Abt *et al* (1989), and

presented as a rough indicator by the authors, so it might have a very narrow range of application, and is being extrapolated without foundation.

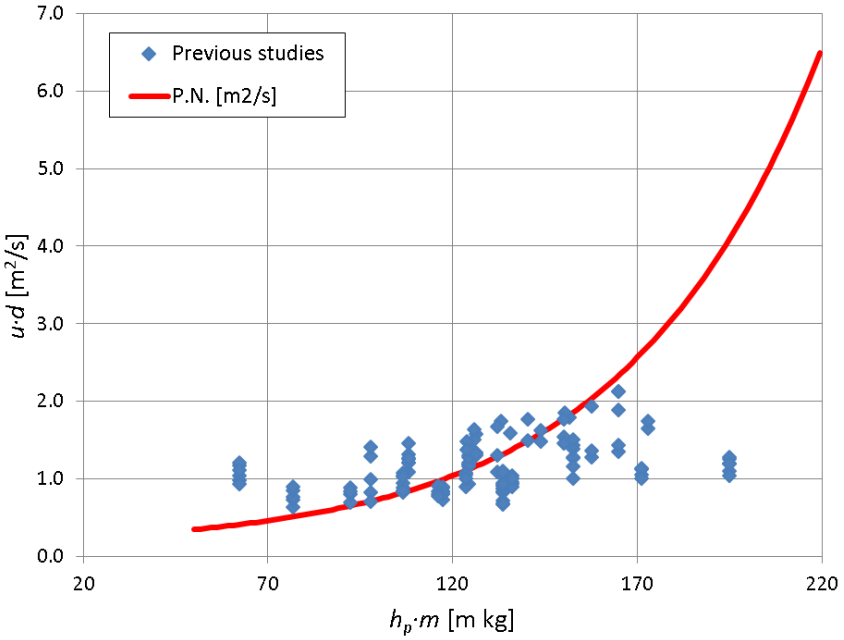


**Figure 3.23**: P.N. prediction based on Abt *et al.* (1989) plotted together with data from literature (Abt et al, 1989; Endoh and Takahashi, 1995; RESCDAM, 2001; Jonkman and Penning-Rowsell, 2008).

A different approach has been proposed in more recent studies, based upon a consideration of the mechanism that can lead to a loss of human stability. The earliest but still most complete analysis found is that of Endoh and Takahashi (1995) who identified two general falling mechanisms, called "slipping" and "tumbling".

*Slipping* is related with a lack of sufficient friction between the subject´s footwear and the surface on which the person is standing. When the drag force of the flow is bigger than the available friction, the subject will fall due to this mechanism. *Tumbling* occurs when the person is knocked over by the moment generated by the flow, *i.e.* the destabilising moment due to the flow exceeds to restoring moment due to the person's weight. In such a case, the person is rotated around its pivot point, suffering fall. As previously observed, when people fall due to *slipping* they tend to

fell with their legs pointing downstream, whereas when the main mechanism is *tumbling*, they tended to fall with their head pointing downstream.

According to this methodology the stability depends not only on the person's weight and height, but is also influenced by the position of the person, *e.g.* their way of standing, and also by the coefficient of friction between shoe sole and ground. The analysis for each mechanism of instability can be derived as follows (after Endoh and Takahashi, 1994):

- **Friction stability** (see Figure 3.24)
  (based on Endoh and Takahashi 1994)

$$F_f - F_r = 0$$

$F_f$ is the drag force of the flow and it is function of the velocity, depth, the shape of the submerge body and the drag coefficient. $F_r$ is the friction resistance function of the body weight and friction coefficient.

$$C_d \cdot \frac{\rho}{2} \cdot u^2 \cdot B \cdot d - \mu \cdot m \cdot g = 0$$

From this equation the critical combination *u-d* for the fiction instability can be found.

$$u^2 \cdot d = \frac{2 \cdot \mu \cdot m \cdot g}{C_d \cdot \rho \cdot B} \qquad (3.4)$$

- **Momentum stability** (see Figure 3.24)
  (based on Endoh and Takahashi 1994)

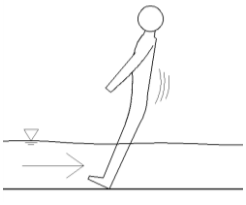

$$M_r - M_f = 0$$

The moment generated by the flow ($M_f$) can be calculated as the drag force applied at the half of the depth. On the other hand the restoring moment ($M_r$) is function of the person weight and distance to the pivot point ($d_1$).

$$m \cdot g \cdot d_1 - F_f \cdot \frac{d}{2} = 0$$

Replacing the value of the drag force the critical combination u-d for the moment stability can be found:

$$| m \cdot g \cdot d_1 - C_d \cdot \frac{\rho}{2} \cdot u^2 \cdot B \cdot d \cdot \frac{d}{2} = 0$$

$$u \cdot d = 2 \cdot \sqrt{\frac{m \cdot g \cdot d_p}{C_d \cdot \rho \cdot B}} \tag{3.5}$$

with:

$F_f = C_d \cdot \frac{\rho}{2} \cdot u^2 \cdot A$, drag force of the flow [N]

$C_d$ = drag coefficient [-], calculated according to Endoh and Takahashi (1995)

$$C_d = 1.1 \cdot (1 - \frac{L_f}{h_p}) \quad \theta = 0^o$$

$$C_d = 1.1 \cdot (1 + \frac{L_f}{h_p}) \quad \theta = 45^o, 90^o$$

$u$ = average flow velocity [m/s]

$d$ = average flow depth [m]

$\rho$ = density of the water [kg/m$^3$]

$\mu$ = coefficient of friction between shoe sole and ground [-]

$g$ = gravitational acceleration [9.81 m/s$^2$]

$m$ = subject´s mass [kg]

$L_f$ = width between the feet [m]

$\theta$ = angle of the person against the current [°]

$h_p$ = person height [m]

$B$ = average diameter of the subject legs [m]

$A$ = the projected area of the submerged part of the body normal to the flow $= B\,d$ [m$^2$]

$d_1$ = distance from pivot point to the centre of gravity [m]

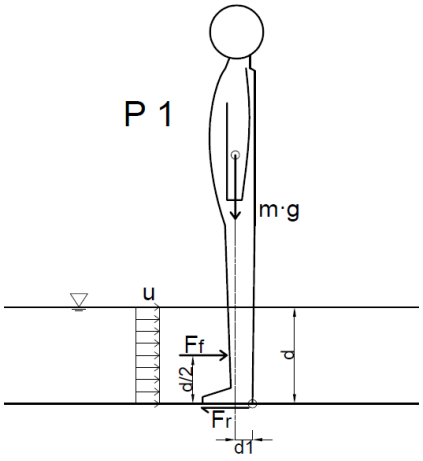


**Figure 3.24**: Human model standing in front of the flow, position 1.

To find the stability zone with this methodology, several assumptions had to be made. First, a human model had to be assumed standing in a certain position against the flow, as a first iteration the position 1 (P1) show in Figure 3.24 was used in this work. This position assumed here represents a very conservative assumption because it represents a person who is taken by surprise by the flow and has not adjusted position to one more suitable to resist the flow. It was also necessary to define the person´s height and weight, the average of the subject's height and weight from the previous experiments was used, see table B.2 Appendix B. The subjects are not separated by their physical characteristics at this time. Figure 3.25 show the prediction and the data of the previous studies plotted together. In addition, all the new video data is included in order to check whether they lie in the hazard zone of the graph.

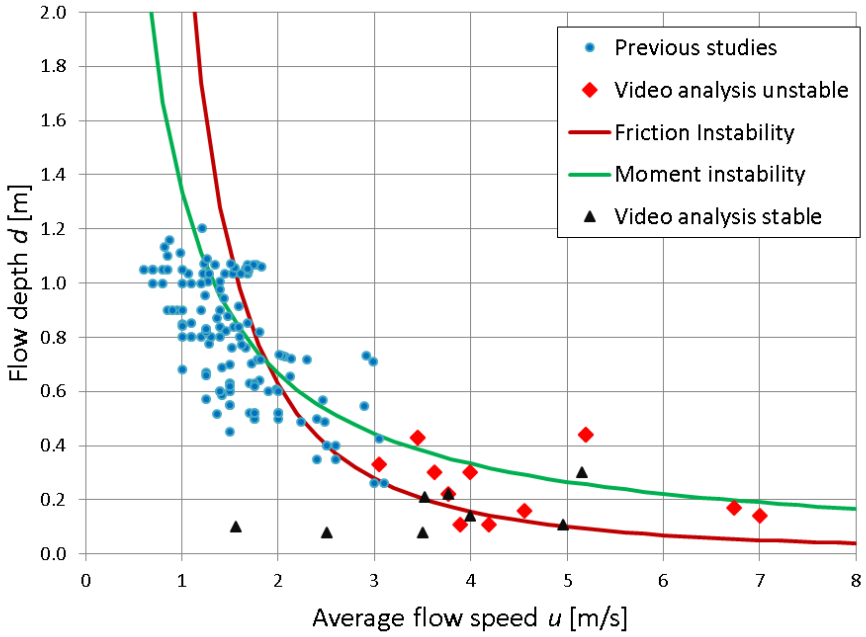


**Figure 3.25:** Comparison of instability prediction and data from the video analysis of actual event and the results of studies from literature (Abt *et al*, 1989; Endoh and Takahashi, 1995; RESCDAM, 2001; Jonkman and Penning-Rowsell, 2008). The following assumptions were made: mass = 72.54 kg (average for subjects in figure 3.8); hp=1.76 m. (average for subjects in figure 3.8); B (leg diameter)= 0.2 m; Lf (leg separation)= 0.2·hp; Lg (foot length)= 0.125·hp; friction coefficient μ=0.62 (wet, smooth concrete, based on Endoh and Takahashi 1995) and ρ (of the water) = 1000 kg/m$^3$.

Firstly, it can be seen that the two mechanisms occupy different zones where they are the dominant cause of instability. The friction instability takes place in shallow and fast waters and, in contrast, the moment instability is dominant in deeper and slower waters. This is explained because in order for the moment instability mechanism to be the one responsible for knocking down a person, a considerable depth is needed to generate a large enough moment to defeat the restoring moment due to the person's weight. By the equations (3.4) and (3.5) is possible to find the condition of *u* and *d* where the transition occurs.

$$d_{tr} = \frac{2 \cdot d_p}{\mu} \tag{3.6}$$

$$u_{tr} = \mu \cdot \sqrt{\frac{m \cdot g}{C_d \cdot \rho \cdot B \cdot d_p}} \tag{3.7}$$

Good agreement is observed considering the shape of the instability curve and the distribution of the critical points, but only the 34% of the points are located in the hazard zone. It can be seen that in the lower part of the graph (friction instability) the prediction work better, on the other hand in deeper water the models are less accurate. In general the points calculated in the video analysis are located more or less in the zone of the graph where they supposed to be, even though they include the data due to cyclists too. The exception to this good agreement is the one stable point located very inside the unstable zone (with $u$=5.15m/s and $d$=0.3). This particular case can be explained because that point corresponds to the case of a cyclist who received three overtopping flows, with this being the last one. This time, the subject used the bicycle as an extra point of support and was also more aware of the situation, and thus was more prepared to receive this last flow.

In the upper part of the graph the prediction lines lie significantly above the trend of the data. This could be explained by the buoyancy not being considered as one of the forces acting on the person in the derivations of the models. This produces an unrealistic prediction in situations where the depth is similar to or greater than the subject's height. In such a case, it would be expected that the resistance to being swept away by the flow will reduce to zero, since the available ground-to-footwear friction will disappear. This omission could produce and overestimation of the stability under considerable deep flows. This is addressed for the first time in the following analysis.

### 3.5.1 Influence of buoyancy on stability

The buoyancy force is simply weight of the water displaced by the submerged body. This adds another source of variability in this study, because it depends upon the shape of the human body, changing from person to person, and the clothing could also affect considerable (such as waders and survival suits). Assumptions must therefore be made in order to solve the problem. Figure 3.26 shows a simplification of the shape of the human body with a uniform distribution of its volume over the height of the person. Using this model the buoyancy can be calculated as function of the flow depth, equation 3.8.

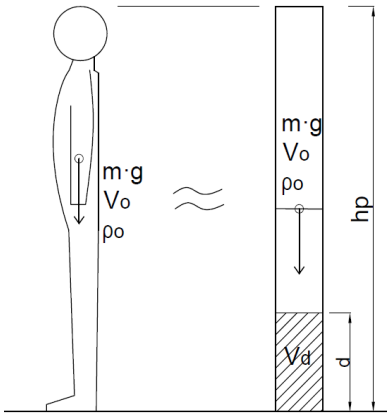


$$V_d(d) = \frac{V_o}{h_p} \cdot d$$

$$V_d(d) = \frac{m}{\rho_o \cdot h_p} \cdot d$$

**Figure 3.26**: Proposed, simplified model of the distribution of a person´s volume with height.

$$Fb(d) = \begin{cases} \dfrac{m}{\rho_o \cdot h_p} \cdot d \cdot \rho \cdot g & for\, 0 \le d \le h_p \\ V_o \cdot \rho \cdot g = \dfrac{m}{\rho_o} \cdot \rho \cdot g & for\, h_p \le d \end{cases} \tag{3.8}$$

where:

$F_b(d)$= buoyancy force as a function of $d$ [N]

$V_d(d)$= submerged volume of the body as a function of $d$ [$m^3$]

$d$ = water depth [m]

$\rho$ = water density [1000 $kg/m^3$]

$g$ = gravitational acceleration [9.81 $m/s^2$]

$m$ = subject´s mass [kg]

$\rho_o$ = density of the human body [≈1,062 $kg/m^3$]

$h_p$ = subject´s height [m]

$V_o$ = total volume of the subject [m]

Including the buoyancy force in the derivation of the model leads to the following expressions:

- **Friction instability for** $0 \le d \le h_p$, (see Figure 3.24 and 3.26)

$$F_f - F_r = 0$$

Now the friction resistance is reduced by the buoyancy force.

$$C_d \frac{\rho}{2} u^2 B d - \mu \cdot \left( m g - V_d \rho g \right) = 0$$

Using the assumption of Figure the $V_d$ can be estimated,

$$C_d \cdot \frac{\rho}{2} \cdot u^2 \cdot B \cdot d - \mu \cdot \left( m \cdot g - \frac{m \cdot d}{\rho_o \cdot h_p} \cdot \rho \cdot g \right) = 0$$

The relation between $u$ and $d$ can now be found:

$$u = \sqrt{C_F \, m} \cdot \sqrt{\frac{1}{d}} \cdot \sqrt{\left( 1 - \frac{d \rho}{\rho_o h_p} \right)} \quad \text{with} \quad C_F = \frac{2 \cdot g \cdot \mu}{\rho \cdot C_d \cdot B} \tag{3.9}$$

- **Moment instability for** $0 \le d \le h_p$, (see Figure 3.24 and 3.26)

$$F_r \cdot d_1 - F_f \cdot \frac{d}{2} = 0$$

As the friction resistance, here the restoring moment is reduced by the buoyancy force.

$$\left( m \cdot g - V_d \cdot \rho \cdot g \right) \cdot d_1 - C_d \cdot \frac{\rho}{2} u^2 \cdot B \cdot d \cdot \frac{d}{2} = 0$$

Now the relation between $u$ and $d$ can be found for the moment instability:

$$u = \frac{2}{d} \cdot \sqrt{\frac{m \cdot g \cdot d_1}{C_d \cdot \rho \cdot B} \cdot \left( 1 - \frac{d \cdot \rho}{\rho_o \cdot h_p} \right)}$$

$$u = \frac{C_M}{d} \cdot \sqrt{m} \cdot \sqrt{\left( 1 - \frac{d \cdot \rho}{\rho_0 \cdot h_p} \right)} \quad \text{with} \quad C_M = 2 \cdot \sqrt{\frac{g \cdot d_1}{C_d \cdot \rho \cdot B}} \tag{3.10}$$

For conditions where the depth is greater than a person's height, d $\geq$ $h_p$, it was considered than a person will not be able to offer any resistance at all against the flow. The new equations derived (equation 3.10) gives, for the first time, a physically rational behaviour for the deepest flows.

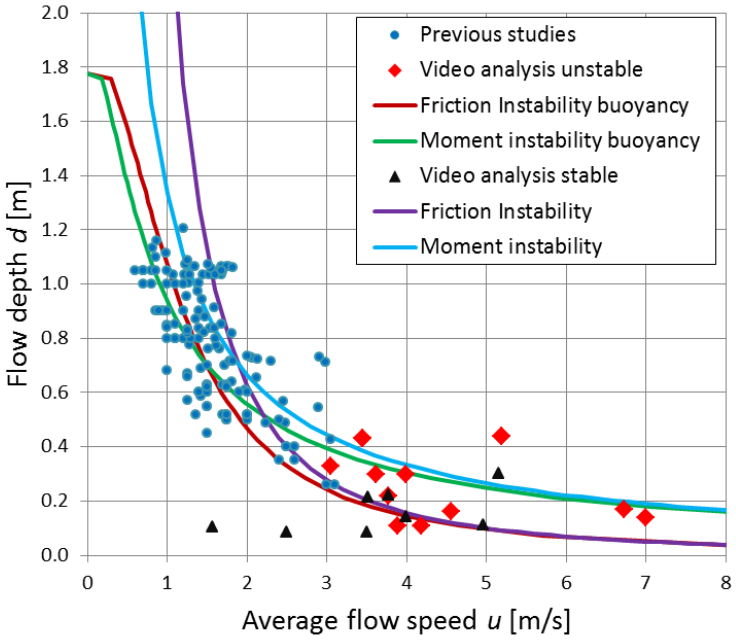


**Figure 3.27**: Comparison of instability prediction regardless buoyancy (purple and blue lines)and considering buoyancy (red and green lines) and data from the video analysis of actual event and the results of studies from literature (Abt *et al*, 1989; Endoh and Takahashi, 1995; RESCDAM, 2001; Jonkman and Penning-Rowsell, 2008). The following assumptions were made: mass = 72.54 kg (average for subjects in figure 3.8); hp=1.76 m. (average for subjects in figure 3.8); B (leg diameter)= 0.2 m; Lf (leg separation)= 0.2·hp; Lg (foot length)= 0.125·hp; fraction coefficient μ=0.62 (wet, smooth concrete, based on Endoh and Takahashi 1995) and ρ (of the water) = 1000 kg/m$^3$.

Figure 3.27 shows the new prediction of the models including the buoyancy force. It can be seen that the new prediction gives a better agreement in the higher part of the graph, now the 70% of the points are well located in the hazardous zone of the graph, which give us the indication that the buoyancy force has a significant effect in the stability of the subjects under deeper waters. Also it is important that the good agreement in lower part of the graph is not lost due to the modification of the equations because in shallow waters, the buoyancy force does not play a significant role in comparison with the person´s weight. It can be seen that above depths of c. 0.4m –around the 20% of a person´s height– the buoyancy force begins to reduce the prediction of the onset of instability to a significant extent. It can also be noted that when the buoyancy force is taken in consideration, the difference between the moment model and the friction model is smaller when $u < u_{tr}$ compared with figure 3.25.

### 3.5.2 Influence of person features on stability

As noted earlier, a wide scatter exists in the data due to the range of characteristics of the subjects used and test conditions. In order to explore that scatter, the data is now separated by gender, so that persons with somewhat more similar characteristics are compared. Separating the data by female and male, and taking for each group the average heights and weights of the samples used in the literature studies (table B.2) gives the results shown in Figure 3.28.

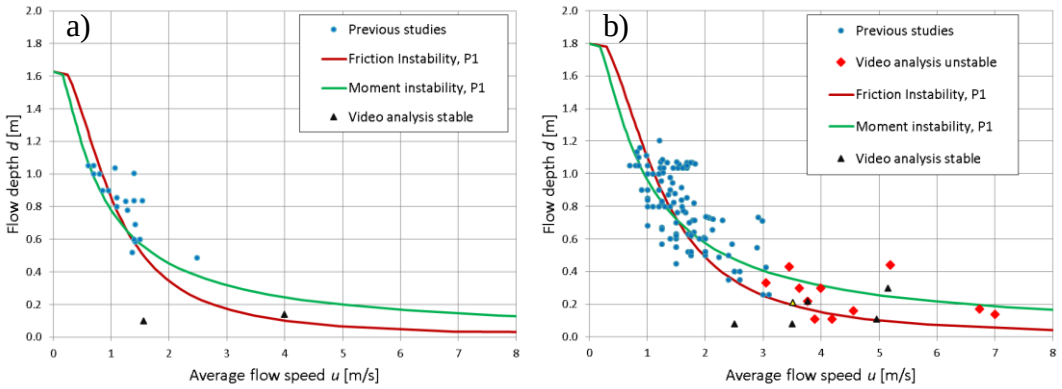


**Figure 3.28:** Comparison of instability prediction considering buoyancy force and data from the video analysis of actual event and the results of studies from literature (Abt et al, 1989; Endoh and Takahashi, 1995; RESCDAM, 2001; Jonkman and Penning-Rowsell, 2008), **a)** female subjects and **b)** male subjects. The following assumptions were made: mass = 49.82 kg (average for females subjects in figure 3.8) and mass = 76.63 kg (average for males subjects in figure 3.8); hp=1.61 m. (average for females subjects in figure 3.8) and hp=1.78 m. (average for males subjects in figure 3.8); B (leg diameter)= 0.2 m; Lf (leg separation)= 0.2·hp; Lg (foot length)= 0.125·hp; fraction coefficient μ=0.62 (wet, smooth concrete, based on Endoh and Takahashi 1995), ρ (of the water) = 1000 kg/m3 and ρo (of the body) = 1062 kg/m3.

From figure 3.28 it can be seen that exist more male data than female. In both graphs it is appreciated a better identification of the hazardous zone, in case of the prediction for female 86% of the point are well located in the graph and 72% case of the male prediction. A bigger scatter is observed in the male graph due to the bigger number of data.

The use of the average height and weight of the sample of the studies may explain why some of the data points that are located in the stable zone although reported as a critical flow situation. In order to obtain a more conservative prediction, the minimum height and weight of the subjects was used instead of the average.

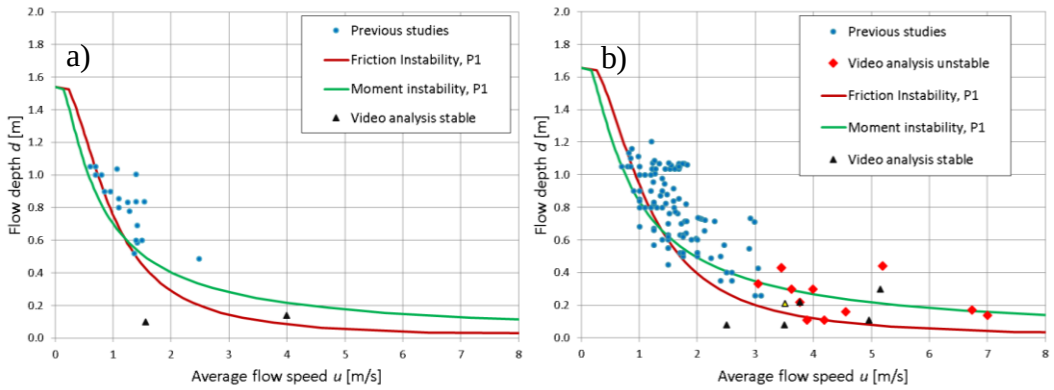


**Figure 3.29:** Comparison of instability prediction considering buoyancy force and data from the video analysis of actual event and the results of studies from literature (Abt et al, 1989; Endoh and Takahashi, 1995; RESCDAM, 2001; Jonkman and Penning-Rowsell, 2008), **a)** female subjects and **b)** male subjects. The following assumptions were made: mass = 40.9 kg (minimum for females subjects in figure 3.8) and mass = 59.1 kg (minimum for males subjects in figure 3.8); hp=1.52 m. (minimum for females subjects in figure 3.8) and hp=1.64 m. (minimum for males subjects in figure 3.8); Wl (leg diameter)= 0.2 m; Lf (leg separation)= 0.2·hp; Lg (foot length)= 0.125·hp; fraction coefficient μ=0.62 (wet, smooth concrete, based on Endoh and Takahashi 1995), ρ (of the water) = 1000 kg/m3 and ρo (of the body) = 1062 kg/m3.

It can be seen (figure 3.29) that considering the minimum height and weight of the subjects a more conservative prediction is obtained. For the female prediction 91% of the critical points are well located in the unstable zone. On the other hand, in the male prediction 90% of the points are correctly located, which represented a significant improvement compared with accuracy in Figure 3.24.

### 3.5.3 Influence of standing position on stability

The influence of the change of position in the resistance to fall by the flow can now, for the first time, be explored *via* an adjustment to the analytical model. A new position more suitable to resist the flow is proposed –see Figure 3.30. In this case, it is supposed that the person reacts to the flow by moving one leg back – thought to be an instinctive reaction of a person in this kind of situation. This response generates a larger distance between the pivot point and the centre of gravity, $d_1$, increasing the restoring moment available. In addition, the projected area exposed to the flow decreases, as only one leg is receiving the drag force directly.

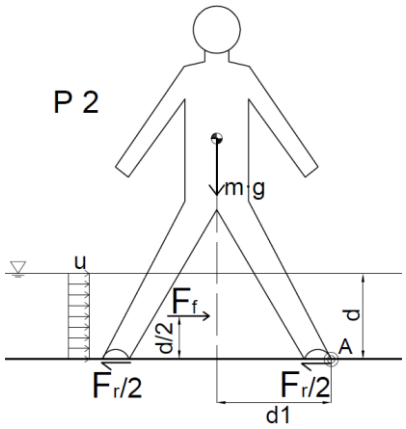


**Figure 3.30**: Stability mechanism, position 2 (P2). Flow from left to right.

From figure 3.31 it can be seen that the change of position from P1 to P2 increase considerably the moment resistance, due to the increase of $d_1$, but it does not have a significant affect on the friction stability model since even though the area against the flow get reduced, the factor Cd increases its value. From this, it follows that the change of position will be more effective in case of deeper-slow flows than in shallow-faster waters. However, the changes to the envelope are not great.

From the comparison with the data, 77% of the points are well located in the unstable zone in the female prediction and 74% in the male prediction. This represents a decrease in the accuracy to predict the hazardous zone in comparison with figure 3.29. This reduction is concentrated in the higher part of the graph where the moment instability is the critical mechanism. Therefore assuming P1 and a person with height and weight equal to the minimum, it is possible to obtain a good and conservative model to predict the potential hazardous flow condition for pedestrians and cyclists.

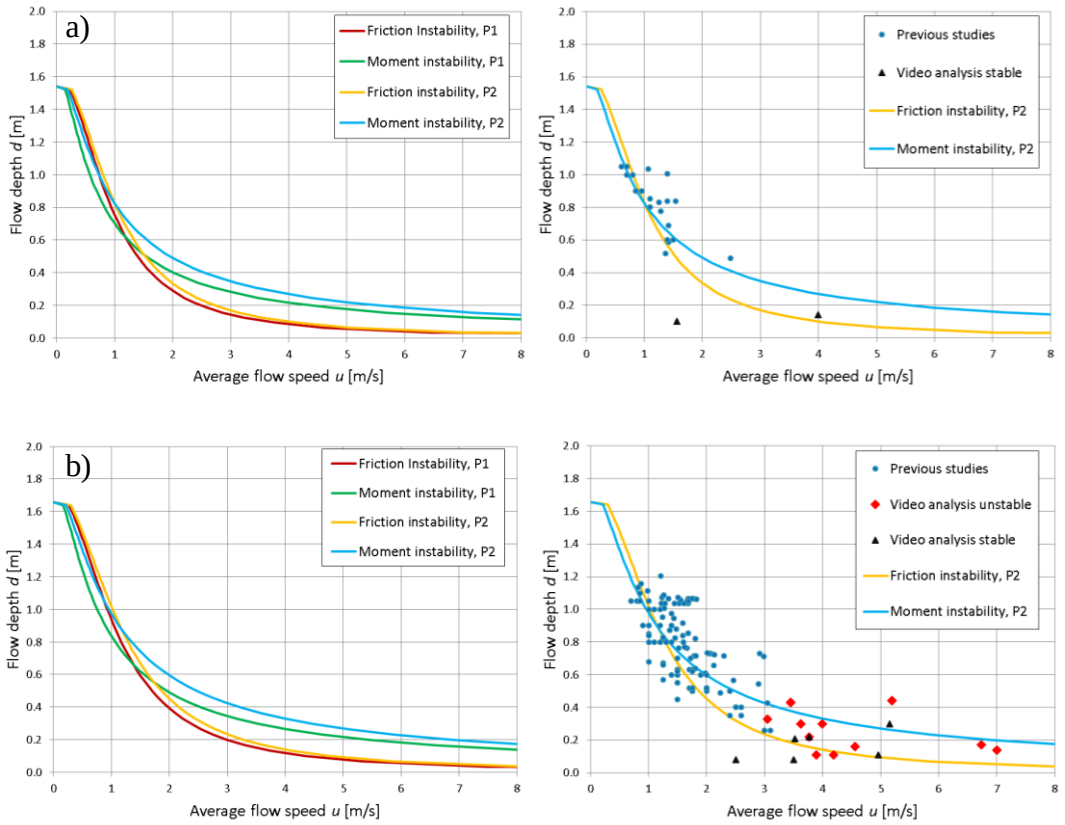


**Figure 3.31**: Comparison of instability prediction between position 1 and position 2, plotted together with data from the video analysis of actual event and the results of studies from literature (Abt *et al*, 1989; Endoh and Takahashi, 1995; RESCDAM, 2001; Jonkman and Penning-Rowsell, 2008). **a)** female subjects and **b)** male subjects. The following assumptions were made: mass = 40.9 kg (minimum for females subjects in figure 3.8) and mass = 59.1 kg (minimum for males subjects in figure 3.8); hp=1.52 m. (minimum for females subjects in figure 3.8) and hp=1.64 m. (minimum for males subjects in figure 3.8); Wl (leg diameter)= 0.2 m; Lf (leg separation)= 0.2·hp; Lg (foot length)= 0.125·hp; fraction coefficient μ=0.62 (wet, smooth concrete, based on Endoh and Takahashi 1995), ρ (of the water) = 1000 kg/m$^3$ and $\rho_o$ (of the body) = 1062 kg/m$^3$.

## 3.6 Chapter conclusions

During the literature review, four important studies related with the human stability under flood flows were found: Abt *et al*. (1989); Endoh and Takahashi (1995); RESCDAM (2001), and Jonkman and Penning-Rowsell (2008). Three of these were conducted in controlled laboratory environments and one under more realistic conditions in an open channel, all of them used human subjects. The flow´s velocity,

$u_{cr}$, and depth, $d_{cr}$, which resulted in the subjects becoming unable to remain stable or move anymore, was recorded. All these results were gathered together in Figure 3.9.

Due to the paucity of data on wave overtopping flows, an extensive video research of human interaction with wave overtopping was conducted; three videos were found with sufficient quality to make a quantitative analysis of the flow parameters. This new and unique data gave and estimation of the velocities and depth which can cause hazard for people in real overtopping accident, Figure 3.19 and 3.20. Overtopping flows with depth between 0.11m and 0.44m and velocities between 3m/s to 7m/s were estimated.

Comparing this videos-derived data against that found in the literature it was found that the last one explore deeper and slower flows than the ones found in the video analysis. No flows faster than 3 m/s were included in the studies reported in the literature, whereas, in stark contrast, flows no slower than 3 m/s were estimated in the wave overtopping flows of the videos. Moreover, the flow depths in most of the literature study's results are much greater than the estimations of the video analysis. It was found that all the accidents that were analysed occurred with flow depths lower than the person's knees, but in the literature tests, some subjects were able to resist flows deeper than one meter.

It was found that the wave overtopping flow events could be very violent, with rapid changes in flow depth and speed. They also appeared to be very turbulent, exposing the person to different flow condition in a very short time. In addition, splashes or jets of water can occur near the defence line, exposing people in a totally different situation than the ones explored in the literature studies. It was seen in the videos that all the people who received the jets water were more easily knock over than the persons who received the flow at the feet level

The reaction of the person also represents a variable in the process. It was observed in the videos that different people respond very differently to a similar situation. Some people run away from the flow; others tried to resist in their position, while others were taken by surprise and did not have time to react at all. All this variability of combinations of flow conditions and human responses make very difficult to generate a model which works well for each one of them. Instead, this implies that a

lowest resistance will need to be considered for design and risk assessment. In video 3 it was observed a tendency that the persons which did not move had a lower resistance to the flow than the persons who run.

Two methodologies to predict which flow conditions could generate a hazard condition were analysed. The first one, Abt. *et al* (1989), proposed a formulation function based upon the height and weight of the person. This model did not give a good agreement with all the data compiled, literature and video analysis. This could be because their model was calibrated only with the results of their own experiment, producing a narrow range of applicability. The second model analysed has a stronger physical rationalisation, identifying two main mechanisms of instability: people will fall due to a lack of friction resistance between footwear and the ground (termed "friction instability"), or because the flow is strong enough to rotate the person around their pivot point (termed "moment instability"). These models are functions of the human´s height and weight, but they also take in consideration the person´s position against the flow and the friction coefficient between the footwear and the ground.

In the present study the second model—"friction and moment instability"— was improved. The buoyancy force was considered, resulting an improvement with a factor of 2.6 in its capability to predict the potential hazardous flows compared with the original formulation. Even though there is no consideration of the violent of the flow in the models (and jets/splash) they can satisfactory predict the unstable zone after considering a conservative scenario: a person standing in front of the flow; smooth and wet concrete and a person with height and weight equal to the minimum of the subjects used in the studies.

Therefore the improved model offers significantly enhanced confidence in the ability to predict the depth and the speed of a hazardous wave overtopping flow. It could thus be possible to forecast a hazard situation for flows that reach a person at the floor level, no water jets, as fluvial flooding, tsunamis or overtopping events composed mainly by green water. In the next chapter the methodology and studies related with the prediction of the overtopping flows are presented.

# Chapter 4

# Wave Overtopping Flow Description

## 4.1 Introduction

In the previous Chapter the stability of humans under overtopping flows was studied and a methodology to predict when a certain flow could destabilize a person was proposed. This was validated with data from analysis of video of real overtopping events and data form previous published studies. This model identifies the velocity ($u$) and the depth ($d$) of the flow as the major hydraulic parameters responsible for knocking over a person. The method is applicable for the cases of overtopping events composed by principally of green waters.

Here first is reviewed one of the methodology more use and validated to design a seadike by wave overtopping, the EurOtop (2007), which gives the method to calculate the basic parameters to describe the overtopping process.

In this chapter it is study the methodologies to predict the overtopping flow depth ($d$) and velocity ($u$)[1] from a wave condition and the geometry of the coastal defence. This is done by the compilation of results of previous study,

The study of wave overtopping has focused primarily in the prediction of the mean discharge ($q$) and the distribution of individual overtopping event volumes ($V$) during a storm. Less attention has taken the study of the wave overtopping flow and its hydraulics parameters as the depth ($d$) the velocity ($u$).

A description of the wave overtopping is presented in this chapter. Three parameters were identified as the main ones to describe an overtopping flow: First is the duration of the overtopping flow ($T_{ovt}$), which is defined as the duration over which the depth is greater than zero at a given section of the protected surface. The next two main

[1] It is noted that the real interpretation of the parameter $u$ is the speed of the flow, but in order to maintain the same notation of the previous studies it will be called velocity.

parameters are the maximum depth ($d$) and velocity ($u$), which occurred within $T_{ovt}$. Relevant literature was found for each parameter but only applicable for seadikes. This information was used to propose a method to describe an overtopping flow in function of the wave condition and the geometry of the seadike.

## 4.2 Existing (EurOtop, 2007) methodology to predict wave overtopping

The study of the wave overtopping has been conducted for many decades. Most recently, improvements to the UK, Netherlands and German guidelines, drawing on previous guidance and research outcomes from projects such as OPTICREST (De Rouck 1998), PROVERBS (Oumeraci 2001), CLASH (De Rouck *et al.* 2009), VOWS (Bruce et al. 2001) have resulted in the most widely accepted and validated guidance brought together in the European Manual on Wave Overtopping (EurOtop, 2007). EurOtop (2007) will be used for all further calculations in this thesis.

Currently the most common way to design by wave overtopping is limiting the volume flow rate, or discharge, of water that will overtop the defence. This methodology implies the calculation of a mean discharge, $q$, per metre structure width during the duration under consideration, typically units of, $m^3/s/m$ of l/s/m. This parameter gives an averaged value, over time, of the wave overtopping within the storm. Due to significant differences of the process between different structures, the study of wave overtopping has been sub-divided by type of coastal defence. EurOtop (2007) classifies the structures into three general categories:

A) Coastal dikes and embankment seawalls

B) Armoured rubble slopes and mound

C) Vertical and steep seawalls.

Due to this thesis is focused in coastal dikes, only its procedure of design will be reviewed.

A coastal dike or seadike is a sloped coastal defence composed by seaward slope, a crest, and a landward slope, Figure 4.1. This are usually used to prevent flooding in

low lands. The surface of this structure is usually covered by concrete, asphalt or grass.

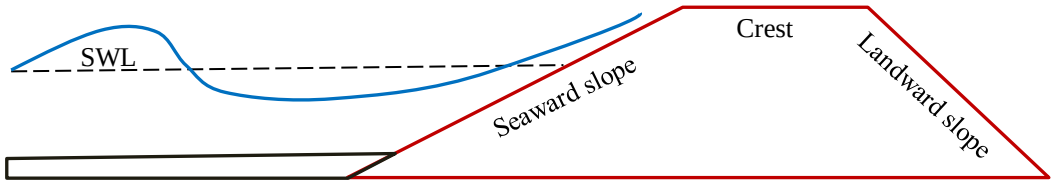


**Figure 4.1**: Typical seadike configuration.

### 4.2.1 Coastal dikes and embankments

The calculation of the run-up, *R*, and the mean discharge, *q*, for coastal dikes and embankment have been developed from empirical formulations calibrated by experimental models and full scale field data. One of the most important conditions that influences the overtopping discharge is the nature of the waves, at the structure - breaking, or non-breaking. For sloping structures, that is characterised by the "breaker parameter" (or "Iribarren number", or "surf similarity parameter"), $\xi_{m-1,0}$. In general a breaker parameter under 1.8 is considered a breaking condition and over 1.8, a non breaking condition.

$$\xi_{m-1,0} = \frac{\tan\alpha}{\sqrt{s_0}} = \frac{\tan\alpha}{\sqrt{H_{m0}/L_0}} \tag{4.1}$$

with: $\xi_{m-1,0}$ = breaker parameter

$L_0$ = deep water wavelength based on $T_{m-1,0}$, $= g\,T_{m-1,0}{}^2/2\pi$ [m]

$\alpha$ = angle of seaward slope [°]

The run-up can be calculated by the following equations:

$$\frac{R_{2\%}}{H_{m0}} = \min\left\{1.65\gamma_b\,\gamma_f\,\gamma_\beta\,\xi_{m-1,0};1.00\gamma_b\,\gamma_f\,\gamma_\beta\left(4.0-\frac{1.5}{\sqrt{\xi_{m-1,0}}}\right)\right\} \tag{4.2}$$

where: $R_{2\%}$ = wave run-up height exceed by the 2% of the incoming waves [m]

$H_{m0}$ = significant wave height from spectral analysis at the toe of the structure [m]

$\gamma_b$ = influence factor for a berm

$\gamma_f$ = influence factor for roughness elements

$\gamma_\beta$ = influence factor of oblique waves

This formula is valid for the range of $0.5 \leq \gamma_b \, \xi_{m-1,0} \leq 8$ to 10.

For the range of breaking waves, $\xi_{m-1,0} < 1.8$, the run-up height increases linearly with the breaker parameter, until the transition to non-breaking waves is reached, from where run up increases more slowly.

Wave overtopping occurs when the run-up is higher than the freeboard ($R_c$), defined as the difference between the still water level (SWL), and the level of the seadike's crest. As for $R_{u2\%}$ equations, the overtopping equations were developed from empirical formulation calibrated with results from experimental models.

The mean overtopping discharge can be calculated with the following equation:

$$\frac{q}{\sqrt{g\,{H_{m0}}^3}} = \min\left\{\frac{0.067}{\sqrt{\tan\alpha}}\,\gamma_b\,\xi_{m-1,0}\exp\left(-4.75\frac{R_c}{H_{m0}\,\xi_{m-1,0}\,\gamma_b\,\gamma_f\,\gamma_\beta\,\gamma_\nu}\right); 0.2\exp\left(-2.6\frac{R_c}{H_{m0}\,\gamma_f\,\gamma_\beta}\right)\right\}$$

$$\text{for } \xi_{m-1,0} < 5 \qquad (4.3)$$

$$\frac{q}{\sqrt{g\,{H_{m0}}^3}} = 10^{-0.92}\exp\left(-\frac{R_c}{H_{m0}\,\gamma_f\,\gamma_\beta\,(0.33+0.022\,\xi_{m-1,0})}\right) \quad \text{for } \xi_{m-1,0} > 7 \qquad (4.4)$$

With: $q$ = mean overtopping discharge [$m^3/s/m$]

$R_c$ = freeboard [m]

$\gamma_\nu$ = correction factor for a vertical wall on the slope

$g$ = gravitational acceleration, = 9.81 [$m/s^2$]

For $5 \leq \xi_{m-1,0} \leq 7$ a linear interpolation between equations (4.3) and (4.4) is recommended.

Like in the run-up equations the mean overtopping discharge depends directly upon the breaker parameter and the characteristics of the dikes.

The effects of the surface roughness ($\gamma_f$), a composite slope ($\gamma_b$), the angle of incident of the incoming waves ($\gamma_\beta$) and the existence of a crest wall ($\gamma_\upsilon$), are present in the equations of the run-up and overtopping discharge by the used of reduction factors. More information can be found in EurOtop chapter 5.

Although *q* is a very useful parameter for design, and gives a good estimation of the requirement that the defence will have to resist, it doesn't give information about the volume of water which will overtop in an individual event. Because q is a mean parameter, several wave conditions could produce the same q, but they can be quite different in the distribution of volume per wave overtopping, producing different overtopping´s flows and therefore different levels of hazard.

It have been demonstrated that the Weibull distribution describes the distribution of individual wave overtopping volumes within a sea state with good agreement to measurements. Equation 4.5 shows the Weibull distribution which depend of two parameters: the scale parameter (*a*) and the shape parameter (*b*). The last gives a lot of information of the distribution during time. Figure 4.2 shows various distributions depending on the value of *b* and it can be seen that steeper curves are generated by lower values of *b*. The distribution of the overtopping volume is described by a steep curve. This is explained because during a storm or surge, the mean overtopping discharge *q*, will be caused by many small volumes and just a few big ones. It have been estimated a b value of the Weibull distribution for waves overtopping are within the range 0.6 and 0.9. For smooth slopes, a constant b value of 0.75 is recommended by the EurOtop (2007). Knowing the duration of a storm, t, and the number of waves that produce an overtopping event, $N_{ow}$, it is possible to describe this irregular process quite well.

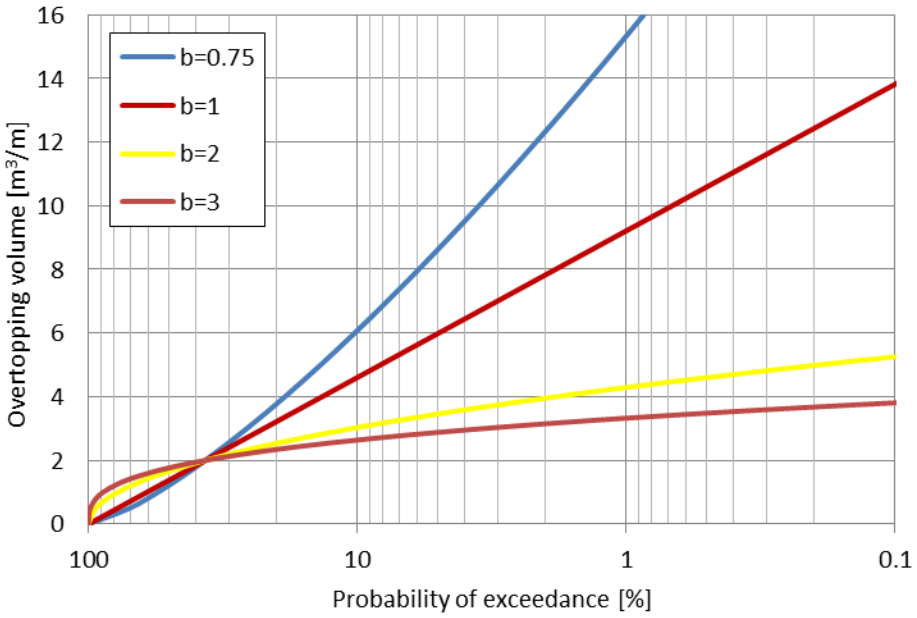


**Figure 4.2**: Probability of exceedance calculated with Weibull with difference values of b.

The non-exceedance probability, $P_v$, of an overtopping volume can be calculated as follow:

$$P_V = P(\underline{V} \le V) = 1 - \exp\left[-\left(\frac{V}{a}\right)^b\right] \tag{4.5}$$

with: $a = 0.84 T_m \frac{q}{P_{ov}} = 0.84 T_m \, q \frac{N_w}{N_{ow}} = 0.84 q \frac{t}{N_{ow}}$ , scale factor (4.6)

$b$ = shape factor, =0.75

$T_m$ = mean wave period [s]

$P_{ov}$ = proportion of waves overtopping, = $\frac{N_{ow}}{N_w}$

$t$ = duration of storm/surge [s]

$N_w$ = number of waves within $t$

$N_{ow}$ = number of waves which produce an overtopping event within $t$.

From equation (4.5) it can be deduced that the maximum volume of overtopping produced by a single wave depends of the duration of the storm, $t$, and the number of overtopping waves, $N_{ow}$ can be calculated by:

$$V_{\max} = a\left[\ln N_{ow}\right]^{4/3} \tag{4.7}$$

Knowledge of the maximum single-event overtopping volume that will occur during a storm it is a very useful tool in order to estimate the hazard and consequences that could happen, but this formulation still gives no information about the flow that this volume will produce. For the same value of volume, quite different flows could happen, generating different level of hazard, *e.g.*: green water with a long duration is less dangerous than green water with a short duration, because in the in the latter case, a deeper and faster flow is expected.

The EurOtop (2007) includes a methodology to estimate the overtopping flow depth and the overtopping flow velocity. These formulae were calibrated with experimental tests at small and large scale, with sloped structures (Schüttrumpf *et al*. 2002).The run-up flow depth at the seaward slope ($h_A$) is assumed to decrease linearly from SWL to the run-up height (figure 4.3). Thus the depth on the seaward slope can be calculated as function of the horizontal position $x_A$, in Figure 4.3. Subsequently over the width of the dike crest ($B_C$) the overtopping depth ($h_C$) decreases as an exponential function (Figure 4.4).

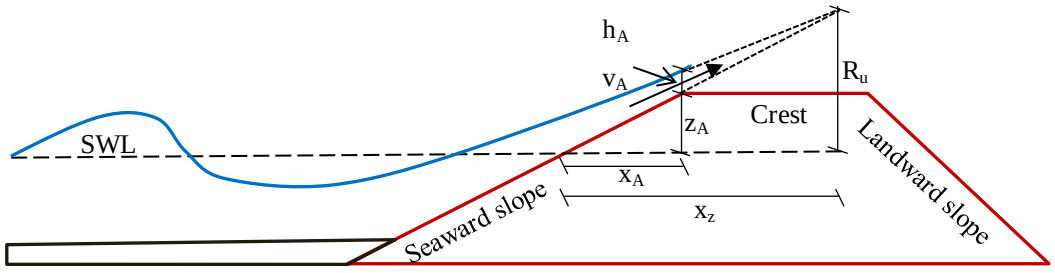


**Figure 4.3**: Flow depth changes and velocity on seaward slope according to EurOtop (2007).

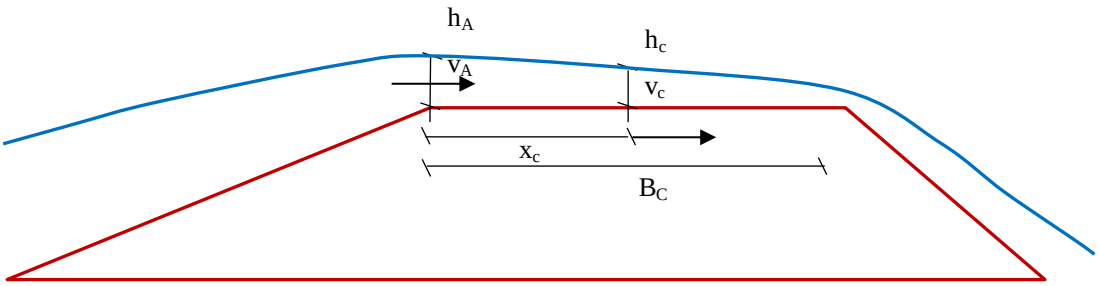


**Figure 4.4:** Flow depth changes and velocity on dike´s crest according to EurOtop (2007).

$$h_A(x^*) = c_2 (x_z - x_A) = c_2\, x^* \tag{4.8}$$

$$\frac{h_c(x_c)}{h_c(x_c=0)} = \frac{c_2(x_c)}{c_2(x_c=0)} = \exp\left(-c_3 \frac{x_c}{B_c}\right) \tag{4.9}$$

The coefficient $c_2$ was calibrated for different probabilities of exceedance, table 4.1 and $c_3$ has a value of 0.89 for TMA spectra, and 1.11 for natural wave spectra.

**Table 4.1:** Values of the coefficient $c_2$. EurOtop (2007).

| | **$c_2$** | **σ'** |
|---|---|---|
| **$h_{A,50\%}$** | 0.028 | 0.15 |
| **$h_{A,10\%}$** | 0.042 | 0.18 |
| **$h_{A,2\%}$** | 0.055 | 0.22 |

The velocity at the seaward slope ($v_A$) and on the dike crest ($v_C$) were deducted from a simplified energy equation and the simplified Navier-Stokes equation, respectively and calibrated by experimental tests.

$$\frac{v_A}{\sqrt{gH_s}} = a_0^* \sqrt{\frac{(R_{u2\%} - z_A)}{H_s}} \tag{4.10}$$

$$v_C = v_{C(xc=0)} \exp\left(-\frac{x_c\, f}{2\, h_c}\right) \tag{4.11}$$

with: $H_s$ = significant wave height [m]

$f$ = friction factor =0.01 for smooth structures

The coefficient $a_0^*$ was calibrated for different probabilities of exceedance, table 4.2.

**Table 4.2**: Values of the coefficient $c_0^*$. EurOtop (2007).

| | $a_0^*$ | **σ'** |
|---|---|---|
| $\mathbf{v_{A,50\%}}$ | 1.03 | 0.23 |
| $\mathbf{v_{A,10\%}}$ | 1.37 | 0.18 |
| $\mathbf{v_{A,2\%}}$ | 1.55 | 0.15 |

## 4.3 General description of wave overtopping flow

Since the earliest 2000s, studies have used physical model tests with the aim of analysis of the flow generated by a wave overtopping event and its influence in the failure mechanism of seadikes. The velocity and the depth of the flow are the main parameters investigated and recorded, generating good information to make a satisfactory description of the wave overtopping flows.

A wave overtopping event will start when the water overpass the seaside of the crest and then the flow will decrease its velocity and depth until it reach the landward slope, where it will increase again its velocity but probably will experience a stretching decreasing its depth. In an overtopping event the predicted run-up height, $R$, is higher than the freeboard, $R_c$, thus it is a virtual run-up.

The present study is focus in the direct hazard for pedestrians, being the crest of the dike the most common area where they can be reached by wave overtopping flows, where coastal path probably will be, thus the theory and findings for the landward slope were not analysed.

In general a wave overtopping flow composed of mainly green water can be imagined to have three stages within its duration. The first one consists of a very rapid increase of flow depth and velocity, which finishes when the maximum values of these parameters are reached. The second stage is this fully developed wave

overtopping flow. In the third stage the flow depth and velocity decrease from the developed flow to zero, with this change being more gradual than the first stage. From the video analysis conducted in the previous chapter and the measurements found in the literature, e.g.: Figure 4.1, three general aspects were observed: Firstly the time which the maximum depth and velocity are (more or less) sustained is very short for large overtopping volumes and longer for small and moderate wave overtopping, *u* and *d* reached their maxima almost at the same time and finally this maximums occur very at the beginning of the flow, showing that these maxima is a very violent flow.

No study has taken the description of the discharge's curves *u(t)* and *d(t)* as its principal aim. Three main parameters are identified here as necessaries to describe an overtopping flow: the maximum flow depth ($d_{max}$), the maximum velocity ($u_{max}$), and the overtopping duration ($T_{ovt}$).

Based on records of *d* and *u*, of previous studies (Schüttrumpf *et al*. (2002), Van Gent (2002), Bosman *et al.* (2007) suggested a triangular shape for the variation of the depth and the velocity, with the flow´s changes described as linear with time (continuous line in Figure 4.6). Due to the short time observed in the data analysed the first stage was omitted, therefore the overtopping flow start with the maximum velocity and depth. In a more recent study, Hughes *et al.* (2012), an analytical analysis was conducted and a relation between the shape of the discharge and the volume was proposed. It was suggested that an increase of the overtopped volume will generated a more convex discharge (shows as the segmented line in Figure 4.6). This was explained because in small overtopping events most of the energy will be dissipated on the seaward slope but, in larger events, the flow will have enough energy to reach the crest with a violent flow. This hypothesis can be checked in Figure 4.5, where it can be seen that the singular events where higher maxima are reached, more convex curves are discernible.

Few studies have analysed the wave overtopping duration ($T_{ovt}$) which is taken as the time that the wave overtopping flow takes to pass a certain section of the coastal defence. In a realistic, three-dimensional setting, this time can vary across the width of the crest due to the flow´s deformation. It is expected that the shortest $T_{ovt}$ will

occur near the seaside of the crest, where the most violent flow changes can occur, with longer $T_{ovt}$ at the land side of the crest where a more gradual flow is expected. In general, for coastal defences with freeboard higher than zero it is expected that the overtopping duration should be no longer that the wave period. Overflows conditions are not being considered in this study.

The parameters which have been most studied are $d_{max}$ and $u_{max}$ but, their understanding is restricted, with methodologies only applicable to seadikes.

In the following sections, a more extensive analysis of the findings for each parameter is presented, information which will be used to define a method to predict and characterise a wave overtopping flow.

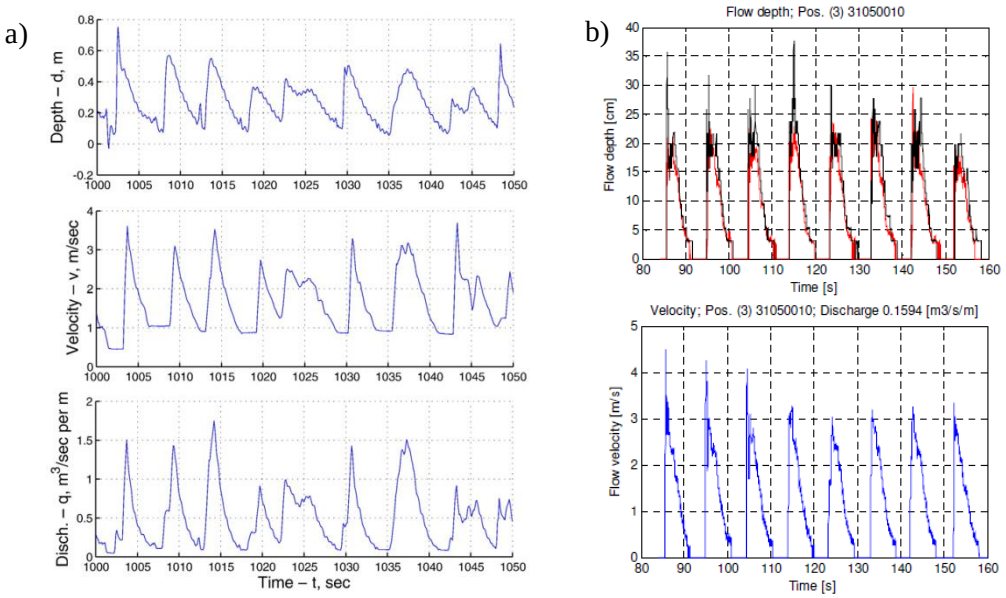


**Figure 4.5:** Examples of measured overtopping flow´s depth and velocity on the crest of a model seadike. Sources: a) Hughes and Nadal (2009), b) Generated by Bosman (2007) and data from Van Gent (2002).

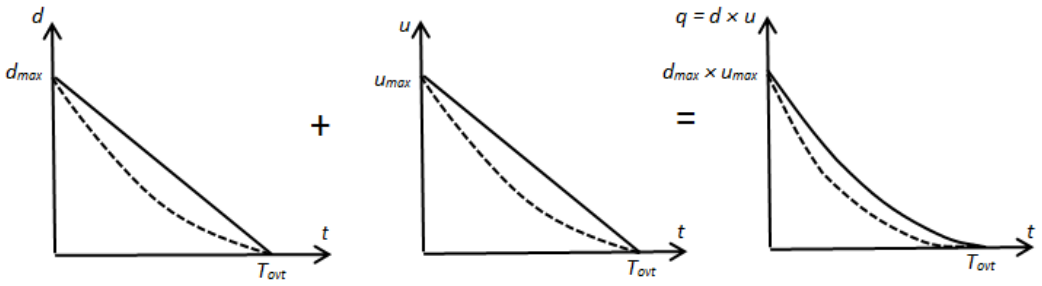


**Figure 4.6**: Records of overtopping flows on the crest of a model seadike, Hughes and Nadal (2009), and simplified model for and individual overtopping event.

## 4.4 Overtopping flow depth and velocity

Three important studies were found in this area: Schüttrumpf *et al*. (2002); Van Gent (2002) and Schüttrumpf and Oumeraci (2005). These projects had similar aims: analyse the principal hydraulic parameters of the wave overtopping flows which are responsible of the failure of a seadike. The run-up and overtopping flows were studied using physical models; the velocity and the thickness (depth) of the water were measured from scale models.

The three studies used the same conceptual analytical model to describe the process of run-up and wave overtopping (Figure 4.7). It was assumed that the water depth, or thickness, decreases linearly on the seaward slope from a maximum at the sea water level (SWL) to zero at the run-up height ($R_c$), equation 4.12.

$$d(z) = c_d \cdot \left(R_{2\%} - z\right) \tag{4.12}$$

For the crest of the dike an exponential function was adjusted to the deformation of the depth across its width, equation 4.13.

$$d_c(x_c) = d(z = R_c) \cdot \exp\left(-c_{dc} \cdot \frac{x_c}{B}\right) \tag{4.13}$$

It is assumed that the initial depth at the seaside of the crest, $d_c(x_c=0)$, it is equal to the final depth of the run-up calculated with equation 4.12 when $z=R_c$, therefore the maximum depth always will be at the initial part of the crest.

From a simplified energy equation, the expression to describe the changes of the run-up velocity on the seaward slope was derived (Schüttrumpf and Oumeraci 2005), equation 4.14. This equation intends to predict the maximum run-up velocity of the front of the flow that occurs in an individual event at any position of the seaward slope. As the depth the velocity has its maximum value at the SWL and becomes zero at the run-up height.

$$\frac{u(z)}{\sqrt{g}} = c_u \cdot \sqrt{(R_{2\%} - z)} \tag{4.14}$$

In order to describe the change of the velocity on the crest an exponential equation was derived, equation 4.15, based on a two-dimensional continuity analysis and momentum equation for an incompressible flow (Schüttrumpf and Oumeraci 2005).

$$u_c(x_c) = u(z = Rc) \cdot \exp\left( - c_{uc} \frac{x_c \cdot f}{d_c(x_c)} \right) \tag{4.15}$$

Like the depth behaviour, the velocity across the crest decreases from a maximum, equal to the final run-up velocity calculated with equation 4.14 for $z = R_c$, to a minimum at the landside, meaning that the maximum velocity is always at the seaside of the crest.

In this model, the depth and the velocity decrease while the flow moves across the crest, behaviour which can be misunderstood as loss of volume in the equations, but this is explained due to the flow´s deformation along the crest, which is a 3D phenomenon not considered in the deduction of the equation but reflected in the coefficient $-c_{dc}$ calibrated with the test results.

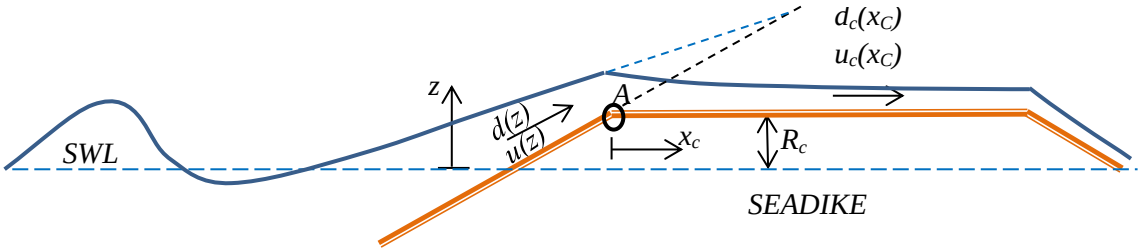


**Figure 4.7**: Run-up and wave overtopping flow deformation on a seadikes, Based on Schüttrumpf (2001).

With: $d(z)$ = Maximum run-up flow depth at z for the individual run-up event [m]

$d_c(x_c)$ = Maximum wave overtopping flow depth on the crest at $x_c$ [m]

$u(z)$ = Maximum front overtopping velocity on seaward slope at $z$ [m/s]

$u_c(x_c)$ = Maximum front overtopping velocity on crest at $x_c$ [m/s]

$R_{2\%}$ = 2% exceedance run-up for the individual event [m]

$B$ = Crest width [m]

$f$ = Friction coefficient = 0.01 for smooth slope

$c_d$ = Coefficient for the run-up depth [-]

$c_{dc}$ = Coefficient for the overtopping depth at the seadike crest [-]

$c_u$ = Coefficient for the run-up velocity [-]

$c_{uc}$ = Coefficient for the overtopping velocity at the seadike crest [-]

These set of equations were then calibrated in each reported project. In Schüttrumpf *et al*. (2002) measurement from a large scale model were used, whereas in Van Gent (2002) and Schüttrumpf and Oumeraci (2005) results from small models were used.

Equations 4.12 and 4.14 require the calculation of the 2% exceedance run-up height, $R_{2\%}$. This was calculated using different formulations in each study. Schüttrumpf *et al.* 2002 estimated the run-up height according to the following hyperbolic function, equation 4.16[2]:

$$\frac{R_{2\%}}{\gamma_f \cdot \gamma_\beta \cdot H_{m0}} = 3 \cdot \tanh(0.65 \cdot \xi_0) \qquad \text{(Schüttrumpf 2001)} \qquad (4.16)$$

[2] Original source (Bosman 2007) used $H_s$ instead of $H_{m0}$ in equation 4.16.

with: $R_{2\%}$ = Run-up with a 2% of exceedance [m]

$\xi_0$ = Breaker parameter [-]

$H_{m0}$ = Significant wave height from spectral analysis [m]

$\gamma_\beta$ = Reduction factor due to angled wave attack [-]

$\gamma_f$ = Reduction factor due to roughness of the surface [-]

On the other hand Schüttrumpf and Oumeraci (2005) based the run-up calculation on Hunt (1959) formulation, (4.17)[3].

$$\frac{R_{2\%}}{H_{m0}} = c_1 \cdot \xi_0 \qquad for\ \xi_0 \le \xi_{tr} = 2 \qquad \text{(Hunt 1959)} \qquad (4.17)$$

$$\frac{R_{2\%}}{H_{m0}} = 3 \qquad for\ \xi_0 > \xi_{tr} = 2$$

With $c_1$ = 1.5 for irregular waves and $\xi_{tr}$ the breaker parameter transition between breaker and non breaker condition.

A different run-up formulation was used in Van Gent (2002) who based its calculation on equation 4.18[4]:

$$\frac{R_{2\%}}{H_{m0}} = c_0 \cdot \xi_{S,-1} \qquad for\ \xi_{S,-1} \le p \qquad \text{(Van Gent 2002)} \qquad (4.18)$$

$$\frac{R_{2\%}}{H_{m0}} = c_1 - \frac{c_2}{\xi_{S,-1}} \qquad for\ \xi_{S,-1} \ge p$$

with: $c_0 = 1.35$

$c_1 = 4.7$

$$c_2 = 0.25 \cdot \frac{{c_1}^2}{c_0} = 4.1$$

$$p = 0.5 \cdot \frac{c_1}{c_0} = 1.74$$

[3] Original source (Schüttrumpf and Oumeraci 2005) used $H_s$ instead of $H_{m0}$ in equation 4.17.
[4] Original source (Van Gent 2002) used $H_s$ instead of $H_{m0}$ in equation 4.18.

In Figure 4.8 these three run-up predictions plus the one recommended in EurOtop (2007), equation 4.2, are plotted together. It can be seen that significant differences exist between the functions, being more similar for breaking parameter under 1.8. For non-breaking conditions, $\xi > 1.8$, the differences are greater. It is especially notable that the Van Gent (2002) function shows the higher trend of all methods. In general, it is apparent that the methodologies which have most similarity over a wide range of breaker parameter are the Hunt (1959) formulas used in Schüttrumpf and Oumeraci (2005) and the formula given in EurOtop (2007).

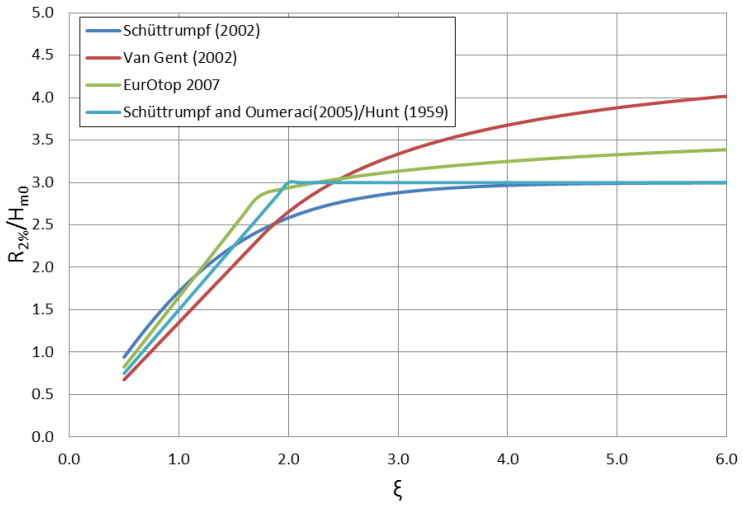


**Figure 4.8:** Run-up methodologies plotted together used in Schüttrumpf *et al.* (2002), Van Gent (2002), Schüttrumpf and Oumeraci (2005) (Hunt 1959) and EurOtop (2007).

### 4.4.1 Schüttrumpf *et al.* (2002) and Schüttrumpf and Oumeraci (2005) research project

In this studies a series of experiments were conducted using small models and a large model. The large scale model tests, Schüttrumpf *et al.* (2002), were conducted in the Grosse Wellen Kanal (GWK), at the Coastal Research Centre (FZK), Hannover, Germany. The flume is 324 m long, 5 m wide and 5 m deep. Waves between 0.4 m and 1.2 m height with period from 2.5 s to 8.0 s were generated, around 200 waves for each test. Regular and irregular waves were tested. Schüttrumpf and Oumeraci (2005) tests were carried out in a medium-scale flume, 100 m long, 2 m wide and 1.25 m deep, at the Leichtweiß-Institute (LWI) of the Technical University of Braunschweig, Germany. Waves with significant heights between 0.08 m and 0.2 m

and period of 1.5 s to 6 s were generated by a flat type paddle. Only short sequences of waves were generated, around 50 waves, in order to avoid interference with the reflected waves. Regular and irregular waves were used. The general characteristic of the models and instrument used are presented in Figure 4.9 and in table 4.3

The water depth, *d*, and the velocity, *u*, of the flow were measured on the dike´s crest and on the landward slope. This data was used to calibrate the equations (4.13), (4.15), (4.19) and (4.20).

**Table 4.3**: General characteristic of Schüttrumpf *et al.* (2002) and Schüttrumpf and Oumeraci (2005) set-ups.

| **Model** | **$h_s$ [m]** | **$H_{m0}$ [m]** | **$T_{m0}$ [s]** | **$R_c$ [m]** | **Seaward slope** | **$B$ [m]** | **Landward slope** | **Velocity measurement** | **Depth Measurement** |
|---|---|---|---|---|---|---|---|---|---|
| Small | 0.6-0.8 | 0.08-0.2 | 1.5-6.0 | 0.0-0.2 | 1:6, 1:4, 1:3 | 0.3 | 1:6, 1:5, 1:4, 1:3, 1:2 | Micro Propellers D=3mm. Video recording | Wave gauges Video recording |
| Large | 4.25-5 | 0.4-1.2 | 2.5-8.0 | 1.0-1.75 | 1:6 | 2.0 | 1:3 | Propellers D=1.5, 2.2cm. Video Recording | Depth gauges Pressure cells Video recording |

Note: $h_s$: Water depth at the toe of the structure, $H_{m0}$: Significant wave height from the spectral analysis, $T_{m0}$: Significant wave height from the spectral analysis, $R_c$: Freeboard, $B$: crest wide.

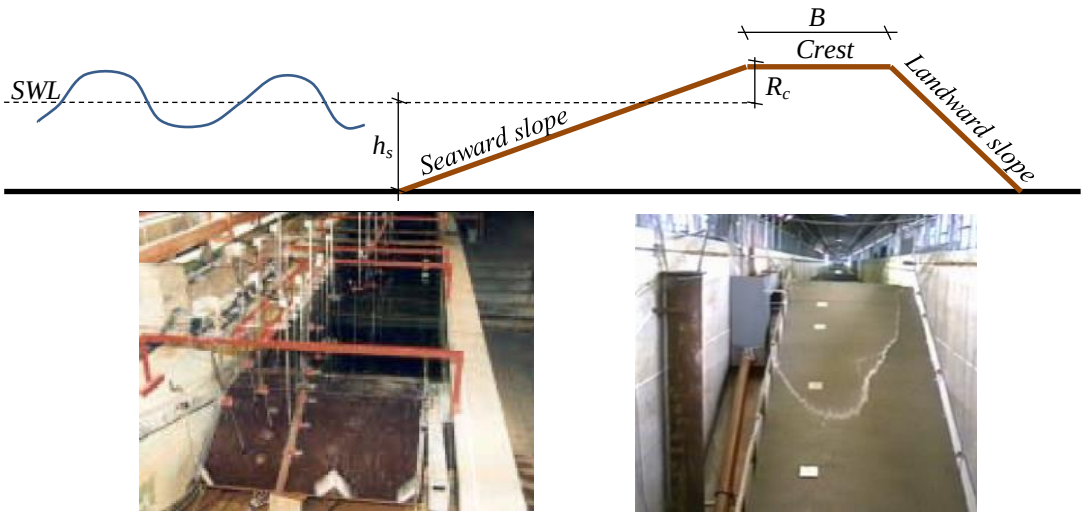


**Figure 4.9**: General layout dike model used by Schüttrumpf *et al*. (2002). Source: Schüttrumpf *et al.* (2002) and Bosman (2007).

The behaviour of the run-up flow was assumed as in Figure 4.7, but slightly different equations of 4.12 and 4.14 were used to estimated *d* and *u* on the seaward slope, 4.19 and 4.20. This time *d* were calculated upon its horizontal position (*x*) on the seaward slope instead of the vertical position (*z*).

$$d(x) = c_2 \left(X_R - x\right) = c_2 \cdot \frac{1}{\tan\alpha}\left(R_{2\%} - z\right) \tag{4.19}$$

In the equation of the velocity now the breaker parameter was included[5].

$$\frac{u(z)}{\left(\frac{\pi \cdot H_{m0}}{T_m}\right)} = a_0^* \cdot n \cdot \xi_0 \cdot \sqrt{\frac{R_{2\%} - z}{H_{m0}}} \quad \text{with} \quad \xi_0 = \xi_0 \frac{\tan\alpha}{\sqrt{H_{m0} / L_0}} \tag{4.20}$$

with: $d(x)$ = Maximum run-up flow depth at x for the individual run-up event [m]

$d_c(x_c)$ = Maximum wave overtopping flow depth on the crest at $x_c$ [m]

$u(z)$ = Maximum front overtopping velocity on seaward slope at *z* [m/s]

$u_c(x_c)$ = Maximum front overtopping velocity on crest at $x_c$ [m/s]

$X_R$ = Horizontal position of the run-up [m]

$\alpha$ = Seaward angle [°]

$n$ = Seaward slope = *1/tanα*

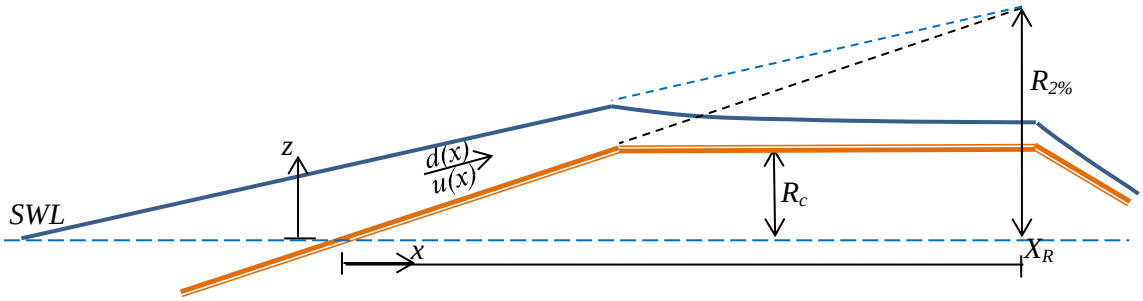


**Figure 4.10:** General layout dike model used by Schüttrumpf *et al*. (2002). Source: Schüttrumpf *et al.* (2002) and Bosman (2007).

The coefficients $c_2$, $c_0^*$, $c_{dc}$ and $c_{uc}$ were calibrated for different probability of exceedance, tables 4.4 and 4.5.

[5] Original source (Schüttrumpf *et al*. 2002) used $H_s$ instead of $H_{m0}$ in equation 4.9.

**Table 4.4**: $c_2$ and $c_{dc}$ values calibrated with different probability of exceedance. Schüttrumpf *et al.* (2002) and Schüttrumpf and Oumeraci (2005).

| | $c_{2,50\%}$ | $c_{2,10\%}$ | $c_{2,2\%}$ | $c_{dc}$ | Model | Seaward slope |
|---|---|---|---|---|---|---|
| Schüttrumpf et al (2002) | 0.028 | 0.042 | 0.055 | 0.89±0.06 | Large scale | 1:6 |
| | 0.028 | -- | -- | -- | Small scale | Not mentioned |
| Schüttrumpf and Oumeraci (2005) | 0.042 | -- | 0.054 | 0.75 | Small scale | 1:4 |
| | 0.028 | -- | 0.035 | | Small scale | 1:6 |

**Table 4.5:** $c_0^*$ and $c_{uc}$ values calibrated with different probability of exceedance. Schüttrumpf *et al.* (2002) and Schüttrumpf and Oumeraci (2005).

| | $a_{0,50\%}^*$ | $a_{0,10\%}^*$ | $a_{0,2\%}^*$ | $c_{uc}$ | Model | Seaward slope |
|---|---|---|---|---|---|---|
| Schüttrumpf et al (2002) | 0.82 | 1.09 | 1.24 | 0.5 | Large scale | 1:6 |
| | 0.75 | -- | -- | -- | Small scale | Not mentioned |
| Schüttrumpf and Oumeraci (2005) | 0.75 | -- | -- | 0.5 | Small scale | 1:4 |

In table 4.4, for the parameter $c_2$ with 50% of probability of exceedance an excellent agreement between the results of the small models and the large model can be seen, but with 2% of probability of exceedance and for a slope of 1:6 there is a significant difference between the large and small results. This could be a sign of: scale effects (more experiments are needed in order to verify this), or also it could be a result of the different run-up equations used in this two projects, equations (4.16) and (4.17).

In addition the influence of the seaward slope in the value of the coefficient $c_2$ was examined and it was found that its value is a function of the slope angle, being $c_2 \cdot 1/\tan\alpha = cte$.

$$c_{d,50\%} = 0.042\times(4/1) = 0.168 \;=\; 0.028\times(6/1) = 0.168 \;\Rightarrow \overline{c_{d,50\%}} = 0.168$$
$$c_{d,2\%} = 0.054\times(4/1) = 0.216 \;\approx\; 0.035\times(6/1) = 0.21 \;\Rightarrow \overline{c_{d,2\%}} = 0.213$$

### 4.4.2 Van Gent (2002) research project

Similar project was carried out by Van Gent. A series of small model test were conducted in a wave flume of 55 m long, 1 m wide and 1.2 m height at the WL/Delft Hydraulics, The Netherlands. The waves generated had significant height between

0.13 m to 0.15 m, with a peak period within 1.59-2.51 s. Regular and irregular conditions with 1,000 waves were generated.

**Table 4.6**: General characteristic of Van Gent 2002 tests.

| Model | $h_s$ [m] | $H_{m0}$ [m] | $T_{m0}$ [s] | $R_c$ [m] | Seaward slope | $B$ [m] | Landward slope | Velocity measurement | Depth Measurement |
|---|---|---|---|---|---|---|---|---|---|
| Small | 0.3-0.5 | 0.13-0.15 | 1.5-2.5 | 0.1-0.3 | 1:4 | 0.2-1.1 | 1:2.5, 1:4 | Micro Propellers D=10mm. | Depth gauges |

The flow and velocity of the run-up and overtopping flows were measured on the dike crest and on the landward slope. With this data the coefficient of the equations (4.12), (4.13), (4.14) and (4.15) were calibrated. In this case Van Gent worked directly with the equations (4.12) and (4.14) so the coefficients $c_d$ and $c_u$ were calibrated, obtaining parameters which were not dependent upon the seaward slope. The coefficients founds are presented in table 4.7.

The main equations used by Van Gent are presented in equation (4.21) to (4.24)[6].

$$d_{2\%}(z) = c_d \frac{(R_{2\%} - z)}{\gamma_f} \tag{4.21}$$

$$d_{c,2\%}(x_c) = d(z = R_c) \cdot \exp\left(-c_{dc} \cdot \frac{x_c}{B}\right) \tag{4.22}$$

$$\frac{u_{2\%}(z)}{\sqrt{g \cdot H_{m0}}} = c_u \cdot \sqrt{\left(\frac{R_{2\%} - z}{\gamma_f \cdot H_{m0}}\right)} \tag{4.23}$$

$$u_{2\%}(x_c) = u_{2\%}(z = R_c) \cdot \exp\left(-c_{uc} \frac{x_c \cdot f}{d_{c,2\%}(x_c)}\right) \tag{4.24}$$

**Table 4.7**: $c_d$, $c_{dc}$, $c_u$ and $c_{uc}$ values calibrated with 2% probability of exceedance in Van Gent (2002).

| Model | $c_{d,2\%}$ | $c_{dc}$ | $c_{u,2\%}$ | $c_{uc}$ | Model | Seaward slope |
|---|---|---|---|---|---|---|
| Van Gent (2002) | 0.15 | 0.15 | 1.3 | 0.75 | Small scale | 1:6 |

[6] Original source (Van Gent 2002) used $H_s$ instead of $H_{m0}$ in equation 4.23.

### 4.4.3 Comparison of results

Very similar analytical and experimental methodologies were used in these studies but, quiet different results were found in some aspects. Due to different run-up equations were used in each study, Figure 4.8, it is not appropriate to compare, simply the value of the coefficients for each seaward slope. Instead, it will be more informative to compare the predictions of the depth and velocity for each study using the run-up equation used for the calibration of particular coefficient. In Figure 4.11 the predictions of dimensionless depth and velocity with a 2% of exceedance are presented for the seaward side of the crest, where the most critical conditions are expected.

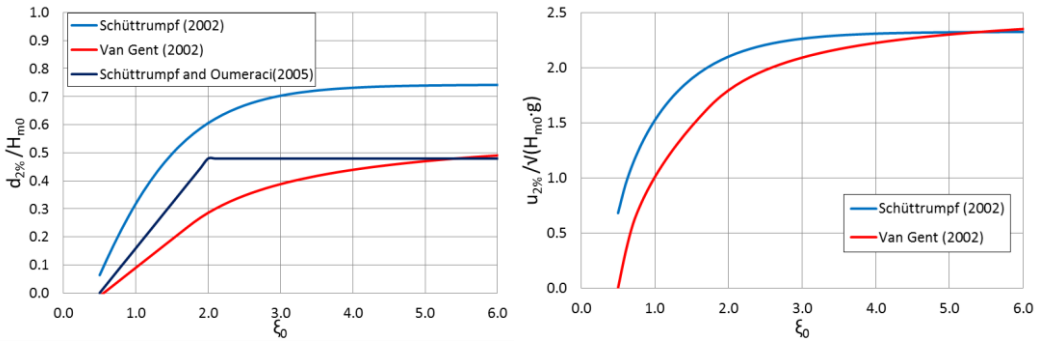


**Figure 4.11:** Prediction of the initial dimensionless wave overtopping flow depth, $d_{2\%}$, and dimensionless velocity,$u_{2\%}$, with a 2% of exceedance based on Schüttrumpf *et al.* (2002), Van Gent (2002), Schüttrumpf and Oumeraci (2005). For $R_c/H_{m0}$=0.75.

From figure 4.11 it can be seen that a significant differences exist in the predictions, with these being more significant for the depth than for the velocity. In both cases Van Gent´s predictions are the smaller. For $d_{2\%}$ it can be seen that the methodologies calibrated with small models, Van Gent (2002) and Schüttrumpf and Oumeraci (2005), produce similar predictions while the one calibrated with results of the large model, Schüttrumpf *et al.* (2002) are significantly different. On the other hand, the predictions for $u_{2\%}$ are significantly closer to each other, with the prediction with the small scale study again the lowest. These differences could be related to different experiments set-ups (Schüttrumpf and Van Gent 2003) or a sign of scale effects, although more tests are needed to explore this fully.

### 4.4.4 Bosman *et al*. (2007)

In Bosman (2007), a complete analysis of the procedures and part of the data obtained in Schüttrumpf et al. (2002) and Van Gent (2002) was made. It was found that the tests were carried out correctly but some possible underestimation could exist in the velocity measurement done in Schüttrumpf et al. (2002). These problems were detected because the maximum velocities recorded by the propeller on the crest, which were used to calibrate the coefficients (table 4.2 and 4.3), were smaller than mean velocities of the front of the flow, but it should be the opposite. A similar effect was not found on the measures done on the inner slope. Taking in consideration this finding, it seems possible that the prediction of the velocity by Schüttrumpf formula in Figure 4.6 should be higher, which would be in line with the difference existing in the depth predictions.

Bosman also recalculated the coefficients, $c_2$, $a_0^*$, $c_{dc}$ and $c_{uc}$, with the part of the data available, finding very similar values to the ones shown in tables 4.3, 4.4 and 4.5. Differences can be attributed to the incomplete data used. In this thesis, only the values derived in the primary sources will be used due to their having been calculated with the complete Schüttrumpf *et al.* (2002) and Van Gent (2002) dataset.

A more recent methodology was proposed in Bosman *et al*. (2007) who, using part of the data compiled during Schüttrumpf *et al*. (2002) and Van Gent (2002), proposed new values for $c_2$, $a_u$, $c_{dc}$ and $c_{uc}$.

Bosman carried out analysis based upon the run-up physics, suggesting that those coefficients have to depend on the slope of the dike an aspect that could explain the differences on the values estimated in the previous studies, which were carried out with different slopes, 1:6 and1:4 (Figure 4.11).

For the seaward slope the same equations of (4.12) and (4.14) were found to describe the process quite well, but new coefficients function of the *sine* of the seaward slope were calibrated. New formulations were proposed to describe the change of depth and velocity on the crest, equation (4.25) and (4.26). These new equations included a transition coefficient, $c_{trans}$, which intends to include the reduction of the flow depth when it passes from a sloped surface to a horizontal one. Therefore now the initial flow depth of the overtopping flow is not equal to the one calculated by equation

(4.12) for $z=R_c$, but is instead reduced by $c_{trans}$. Moreover, Bosman found the change of depth on the crest is related to the wavelength instead of the crest width.

$$d_{c,2\%}(x_c) = d(z = R_c) \cdot c_{trans} \cdot \exp\left( - c_{dc,B} \cdot \frac{x_c}{\gamma_c \cdot L_0} \right) \tag{4.25}$$

$$u_{2\%}(x_c) = u_{2\%}(z = R_c) \cdot \exp\left( - c_{uc,B} \frac{x_c}{\gamma_c \cdot d_{c,2\%}(x_c)} \right) \tag{4.26}$$

**Table 4.8:** Values of $c_d$, $c_{dc,B}$, $c_u$ and $c_{uc,B}$ estimated by Bosman *et al.* 2007.

| **Model** | $\mathbf{c_{d,2\%}}$ | $\mathbf{c_{tran}}$ | $\mathbf{c_{dc,B}}$ | $\mathbf{c_{u,2\%}}$ | $\mathbf{c_{uc,B}}$ |
|---|---|---|---|---|---|
| Bosman *et al.* (2007) | $\frac{0.010}{\sin^2 \alpha}$ | 0.81 | 15 | $\frac{0.30}{\sin\alpha}$ | 0.042 |

*Value obtained from Velocity and flow depth variations during wave overtopping, Bosman G., 2007, Master thesis.

This new formulation was calibrated with part of the data from Schüttrumpf *et al*. (2002) and Van Gent (2002) and checked with the results of different studies, Schüttrumpf and Oumeraci (2005) and Van der Meer (1987). A good agreement was found by the authors in all the parameters.

In Figure 4.12 and 4.13 is presented a comparison between the studies analysed previously and the formulation proposed by Bosman. It can be seen that in general, a good agreement for $d_{2\%}$ and $u_{2\%}$ is observed between the Bosman predictions and Schüttrumpf *et al*. (2002) and Van Gent (2002). This is expected because Bosman´s was calibrated by data of these projects. A different picture emerges when the results from Schüttrumpf and Oumeraci (2005) are also taken into account. It can be seen that for a slope of 1:6, the Schüttrumpf and Oumeraci (2005) prediction is significantly smaller than the other two, (Figure 4.12, a). On the other hand, for a slope 1:4, the three predictions have a good agreement. This could be another sign of scale effects in view of Figure 4.12 b) shows only results calibrated with small models, whereas Figure 4.12 a) shows the study calibrated with a small model, (Schüttrumpf and Oumeraci, 2005), to be quite different to the others calibrated with a large model. Thus it is not clear whether the new coefficients calibrated by Bosman

are reducing the uncertainties due to the seaward slope or the scales effects. More tests are needed to clarify this discrepancy.

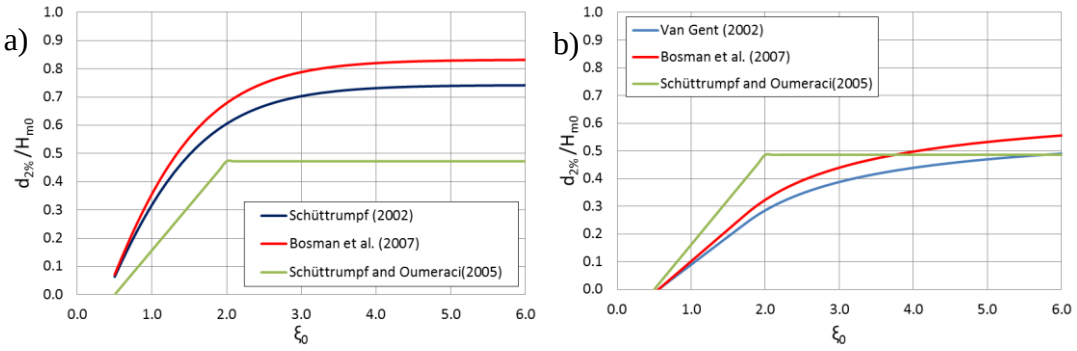


**Figure 4.12:** Dimensionless flow depth Bosman comparison a) seaward slope 1:6, b) seaward slope 1:4.

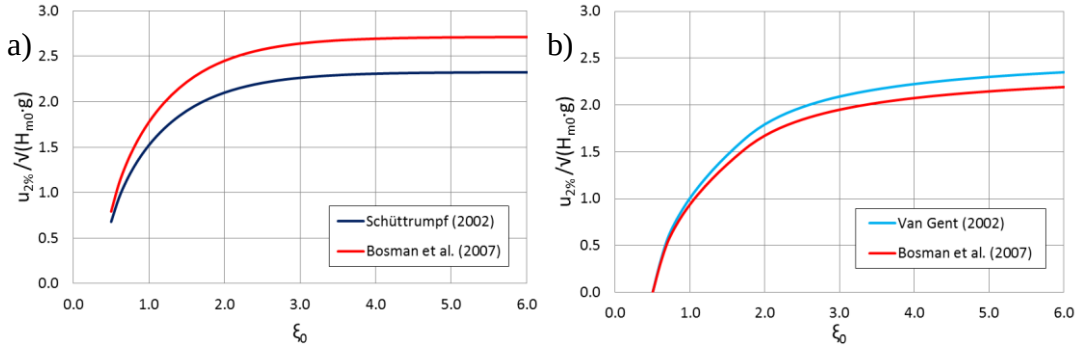


**Figure 4.13:** Dimensionless flow velocity Bosman comparison a) seaward slope 1:6, b) seaward slope 1:4.

## 4.5 Wave overtopping duration $T_{ovt}$

The overtopping duration, $T_{ovt}$, is time that the flow takes to pass through a certain section of the coastal defence´s crest. Different $T_{ovt}$ can be found in different parts of the crest due to the along-crest deformation that the flow experiences. The duration is a very useful measure of how violent a wave overtopping event is. For events with the same volume but different duration, higher velocities and deeper water will be expected for the shorter event. Thus, a more violent flow will be expected, with greater potential to create hazard.

Few studies have analysed the overtopping duration and no clear methodology has been found. The earliest estimation found (Van der Meer *et al.* 2006) showed that for larger overtopping volume duration between 0.5 and 0.8 $T_p$ can be expected and for smaller volume the duration could about 0.3-0.5 $T_p$, therefore a relation between the wave overtopping duration and the wave period have been suggested.

A more complete analysis was found in Bosman *et al.* 2007 who, from an analytical deduction based in the lineal decreased of the run-up's depth and velocity on the seaward slope, and using part of the data from Schüttrumpf *et al.* (2002) and Van Gent (2002), derived an equation to predict the overtopping duration with a 2% probability exceedance at the sea side of the crest for an individual overtopping event, equation (4.27)[7].

$$\frac{T_{ovt,2\%}(z=R_c)}{T_{m-1,0}} = 1.15 \cdot \sqrt{\left(\frac{R_{2\%}-R_c}{\gamma_f \cdot H_{m0}}\right)} \tag{4.27}$$

This formulation is a function of the run-up, $R_{2\%}$ , the wave height and period. The equation was calibrated with data from Schüttrumpf *et al.* (2002) and Van Gent (2002). A relation $T_{ovt,2\%}/T_{m-1.0}$ bigger than 1 was found in the data, contradicting the first estimation mentioned earlier where $T_{ovt}$ is always shorter than the wave period.

A more recent study was conducted in Hughes *et al.* 2012 where a relation between the individual wave overtopping volume and the overtopping duration was proposed, equation (4.28).

$$T_{ovt} = 3.9 \cdot V^{0.46} \tag{4.28}$$

[7] Original source (Bosman *et al.* 2007) used $H_s$ instead of $H_{m0}$ in equation 4.25.

Data from a previous experiment carried out in Hughes and Nadal 2009 were used to adjust the parameters of the expression. The principal objective of Hughes and Nadal (2009) was study the wave overtopping on seadikes under condition of negative freeboard where a combination of overflow and wave overtopping will occur. Dimensionless freeboards ($R_c/H_{m0}$) from -2.03 to -0.1 were tested in three seadike models with -0.29 m., -0.81m. and -1.3 m. freeboards (prototype equivalent). Under such negative conditions probably all of the flows generated on the dikes were hazardous for people, so the results lie far above the line in Figure 3.2, rather than close to the critical situations. For the elaboration of equation 4.16 only the data with freeboard -0.29 m. was used in order to reduce the overflow effects in the results. The use of very low freeboard could produce an overestimation of the overtopping durations when is applied for condition with positive freeboard, where no overflow is expected and therefore no overtopping duration much longer than the wave´s period should occur. Sadly, is not given in Hughes et al. (2012) the relation between the overtopping duration and the wave period for the data used. There is therefore no way to know whether overflow has a significant effect on the equation.

From the 2,100 data pairs analysed in Hughes *et al.* (2012), it is possible to discern a trend between the individual wave overtopping volume and the duration of each event, but with large scatter, common for studies of overtopping due to the highly turbulent nature of this kind of flow. An important aspect which is not mentioned on the paper is for what section of the dike´s crest this prediction of duration will be valid, from the video analysis it was appreciated that the overtopping duration could change significantly depending on the location of the crest. Despite these sources of uncertainty, it seems logical that there exists a relation between the volume of water overtopped and the duration of the flow. As previously noted, however, different waves could generate the same overtopping volume, with quite different flows resulting different overtopping duration, an aspect which is not accounted for this equation. This could explain the wide scatter in the data used to estimate equation 4.28. In order to reduce this problem it is possible that the equation needs to consider the wave properties too.

Due to each equation requiring different input parameters, the method to best compare them is to use a representative wave-structure condition and calculate the

overtopping duration with each formula. Wave conditions of $H_{m0}$ = 1 m, $T_{m-1,0}$ = 3 to 25 ($s_0$ = 0.001 to 0.07) with a duration t=2hr were tested in a seadike with a seaward slope 1:3 with two different freeboards 2m and 1m.

Figure 4.14 shows the calculation of the overtopping duration by Bosman and Hughes versus ($R_{u2\%}$-$R_c$) and $V_{max}$. Bosman´s result corresponds to the duration with a 2% probability of exceedance for the particular wave conditions used. On the other hand Hughes result intends to predict the duration of an individual overtopping volume, with $V_{max}$ used in this case. The definition of each duration is therefore different, and is expected that Bosman prediction will be bigger than Hughes.

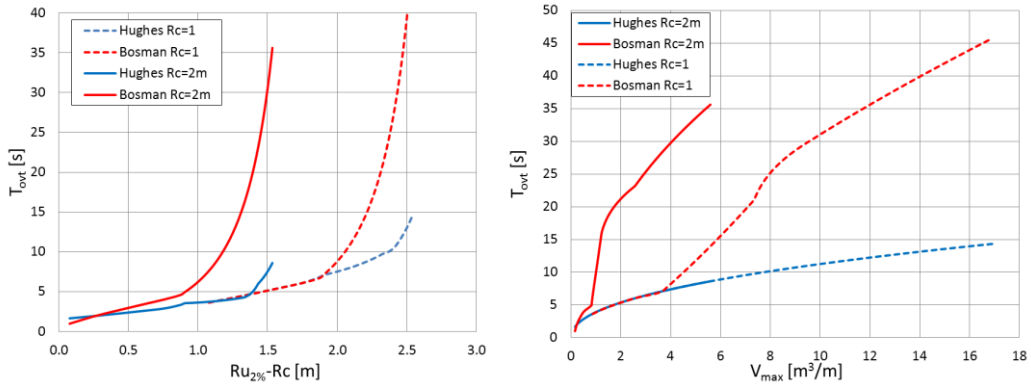


**Figure 4.14:** Comparison of wave overtopping duration, $T_{ovt}$, based on Hughes *et al.* 2012 and Bosman *et al.* 2007, versus ($R_{u2\%}$-$R_c$) and $V_{max}$. Changes in curves upon variation of $T_{m-1,0}$ from 3s to 25s.

It can be seen in Figure 4.14 that the overtopping duration predictions based on equations 4.27 and 4.28 are quite similar at the beginning of each curve, but then Bosman´s equation grows faster than Hughes, as is expected due to the first one is a 2% exceedance value. It is observed that shorter durations are predicted for the higher crest, where smaller ($R_{u2\%}$-$R_c$) and $V_{max}$ are expected.

Figure 4.15 shows the relation between the non-dimensional duration ($T_{ovt}/T_{m-1,0}$) with ($R_{u2\%}$-$R_c$) and $V_{max}$ . Again similarities are observed at the beginning of each curve especially for $R_c$=1m, but then very different behaviours are observed for each equation. In general Hughes's method predicts smaller $T_{ovt}/T_{m-1,0}$ than Bosman, being always smaller than 0.8 for $R_c$=2m, but for $R_c$=1m both equation predict $T_{ovt}/T_{m-1,0}$ larger than 1. Bosman reaches values of 1.8 and Hughes of 1.6. This is in contrast to

the estimation mentioned earlier (Van der Meer *et al.* 2006) where overtopping durations between 0.3 and 0.8 $T_p$ were suggested. Taking, approximately $T_p$=*1.1* $T_{m-1,0,}$ no values of $T_{ovt}/T_{m-1,0}$ bigger than 0.9 should be predicted.

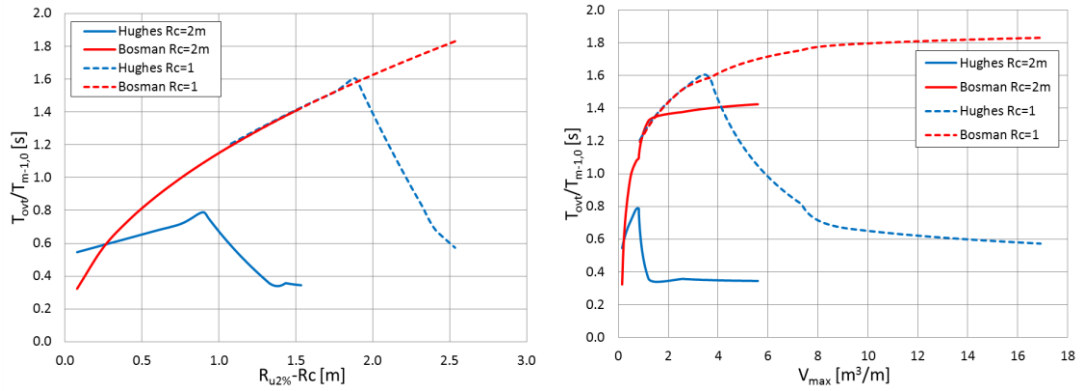


**Figure 4.15:** Comparison of dimensionless wave overtopping duration, $T_{ovt}/T_{m-1.0}$, based on Hughes *et al.* 2012 and Bosman *et al.* 2007, versus ($R_{u2\%}$-$R_c$) and $V_{max}$. Changes in curves upon variation of $T_{m-1,0}$ from 3s to 25s.

The different behaviour of the curves in Figure 4.15 are explained because each equation depends on different parameters, $R_{2\%}$ Bosman and $V_{max}$ Hughes, and they behave differently upon the changes of the breaker parameter, Figure 4.16 a). Figure 4.16 b) shows that for the breaking range the agreement between these two equations is better, but then the dimensionless duration predicted by Hughes decreases, while Bosman increase but in a much smaller rate. It is important to mention that Bosman calibrated its work with wave conditions in the breaking range $\xi_0$<1.8, no information on this subject is given for the data used in Hughes *et al.* 2012. This could explain why the better agreements are found at the beginning of the curves.

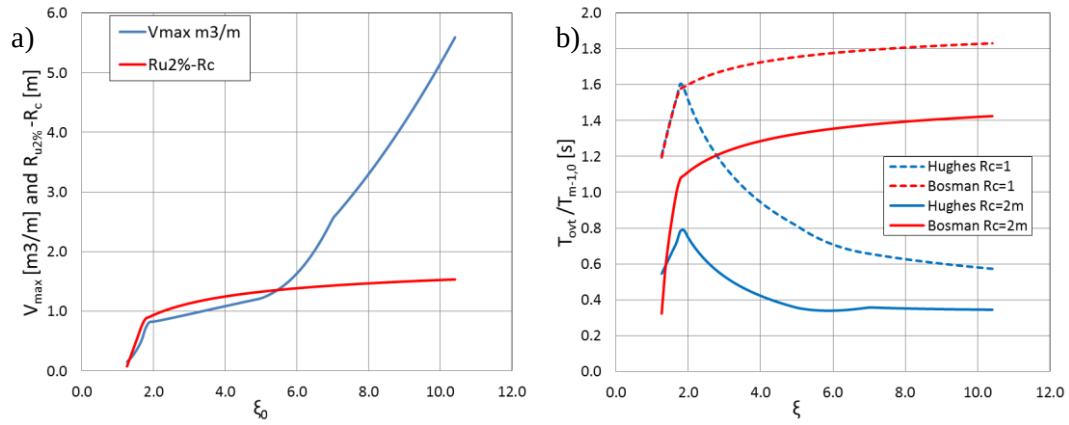


**Figure 4.16:** a) Variation of Vmax and Ru2%-Rc for a range of breaking parameter. b) Comparison of non dimensional duration, $T_{ovt}/T_{m-1.0}$, based on Hughes et al. 2012 and

Bosman et al. 2007 for a range of breaking parameters. Changes in curves upon variation of $T_{m-1,0}$ from 3s to 25s.

## 4.6 Overall description of wave overtopping flow

From the analysis of previous studies (Hughes and Nadal (2009) and Bosman (2007)) it was found that in general, a linear shape of *u(t)* and *d(t)* is a good approximation but, for larger events a more convex curve seems describe better an individual flow. The use of a more convex shape will predict higher $d_{max}$ and $u_{max}$ for a given volume. Due to this project´s aim to describe potentially overtopping flows, the more conservative prediction was selected. Power curves with an exponent of 1.5, eq. (4.29) and (4.30), will be used to describe change of depth and velocity on a seadike's crest.

$$d(t) = d\max \cdot \left(1 + \frac{t}{T_{ovt}}\right)^{1.5} \tag{4.29}$$

$$u(t) = u\max \cdot \left(1 + \frac{t}{T_{ovt}}\right)^{1.5} \tag{4.30}$$

Clear methodology was found (Schüttrumpf *et al*. 2002 and Van Gent 2002) to describe the changes, on the seaward slope and crest, of the flow depth and velocity with a 2% of probability of exceedance. The equations were calibrated by physicals models in three previous projects but different results were found. It is not possible to determine which one of them is the most reliable, and an average of the predictions was thus used for further calculations, Figure 4.17.

Two methods to calculate the overtopping duration ($T_{ovt}$) were found. The first one (Bosman *et al.* 2007) predict a 2% exceedance value, relate the $T_{ovt}$ to the wave period and the run-up, and was calibrated with wave conditions $\xi_0$<1.8. The second one (Hughes *at al.* 2012) is a function only of the overtopping volume. A comparison was conducted, Figures 4.10 to 4.12, and a good agreement between them for $\xi_0$<1.8

was found. For $\xi_0$>1.8 Bosman predicts much longer duration than Hughes, which could produce an underestimation of the depth and velocity of an overtopping flow, and also it was calibrated with a very small database increasing it uncertainties. Since this study is focused upon derivation of a methodology to predict hazardous condition for pedestrian, the more conservative equation and with the smaller uncertainties is selected for the next stage of the project.

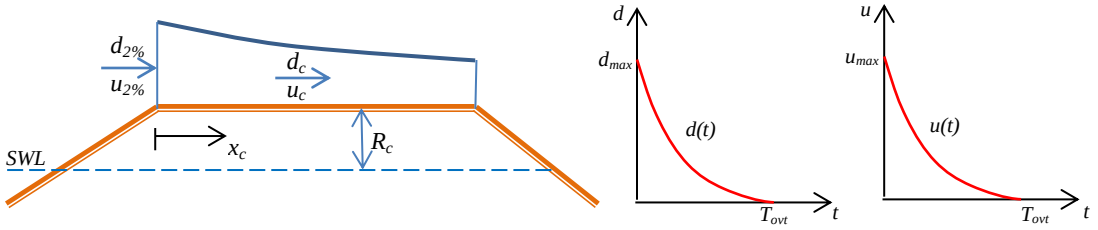


$$d(t) = d_{\max} \times \left(1 - \frac{t}{T_{ovt}}\right)^{1.5} \quad (4.29)$$

$$u(t) = u_{\max} \times \left(1 - \frac{t}{T_{ovt}}\right)^{1.5} \quad (4.30)$$

$$d_{2\%} = c_d \cdot \left(R_{2\%} - R_c\right) \quad (4.31)$$

$$u_{2\%} = c_u \cdot \sqrt{g \cdot \left(R_{2\%} - R_c\right)} \quad (4.32)$$

$$d_c(x_c) = d_{2\%} \cdot \exp\left(-c_{dc} \cdot \frac{x_c}{B}\right) \quad (4.33)$$

$$u_c(x_c) = u_{2\%} \cdot \exp\left(-c_{uc} \frac{x_c \cdot f}{d_c(x_c)}\right) \quad (4.34)$$

$$T_{ovt} = 3.9 \cdot V_{\max}^{0.46} \quad (4.35)$$

| | S *et al* (2002) | VG (2002) | S and *O* (2005) | | **Average** |
|---|---|---|---|---|---|
| $\mathbf{c_{d,2\%}}$ | 0.33 | 0.15 | 0.22 | 0.21 | **0.23** |
| $\mathbf{c_{u,2\%}}$ | 1.55 | 1.3 | -- | -- | **1.43** |
| $\mathbf{c_{dc}}$ | 0.89 | 0.15 | 0.75 | -- | **0.60** |
| $\mathbf{c_{uc}}$ | 0.50 | 0.75 | 0.50 | -- | **0.58** |

S *et al* (2002) = Schüttrumpf *et al.* (2002)
VG (2002) = Van Gent (2002)
S and O (2005) = Schüttrumpf and Oumeraci (2005).

$$\frac{R_{2\%}}{H_{m0}} = \min\left\{1.65\gamma_b\gamma_f\gamma_\beta\xi_{m-1,0}; 1.00\gamma_b\gamma_f\gamma_\beta\left(4.0 - \frac{1.5}{\sqrt{\xi_{m-1,0}}}\right)\right\}$$

$$V_{\max} = a \cdot \left[\ln N_{ow}\right]^{4/3}$$

$f$ = 0.01-0.02 for smooth surfaces

**Figure 4.17:** Resume of methodology to characterise the wave overtopping flow on the crest of a seadike.

With the set of equations selected, it is possible to describe an overtopping flow of a certain volume, *V*, by doing the balance of volume on the crest, equation 4.36.

$$V_o = \int_0^{T_{ovt}} d(t) \times u(t)\, dt$$

$$V_o = \int_0^{T_{ovt}} d_{\max} \times \left(1 - \frac{t}{T_{ovt}}\right)^{1.5} \times u_{\max} \times \left(1 - \frac{t}{T_{ovt}}\right)^{1.5} dt$$

$$V_o = \frac{d_{\max} \times u_{\max}}{T_{ovt}^{\ 3}} \int_0^{T_{ovt}} \left(T_{ovt} - t\right)^3 dt$$

$$V_o = \frac{d_{\max} \times u_{\max}}{T_{ovt}^{\ 3}} \times \left[\frac{-\left(T_{ovt} - t\right)^4}{4}\right]_0^{T_{ovt}}$$

$$V_o = \frac{d_{\max} \times u_{\max} \times T_{ovt}}{4} \qquad (4.36)$$

Some assumptions are necessary: no extra contributions of water occur, such as rain or splash transported by the wind, and no losses of water occur by infiltration. Equation 4.36 relates the total volume overtopped with the three main parameters ($u_{max}$, $d_{max}$ and $T_{ovt}$) studied here. Knowing two of them it is possible to calculate the third one.

Hughes *et al.* (2012) used data from Nadal and Hughes (2009) to analyse the coincidence of $d_{2\%}$ and $u_{2\%}$ and found that there is no reason to expect that both parameters will occur during the same overtopping event. This means that the deeper overtopping flows will not have the maximum velocities and vice versa. This finding implies that equations 4.31 and 4.32 should not be used together to solve equation 4.36. Therefore, two different methods can be used to describe a wave overtopping flow.

**Method 1 (M1d):** $V_o = \frac{d_{\max} \times u_{\max} \times T_{ovt}}{4}$

with: $T_{ovt} = 3.9 \cdot V^{0.46}$

$d_{\max} = d_{2\%} = 0.23 \cdot \left(R_{2\%} - R_c\right)$, for the seaside of the crest

**Method 2 (M2u):** $V_o = \frac{d_{\max} \times u_{\max} \times T_{ovt}}{4}$

with: $T_{ovt} = 3.9 \cdot V^{0.46}$

$u_{\max} = u_{2\%} = 1.43 \cdot \sqrt{g \cdot (R_{2\%} - R_c)}$, for the seaside of the crest

Hence the difference between these two models is that M1d use $d_{2\%}$, equation 4.31, as an input to solve equation 4.36, but M2u use $u_{2\%}$, equation 4.32. These two methods can be use to predict a wave overtopping flow on the crest of a seadike. Using only the equations 4.31 and 4.32 the result will be applicable for the seaside of the crest, to describe the flow in a different part of the crest the equation 4.33 and 4.34 should be use.

Figure 4.18 shows the prediction of these two methods in function of ($R_{u2\%}$-$R_c$) for a given seadike. It can be seen that for ($R_{u2\%}$-$R_c$) smaller than 0.9m, M2u predicts deeper flows than M1d. On the other hand, for ($R_{u2\%}$-$R_c$) smaller 0.9m, M1d predicts faster flows than M2u. In the prediction of the velocity it is also observed that M1d predicts very fast flows, up to 20m/s, for small ($R_{u2\%}$-$R_c$). This is explained because the prediction of the depth in that condition is very small due to the small value of the coefficient in equation 4.31, which produce a high value of $u_{max}$ when equation 4.36 is solved. This could generate unrealistic flows, and a wrong prediction of hazard for low overtopping conditions. It can also be recalled that in the video analysis conducted in Chapter 3 no flow faster than 7m/s where estimated. The effect of this will be extended in Chapter 5.

| $T_{m-1,0}$ [s] | $H_{m-0}$ [m] | $R_c$ [m] | slope | | |
|---|---|---|---|---|---|
| 3 - 25 | 1 | 2 | 1 | in | 3 |

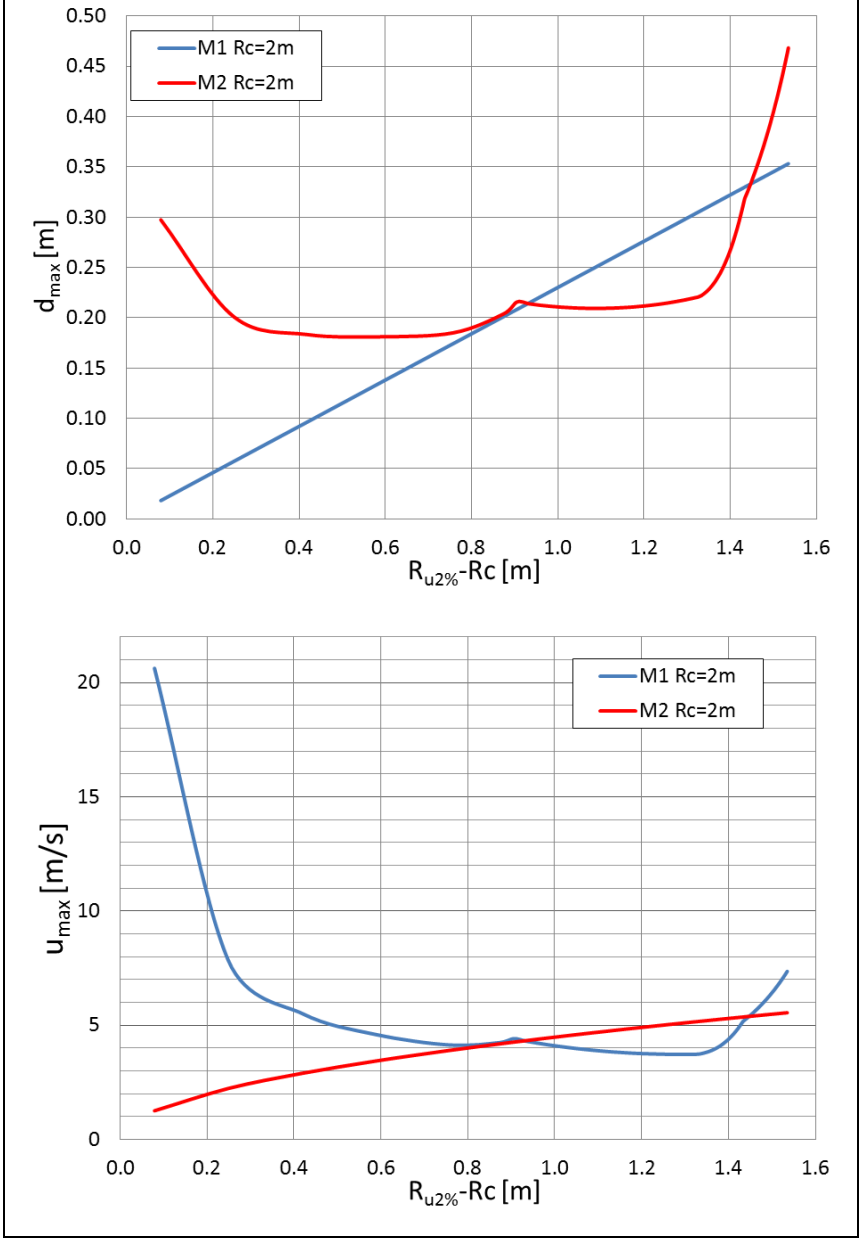


**Figure 4.18**: Comparison $d_{max}$ and $u_{max}$ predicted using M1 and M2 for different ($R_{u2\%}$-$R_c$).

## 4.7 Chapter conclusions

A review of the general methodology for seadikes of the widely accepted EurOtop (2007) was given, which form the basis for the calculations in this research.

The methods to predict overtopping discharge are extended and accepted, but those to estimate the hydraulic parameters of the wave overtopping flows are much less studied. EurOtop (2007) gives a methodology to estimate the flow depth and velocity on a seadike.

An exhaustive review of literature related to wave overtopping flows was also conducted. In general three parameters have been taken into account for previous studies, the maximum flow depth ($d_{max}$), the flow velocity ($u_{max}$) and the overtopping duration ($T_{ovt}$). The first two have a more extensive literature. Although clear methodologies have been proposed for each parameter their applications are very narrow (only for seadikes) and not completely validated with real wave overtopping events. No information was found upon which a general description of an individual overtopping flow of vertical defences could be based. Even though the study of the overtopping flow is not extensive, compared with other aspects of a wave overtopping, important and useful information was found, which can be used to predict the characteristics a overtopping flow produced by a certain wave weather on a specific seadike.

Figure 4.13 shows a resume of the methodologies analysed here and the equations used to developed two methods which can describe a wave overtopping flow with a known volume and run-up. These models predict different conditions: M2u gives deeper and slower flows compared with M1d for smaller ($R_{u2\%}$-$R_c$). It is not yet clear which model produces a more pessimistic scenario for people, due to the human instability models developed in Chapter 3 not being linearly related to the flow depth and velocity.

Taking together the information compiled in this chapter and in Chapter 3 it becomes possible to predict whether a certain wave condition acting at a particular seadike could produce a hazardous condition for pedestrians at the crest. In Chapter 5 this findings are merged together and the hazard potential of different wave conditions is studied for different seadike geometries.

# Chapter 5
# Risk predictions

## 5.1 Introduction

In this chapter the findings for the human stability (Chapter 3) and the prediction of the overtopping flows (Chapter 4) are combined to estimate whether a certain wave condition could generate hazardous overtopping flows for personnel at the crest of a given seadike. A series of hazard matrices and envelopes are derived, and their weaknesses and constraints discussed. Finally a sensitivity analysis of the assumptions is conducted which gives a guide for future work is this field.

## 5.2 Methodology and assumptions

Figure 5.1 presents the general methodology use here to generate the hazard prediction. Two separate areas of calculations are identified; the first one is the calculation of the overtopping flow parameters ($u_{max}$, $d_{max}$), and the second one is the calculation of the human instability curves, which define ($u_{cr}$, $d_{cr}$). Then, in the final stage, it is decided whether the wave condition analyse can produce a hazardous condition for personnel.

The basic oceanographic information to make the calculations of the wave overtopping flow parameters are the wave height ($H_{m0}$), the wave period ($T_{m-1,0}$) and the duration of the storm ($t$). In addition it is necessary to identify the geometric features of the seadike, with the freeboard ($R_c$) and the seaward slope the most important. In the first stage of the calculations, several wave conditions are generated and calculated their characteristics features ($s_0$, $\xi_0$ and $N_w$) in order that only realistic conditions are analysed. If the wave conditions are realistic, the general parameters of wave run-up $R_{u2\%}$ and overtopping $q$ are calculated. If $R_{u2\%}$ is lower than the freeboard then no significant wave overtopping is expected, and this condition is deemed as no hazard "NH". On the other hand, if $R_{u2\%}$ is higher than $R_c$, significant overtopping events may occur and the maximum overtopping volume ($V_{max}$) by a

single event during the storm is calculated. Using this parameter, the overtopping flow duration is estimated, equation 4.23, and then the pairs ($u_{2\%}$ , $d_{2\%}$) are calculated according to the two models proposed in section 4.5 in Chapter 4. It is assumed that this parameters with a 2% of exceedance are very similar to the maximum values therefore ($u_{2\%}$ , $d_{2\%}$)≈($u_{max}$, $d_{max}$).

The two mechanisms for human instability in flow (Chapter 3) predict the combination of velocity and depth ($u_{cr}$, $d_{cr}$) which can generate a critical flow for a person due to overtopping composed by mainly green waters. They are function of the person´s characteristics (mass $m$ and height $h_p$), the position of the person at the moment of receipt of the flow, and the type of surface on which the person stands. Knowing these parameters, the drag force of the flow can be expressed as a function of only $u$ and $d$ and the balance of moment and friction can be done. Solving the equations 3.9 and 3.10, for $0 < d < h_p$ the corresponding $u$ for each type of instability and depth is found, resulting the critical instability curves, ($u_{cr}$, $d_{cr}$), which divide the stability graph (Figure 3.22) in stable and unstable zones.

In the final stage of the procedure the calculated ($u_{max}$, $d_{max}$) is compared with the curve ($u_{cr}$, $d_{cr}$) to determine whether the overtopping flow is located in the stable or unstable zone of the stability graph, and the wave condition classified as not hazardous (NH and green box), or as hazardous (H and red box) accordingly. Given the uncertainties in the calculations, especially in the ones related with the human stability, a yellow band is also included being these wave conditions classified as relative hazardous (RH and yellow box). This yellow band start when the $u_{max}$ calculated is between $0.8 \cdot u_{cr}$ and $1.0 \cdot u_{cr}$. The final results can be show as a risk matrixes or risk envelopes for different seawall configurations.

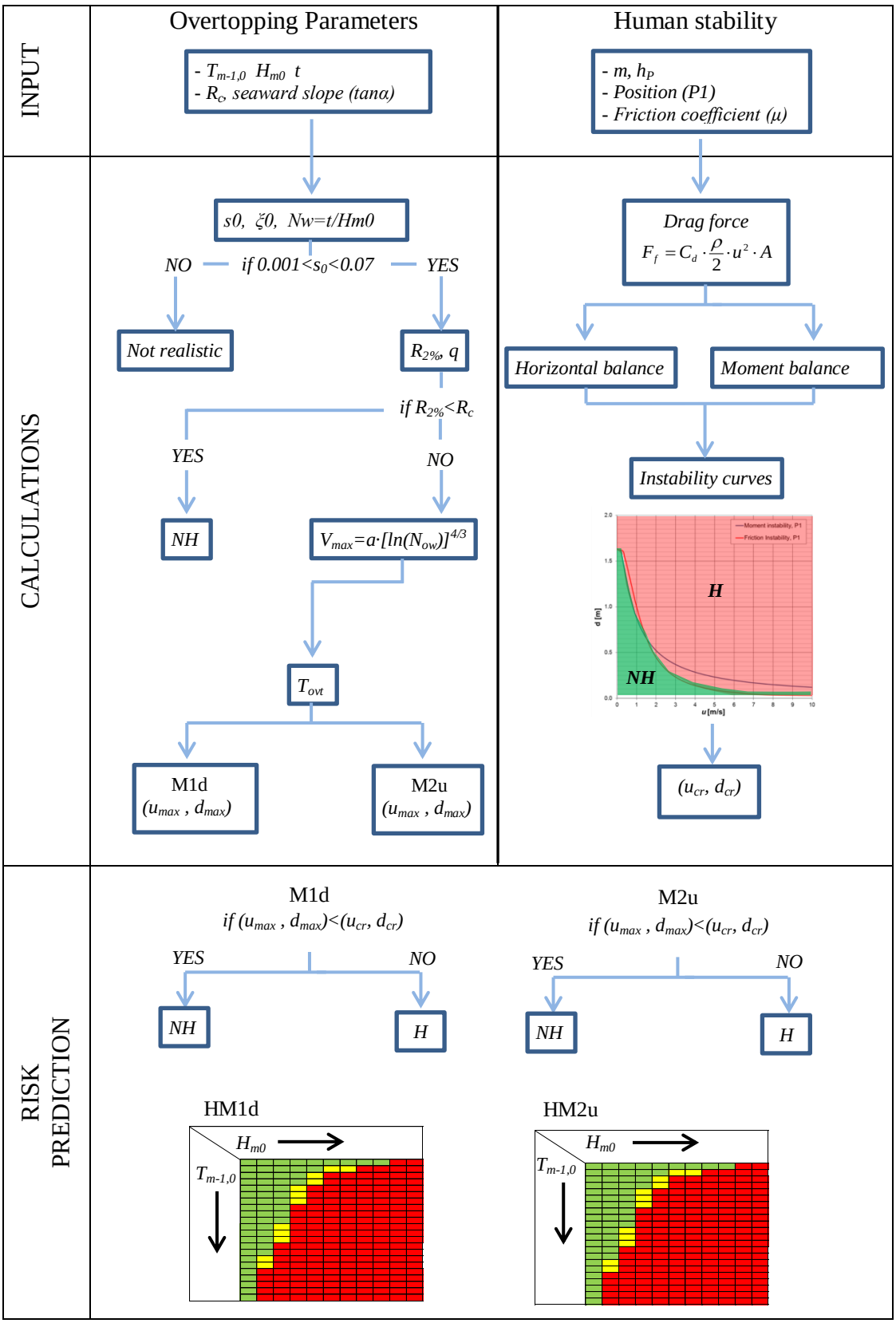


**Figure 5.1:** Methodology of hazard estimation.

### 5.2.1 General assumptions

The prediction elaborated is dependent upon the human features and reaction of the person. Additionally, wave overtopping estimation has inherent uncertainties, and may take several forms, it is therefore necessary to stablish basic assumptions as follows:

Assumptions concerning human stability:

- The person receives the flow while standing in front of the flow and at the seaside of the crest.
- The person does not change her/his position during the overtopping duration, so the moment and friction resistance remain constant during the event.
- The hazard level is only produced by the overtopping flow. The effect of (e.g) water spray, debris and wind can be neglected.

Assumptions concerning overtopping flow:

- The overtopping flows are predominantly "green water" as opposed to "violent" overtopping resulting from wave breaking at very steep or vertical walls. The overtopping flow is in contact with the structure crest.
- The contribution of water due to spray transported by the wind or rain can be neglected.
- No infiltration occurs on the surface of the seawall therefore no losses of water occur.
- There is no presence of debris in the flow; hence the hazard is only produced by the flow´s velocity and depth.
- The velocity profile of the flow is considered uniform with depth and very similar to the velocity of the front of the overtopping flow.
- The storm duration, *t*, is necessary for the calculation of $V_{max}$ and it is assumed equal to 2 hours which covers the peak of the tide, moment with the lowest freeboard and therefore most vulnerable to overtopping.

### 5.2.2 Input data

The input data used to generate the hazard matrices have the objectives to represent realistic scenarios and to generate conservative predictions.

An adult female it is considered as a conservative subject. Height and weight similar to the average of a British woman is assumed, 1.61m and 70 kg (Moody 2013). In addition it is considered that the person is standing in front of the flow according to P1 (Figure 3.24) and remains in that position the whole duration of the flow. With this position it is intended to model people who will be caught by surprise with no time to change posture for one more suitable to resist the flow.

The seaward slope more commonly used in seadikes are 1:2, 1:3 and 1:4, being the steepest slopes more common in urban areas. Due to none of the formulae for flow depth and velocity consider the presence of a crown wall and berms, only simple dikes are considered here.

In table 5.1 the general data used for the development of the hazard prediction is shown.

**Table 5.1:** Input data.

| Parameter | Notation | Value/Range | Unit | Observation |
|---|---|---|---|---|
| Person´s Height | $h_p$ | 1.61 | m | Average UK woman |
| Person´s mass | $m$ | 70 | kg | Average UK woman |
| Density of human body | $\rho_b$ | 1,062 | kg/m$^3$ | |
| Leg width | $W_l$ | 0.2 | m | |
| Leg separation | $L_f$ | 0.2· $h_p$ | m | |
| Rotational distance | $L_g$ | 0.125· $h_p$ | m | |
| Friction coefficient | $\mu$ | 0.62 | - | Rubber shoe/wet smooth concrete* |
| Drag coefficient | $C_d$ | 0.88 | | Endoh and Takahashi (1995) |
| Storm duration | $t$ | 2 | hour | |
| Water depth at toe of the structure | $h$ | 4 | m | |
| Seaward slope | | 1:[2, 3, 4] | | |
| Freeboard | $R_c$ | 1, 2, 3, 4 | m | |

* Endoh and Takahashi 1995.

## 5.3 Results

The following figures present a classification of different wave conditions as hazardous flow (H) or not (NH) for a pedestrian standing on the seaside of the crest of a seadike.

The summary of the 12 seadike conditions explored here are showed in table 5.2

**Table 5.2:** Seadike configuration analysed.

| Parameter | S1 | S2 | S3 | S4 | S5 | S6 | S7 | S8 | S9 | S10 | S11 | S12 |
|---|---|---|---|---|---|---|---|---|---|---|---|---|
| Rc [m] | 4 | 4 | 4 | 3 | 3 | 3 | 2 | 2 | 2 | 1 | 1 | 1 |
| Seaward slope | 1:2 | 1:3 | 1:4 | 1:2 | 1:3 | 1:4 | 1:2 | 1:3 | 1:4 | 1:2 | 1:3 | 1:4 |

Figures 5.3 and 5.4 show the hazard matrices for a person standing on the seaside of the crest of a seadike with $R_c$=4m. and seaward slope 1 in 4, with flow parameters calculated according to M1d and M2u respectively. Three general classifications are shown: a white box represent a wave condition which is not realistic; green is a wave condition which will not produce a flow to unbalance a person, and red identified wave overtopping flows with the potential to unbalance a person. It can be seen that Figure 5.3 is more pessimistic than Figure 5.4 with hazardous flows predicted with smaller wave conditions. $R<R_c$ indicates when the run-up is lower than the freeboard therefore, no overtopping flows are expected. It can be seen in Figure 5.3 that all the no hazard prediction occur due to this, and as soon as $R>R_c$, a hazardous situation is generated. This does not occur in Figure 5.4. For $H_{m0}$=1.25; 1.4; 1.7 and 2.6, before a critical flow is generated, non-hazardous overtopping flows will occur, a prediction which feels more realistic because not all overtopping flows will have the power to unbalance a person. This apparent overestimation occurs when the difference ($R_{2\%}$ - $R_c$) in equation 4.19 is minimal, and thus $d_{max}$ calculated is very low, in turn producing an overestimation of the flow velocity in order to evacuate the overtopping volume within the overtopping duration. The result is a flow with very low depth and an unrealistically high velocity. To avoid this problem it was defined a "always safe" depth $d_s$. If the calculation of $d_{max}$ results in $d_{max}<d_s$, then the wave

condition is classified as non-hazardous. The always safe depth is estimated using the instability curve for the subject, Figure 5.2, and the maximum velocity estimated in the video analysis (Chapter 3), of 7.0 m/s, which is considered as a realistic maximum velocity for an overtopping flow. For that velocity a depth of 5cm will generate a hazardous condition, see Figure 5.2. On the other hand, during the video analysis no flow that caused hazard had a depth less than 10cm. Therefore $d_s$=5cm is considered a good approximation to a "always safe" depth.

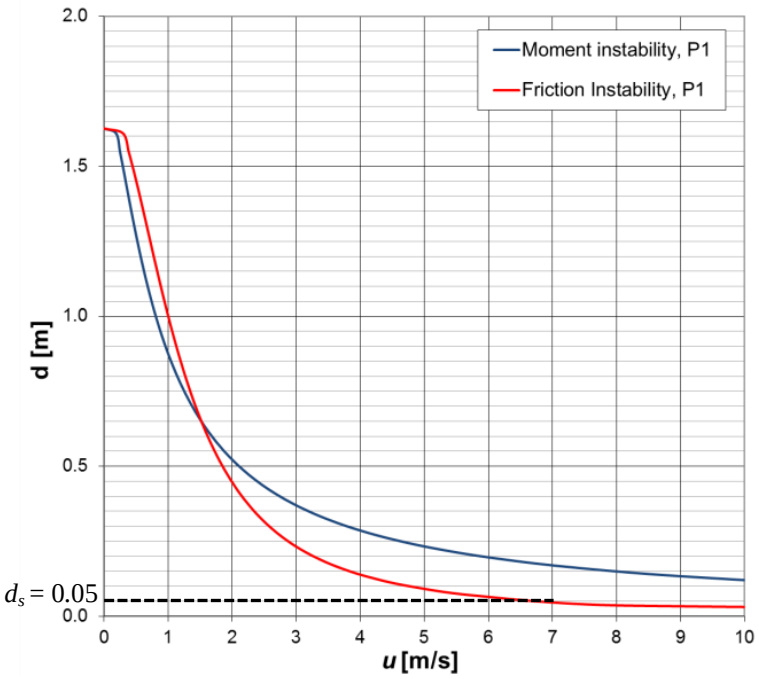


**Figure 5.2:** Instability curve for a person of $m$=70kg, $h_p$=1.61m. and position 1 (P1).

Figure 5.5 shows the adjusted Figure 5.3. Now considering $d_s$, it can be seen that some overtopping events previously classified as H are now classified as NH, which appears to be a more realistic prediction. It can be seen that this new matrix is still more pessimistic that the one generate by M2u, Figure 5.4.

| HM1 | Rc = 4 m | | | slope = 1/4 | | | | | | | | | | | | |
|---|---|---|---|---|---|---|---|---|---|---|---|---|---|---|---|---|
| $H_{m0}$ [m] / $T_{m-1,0}$ [s] | 0.50 | 0.65 | 0.80 | 0.95 | 1.10 | 1.25 | 1.40 | 1.55 | 1.70 | 1.85 | 2.00 | 2.15 | 2.30 | 2.45 | 2.60 | 2.75 |
| 3 | R<Rc | R<Rc | R<Rc | R<Rc | ** | ** | ** | ** | ** | ** | ** | ** | ** | ** | ** | ** |
| 4 | R<Rc | R<Rc | R<Rc | R<Rc | R<Rc | R<Rc | R<Rc | R<Rc | R<Rc | ** | ** | ** | ** | ** | ** | ** |
| 5 | R<Rc | R<Rc | R<Rc | R<Rc | R<Rc | R<Rc | R<Rc | R<Rc | R<Rc | R<Rc | R<Rc | R<Rc | R<Rc | H | H | ** |
| 6 | R<Rc | R<Rc | R<Rc | R<Rc | R<Rc | R<Rc | R<Rc | R<Rc | H | H | H | H | H | H | H | H |
| 7 | R<Rc | R<Rc | R<Rc | R<Rc | R<Rc | R<Rc | H | H | H | H | H | H | H | H | H | H |
| 8 | R<Rc | R<Rc | R<Rc | R<Rc | R<Rc | R<Rc | H | H | H | H | H | H | H | H | H | H |
| 9 | R<Rc | R<Rc | R<Rc | R<Rc | R<Rc | R<Rc | H | H | H | H | H | H | H | H | H | H |
| 10 | R<Rc | R<Rc | R<Rc | R<Rc | R<Rc | R<Rc | H | H | H | H | H | H | H | H | H | H |
| 11 | R<Rc | R<Rc | R<Rc | R<Rc | R<Rc | R<Rc | H | H | H | H | H | H | H | H | H | H |
| 12 | R<Rc | R<Rc | R<Rc | R<Rc | R<Rc | R<Rc | H | H | H | H | H | H | H | H | H | H |
| 13 | R<Rc | R<Rc | R<Rc | R<Rc | R<Rc | H | H | H | H | H | H | H | H | H | H | H |
| 14 | R<Rc | R<Rc | R<Rc | R<Rc | R<Rc | H | H | H | H | H | H | H | H | H | H | H |
| 15 | R<Rc | R<Rc | R<Rc | R<Rc | R<Rc | H | H | H | H | H | H | H | H | H | H | H |
| 16 | R<Rc | R<Rc | R<Rc | R<Rc | R<Rc | H | H | H | H | H | H | H | H | H | H | H |
| 17 | R<Rc | R<Rc | R<Rc | R<Rc | R<Rc | H | H | H | H | H | H | H | H | H | H | H |
| 18 | ** | R<Rc | R<Rc | R<Rc | R<Rc | H | H | H | H | H | H | H | H | H | H | H |
| 19 | ** | R<Rc | R<Rc | R<Rc | R<Rc | H | H | H | H | H | H | H | H | H | H | H |
| 20 | ** | R<Rc | R<Rc | R<Rc | R<Rc | H | H | H | H | H | H | H | H | H | H | H |
| 21 | ** | ** | R<Rc | R<Rc | R<Rc | H | H | H | H | H | H | H | H | H | H | H |
| 22 | ** | ** | R<Rc | R<Rc | R<Rc | H | H | H | H | H | H | H | H | H | H | H |
| 23 | ** | ** | ** | R<Rc | R<Rc | H | H | H | H | H | H | H | H | H | H | H |
| 24 | ** | ** | ** | R<Rc | R<Rc | H | H | H | H | H | H | H | H | H | H | H |
| 25 | ** | ** | ** | ** | R<Rc | H | H | H | H | H | H | H | H | H | H | H |

**Figure 5.3:** HM1 for person at seaside of a seadike crest, $R_c$ = 4m and seaward slope 1:4. Green: No hazard is predicted. Red: Hazardous flow is predicted.

| HM2 | Rc = 4 m | | | slope = 1/4 | | | | | | | | | | | | |
|---|---|---|---|---|---|---|---|---|---|---|---|---|---|---|---|---|
| $H_{m0}$ [m] / $T_{m-1,0}$ [s] | 0.50 | 0.65 | 0.80 | 0.95 | 1.10 | 1.25 | 1.40 | 1.55 | 1.70 | 1.85 | 2.00 | 2.15 | 2.30 | 2.45 | 2.60 | 2.75 |
| 3 | R<Rc | R<Rc | R<Rc | R<Rc | ** | ** | ** | ** | ** | ** | ** | ** | ** | ** | ** | ** |
| 4 | R<Rc | R<Rc | R<Rc | R<Rc | R<Rc | R<Rc | R<Rc | R<Rc | R<Rc | ** | ** | ** | ** | ** | ** | ** |
| 5 | R<Rc | R<Rc | R<Rc | R<Rc | R<Rc | R<Rc | R<Rc | R<Rc | R<Rc | R<Rc | R<Rc | R<Rc | R<Rc | H | RH | ** |
| 6 | R<Rc | R<Rc | R<Rc | R<Rc | R<Rc | R<Rc | R<Rc | R<Rc | RH | H | H | H | H | H | H | H |
| 7 | R<Rc | R<Rc | R<Rc | R<Rc | R<Rc | R<Rc | RH | H | H | H | H | H | H | H | H | H |
| 8 | R<Rc | R<Rc | R<Rc | R<Rc | R<Rc | R<Rc | RH | H | H | H | H | H | H | H | H | H |
| 9 | R<Rc | R<Rc | R<Rc | R<Rc | R<Rc | R<Rc | H | H | H | H | H | H | H | H | H | H |
| 10 | R<Rc | R<Rc | R<Rc | R<Rc | R<Rc | R<Rc | H | H | H | H | H | H | H | H | H | H |
| 11 | R<Rc | R<Rc | R<Rc | R<Rc | R<Rc | R<Rc | H | H | H | H | H | H | H | H | H | H |
| 12 | R<Rc | R<Rc | R<Rc | R<Rc | R<Rc | R<Rc | H | H | H | H | H | H | H | H | H | H |
| 13 | R<Rc | R<Rc | R<Rc | R<Rc | R<Rc | NH | H | H | H | H | H | H | H | H | H | H |
| 14 | R<Rc | R<Rc | R<Rc | R<Rc | R<Rc | NH | H | H | H | H | H | H | H | H | H | H |
| 15 | R<Rc | R<Rc | R<Rc | R<Rc | R<Rc | NH | H | H | H | H | H | H | H | H | H | H |
| 16 | R<Rc | R<Rc | R<Rc | R<Rc | R<Rc | NH | H | H | H | H | H | H | H | H | H | H |
| 17 | R<Rc | R<Rc | R<Rc | R<Rc | R<Rc | NH | H | H | H | H | H | H | H | H | H | H |
| 18 | ** | R<Rc | R<Rc | R<Rc | R<Rc | NH | H | H | H | H | H | H | H | H | H | H |
| 19 | ** | R<Rc | R<Rc | R<Rc | R<Rc | RH | H | H | H | H | H | H | H | H | H | H |
| 20 | ** | R<Rc | R<Rc | R<Rc | R<Rc | RH | H | H | H | H | H | H | H | H | H | H |
| 21 | ** | ** | R<Rc | R<Rc | R<Rc | RH | H | H | H | H | H | H | H | H | H | H |
| 22 | ** | ** | R<Rc | R<Rc | R<Rc | H | H | H | H | H | H | H | H | H | H | H |
| 23 | ** | ** | ** | R<Rc | R<Rc | H | H | H | H | H | H | H | H | H | H | H |
| 24 | ** | ** | ** | R<Rc | R<Rc | H | H | H | H | H | H | H | H | H | H | H |
| 25 | ** | ** | ** | ** | R<Rc | H | H | H | H | H | H | H | H | H | H | H |

**Figure 5.4:** HM2 for person at seaside of a seadike crest, $R_c$ = 4m and seaward slope 1:4. Green: No hazard is predicted. Red: Hazardous flow is predicted. Yellow: Relative hazard.

| HM1 | Rc = 4 m | | | slope = 1/4 | | | | | | | | | | | | |
|---|---|---|---|---|---|---|---|---|---|---|---|---|---|---|---|---|
| $T_{m-1,0}$ [s] \ $H_{m0}$ [m] | 0.50 | 0.65 | 0.80 | 0.95 | 1.10 | 1.25 | 1.40 | 1.55 | 1.70 | 1.85 | 2.00 | 2.15 | 2.30 | 2.45 | 2.60 | 2.75 |
| 3 | R<Rc | R<Rc | R<Rc | R<Rc | ** | ** | ** | ** | ** | ** | ** | ** | ** | ** | ** | ** |
| 4 | R<Rc | R<Rc | R<Rc | R<Rc | R<Rc | R<Rc | R<Rc | R<Rc | R<Rc | ** | ** | ** | ** | ** | ** | ** |
| 5 | R<Rc | R<Rc | R<Rc | R<Rc | R<Rc | R<Rc | R<Rc | R<Rc | R<Rc | R<Rc | R<Rc | R<Rc | R<Rc | NH | NH | ** |
| 6 | R<Rc | R<Rc | R<Rc | R<Rc | R<Rc | R<Rc | R<Rc | R<Rc | NH | NH | H | H | H | H | H | H |
| 7 | R<Rc | R<Rc | R<Rc | R<Rc | R<Rc | R<Rc | NH | H | H | H | H | H | H | H | H | H |
| 8 | R<Rc | R<Rc | R<Rc | R<Rc | R<Rc | R<Rc | NH | H | H | H | H | H | H | H | H | H |
| 9 | R<Rc | R<Rc | R<Rc | R<Rc | R<Rc | R<Rc | H | H | H | H | H | H | H | H | H | H |
| 10 | R<Rc | R<Rc | R<Rc | R<Rc | R<Rc | R<Rc | H | H | H | H | H | H | H | H | H | H |
| 11 | R<Rc | R<Rc | R<Rc | R<Rc | R<Rc | R<Rc | H | H | H | H | H | H | H | H | H | H |
| 12 | R<Rc | R<Rc | R<Rc | R<Rc | R<Rc | R<Rc | H | H | H | H | H | H | H | H | H | H |
| 13 | R<Rc | R<Rc | R<Rc | R<Rc | R<Rc | NH | H | H | H | H | H | H | H | H | H | H |
| 14 | R<Rc | R<Rc | R<Rc | R<Rc | R<Rc | NH | H | H | H | H | H | H | H | H | H | H |
| 15 | R<Rc | R<Rc | R<Rc | R<Rc | R<Rc | NH | H | H | H | H | H | H | H | H | H | H |
| 16 | R<Rc | R<Rc | R<Rc | R<Rc | R<Rc | NH | H | H | H | H | H | H | H | H | H | H |
| 17 | R<Rc | R<Rc | R<Rc | R<Rc | R<Rc | NH | H | H | H | H | H | H | H | H | H | H |
| 18 | ** | R<Rc | R<Rc | R<Rc | R<Rc | NH | H | H | H | H | H | H | H | H | H | H |
| 19 | ** | R<Rc | R<Rc | R<Rc | R<Rc | NH | H | H | H | H | H | H | H | H | H | H |
| 20 | ** | R<Rc | R<Rc | R<Rc | R<Rc | NH | H | H | H | H | H | H | H | H | H | H |
| 21 | ** | ** | R<Rc | R<Rc | R<Rc | H | H | H | H | H | H | H | H | H | H | H |
| 22 | ** | ** | R<Rc | R<Rc | R<Rc | H | H | H | H | H | H | H | H | H | H | H |
| 23 | ** | ** | ** | R<Rc | R<Rc | H | H | H | H | H | H | H | H | H | H | H |
| 24 | ** | ** | ** | R<Rc | R<Rc | H | H | H | H | H | H | H | H | H | H | H |
| 25 | ** | ** | ** | ** | R<Rc | H | H | H | H | H | H | H | H | H | H | H |

**Figure 5.5:** HM1 for person at seaside of a seadike crest, $R_c$ = 4m, seaward slope 1:4, and $d_s$<5cm. Green: No hazard is predicted. Red: Hazardous flow is predicted.

Comparing figure 5.4 and 5.5 it can be seen that the risk matrix calculated with M1d, Figure 5.5, does not has a yellow band, this is also produced because of the overestimation of the velocity of the flow. If it is only considered the onset of hazard, red boxes, the differences between the two predictions are not very significant, condition which remain for others freeboard and slopes. However, the prediction generated with M2u does not have the problem of overestimated depth, producing more realistic flows. This is also verified further in Figure 5.18 which shows that the flows calculated with M2u are more similar to the one estimated in the video analysis. For these reason the prediction generated with M2u is considered for the next analysis. The results calculated with M1d are presented in Appendix C.

Figure 5.6 shows the hazard matrix for a seadike slope 1:4 with a lower freeboard of 2 m. As is expected, now smaller wave conditions can generate a critical overtopping flow.

| HM2 | Rc = 2 m | | | slope = 1/4 | | | | | |
|---|---|---|---|---|---|---|---|---|---|
| $T_{m-1,0}$ [s] \ $H_{m0}$ [m] | 0.50 | 0.65 | 0.80 | 0.95 | 1.10 | 1.25 | 1.40 | 1.55 | 1.70 |
| 3 | R<Rc | R<Rc | R<Rc | R<Rc | ** | ** | ** | ** | ** |
| 4 | R<Rc | R<Rc | R<Rc | NH | NH | RH | RH | H | H |
| 5 | R<Rc | R<Rc | RH | H | H | H | H | H | H |
| 6 | R<Rc | R<Rc | RH | H | H | H | H | H | H |
| 7 | R<Rc | NH | RH | H | H | H | H | H | H |
| 8 | R<Rc | NH | RH | H | H | H | H | H | H |
| 9 | R<Rc | NH | RH | H | H | H | H | H | H |
| 10 | R<Rc | NH | RH | H | H | H | H | H | H |
| 11 | R<Rc | NH | H | H | H | H | H | H | H |
| 12 | R<Rc | NH | H | H | H | H | H | H | H |
| 13 | R<Rc | NH | H | H | H | H | H | H | H |
| 14 | R<Rc | NH | H | H | H | H | H | H | H |
| 15 | R<Rc | NH | H | H | H | H | H | H | H |
| 16 | R<Rc | NH | H | H | H | H | H | H | H |
| 17 | R<Rc | NH | H | H | H | H | H | H | H |
| 18 | ** | RH | H | H | H | H | H | H | H |
| 19 | ** | RH | H | H | H | H | H | H | H |
| 20 | ** | RH | H | H | H | H | H | H | H |
| 21 | ** | ** | H | H | H | H | H | H | H |

**Figure 5.6:** Risk matrix for person at seaside of a seadike crest, $R_c$ = 2m and seaward slope 1:4. Green: No hazard is predicted. Red: Hazardous flow is predicted. Yellow: Relative hazard.

Figures 5.7 and 5.8 show the risk prediction for a seadike with slope 1 in 2 and freeboards 4m and 2m respectively. As is expected in a seaward slope of 1:2, smaller waves are needed to produce a hazard compared with a slope of 1:4.

| HM2 | Rc = 4 m | | | slope = 1/2 | | | | | |
|---|---|---|---|---|---|---|---|---|---|
| $T_{m-1,0}$ [s] \ $H_{m0}$ [m] | 0.50 | 0.65 | 0.80 | 0.95 | 1.10 | 1.25 | 1.40 | 1.55 | 1.70 |
| 3 | R<Rc | R<Rc | R<Rc | R<Rc | ** | ** | ** | ** | ** |
| 4 | R<Rc | R<Rc | R<Rc | R<Rc | R<Rc | R<Rc | RH | H | H |
| 5 | R<Rc | R<Rc | R<Rc | R<Rc | R<Rc | R<Rc | RH | H | H |
| 6 | R<Rc | R<Rc | R<Rc | R<Rc | R<Rc | R<Rc | RH | H | H |
| 7 | R<Rc | R<Rc | R<Rc | R<Rc | R<Rc | NH | H | H | H |
| 8 | R<Rc | R<Rc | R<Rc | R<Rc | R<Rc | NH | H | H | H |
| 9 | R<Rc | R<Rc | R<Rc | R<Rc | R<Rc | NH | H | H | H |
| 10 | R<Rc | R<Rc | R<Rc | R<Rc | R<Rc | NH | H | H | H |
| 11 | R<Rc | R<Rc | R<Rc | R<Rc | R<Rc | RH | H | H | H |
| 12 | R<Rc | R<Rc | R<Rc | R<Rc | R<Rc | H | H | H | H |
| 13 | R<Rc | R<Rc | R<Rc | R<Rc | R<Rc | H | H | H | H |
| 14 | R<Rc | R<Rc | R<Rc | R<Rc | R<Rc | H | H | H | H |
| 15 | R<Rc | R<Rc | R<Rc | R<Rc | R<Rc | H | H | H | H |
| 16 | R<Rc | R<Rc | R<Rc | R<Rc | R<Rc | H | H | H | H |
| 17 | R<Rc | R<Rc | R<Rc | R<Rc | R<Rc | H | H | H | H |
| 18 | ** | R<Rc | R<Rc | R<Rc | R<Rc | H | H | H | H |
| 19 | ** | R<Rc | R<Rc | R<Rc | R<Rc | H | H | H | H |

**Figure 5.7:** Risk matrix for person at seaside of a seadike crest, $R_c$ = 4m and seaward slope 1:2. Green: No hazard is predicted. Red: Hazardous flow is predicted. Yellow: Relative hazard.

| HM2 | Rc = 2 m | | | slope = 1/2 | | | | |
|---|---|---|---|---|---|---|---|---|
| $T_{m-1,0}$ [s] \ $H_{m0}$ [m] | 0.50 | 0.65 | 0.80 | 0.95 | 1.10 | 1.25 | 1.40 | 1.55 |
| 3 | R<Rc | R<Rc | NH | H | ** | ** | ** | ** |
| 4 | R<Rc | NH | RH | H | H | H | H | H |
| 5 | R<Rc | NH | RH | H | H | H | H | H |
| 6 | R<Rc | NH | RH | H | H | H | H | H |
| 7 | R<Rc | NH | RH | H | H | H | H | H |
| 8 | R<Rc | NH | H | H | H | H | H | H |
| 9 | R<Rc | NH | H | H | H | H | H | H |
| 10 | R<Rc | RH | H | H | H | H | H | H |
| 11 | R<Rc | RH | H | H | H | H | H | H |
| 12 | R<Rc | RH | H | H | H | H | H | H |
| 13 | R<Rc | H | H | H | H | H | H | H |
| 14 | R<Rc | H | H | H | H | H | H | H |
| 15 | R<Rc | H | H | H | H | H | H | H |
| 16 | R<Rc | H | H | H | H | H | H | H |
| 17 | R<Rc | H | H | H | H | H | H | H |
| 18 | ** | H | H | H | H | H | H | H |
| 19 | ** | H | H | H | H | H | H | H |

**Figure 5.8:** Risk matrix for personal at seaside of a seadike crest, with $R_c$ = 2m and seaward slope 1:2. Green: No hazard is predicted. Red: Hazardous flow is predicted. Yellow: Relative hazard.

In order to compare, on a single graph, different structures for easier analysis, a series of envelopes of risk were generated. These graphs show the curves which separate the hazardous wave conditions, under the line, from the condition which can generate an overtopping flow with the energy to knock over a person.

Figures 5.9, 5.10 and 5.11 show the change of the risk envelope for a seadike with a defined seaward slope but with a variation of freeboard.

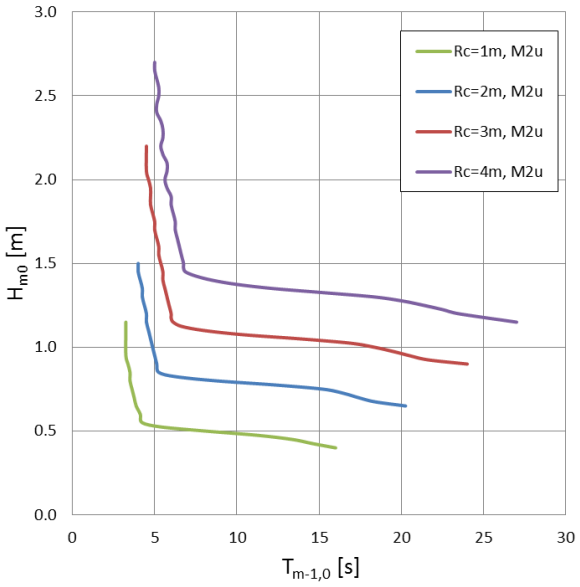


**Figure 5.9:** Risk envelopes for seadike with seaward slope 1 in 4 and Rc={1,2,3,4} calculated with M2u.

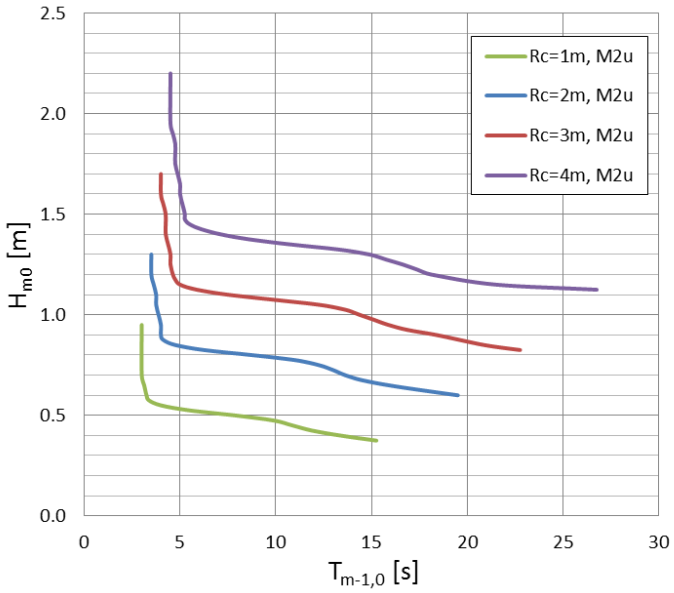


**Figure 5.10:** Risk envelopes for seadike with seaward slope 1 in 3 and Rc={1,2,3,4} calculated with M2u.

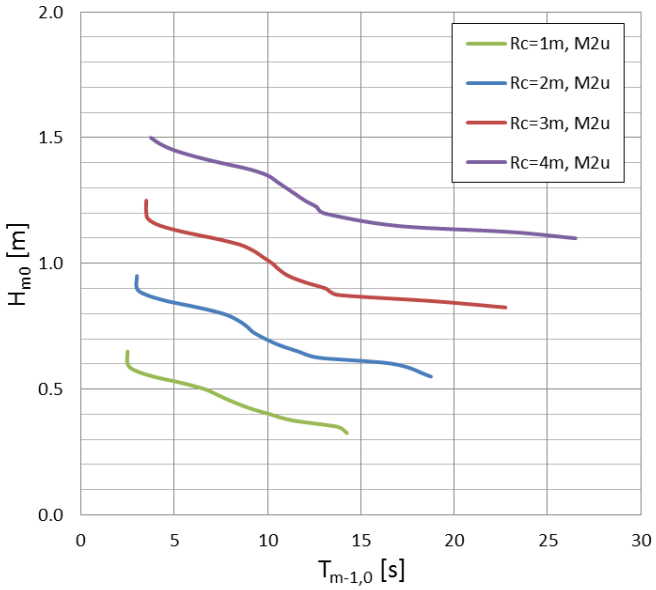


**Figure 5.11:** Risk envelopes for seadike with seaward slope 1 in 2 and Rc={1,2,3,4} calculated with M2u.

Figures 5.12, 5.13, 5.14 and 5.15 show the variation of the hazard envelopes in response to the variation of the freeboard height. It can be seen that the envelopes do not experience such a significant change in comparison with response to variation of the freeboard (previous figures).

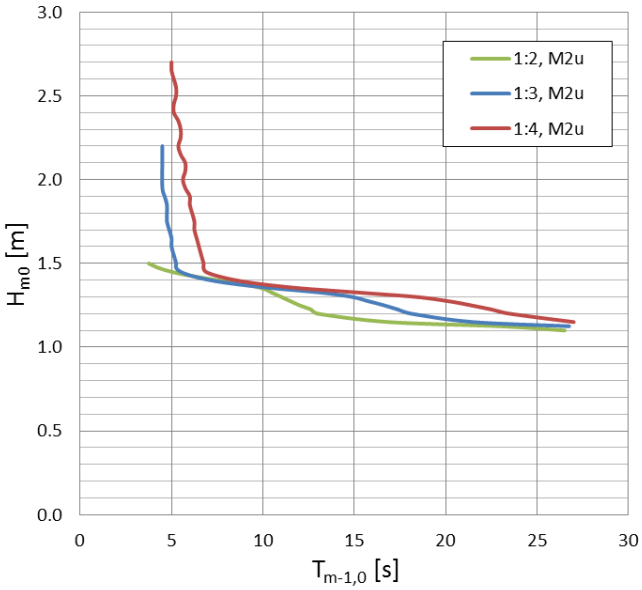


**Figure 5.12:** Risk envelopes for seadike with $R_c$= 4m. and seaward slopes 1:2, 1:3 and 1:4. calculated with M2u.

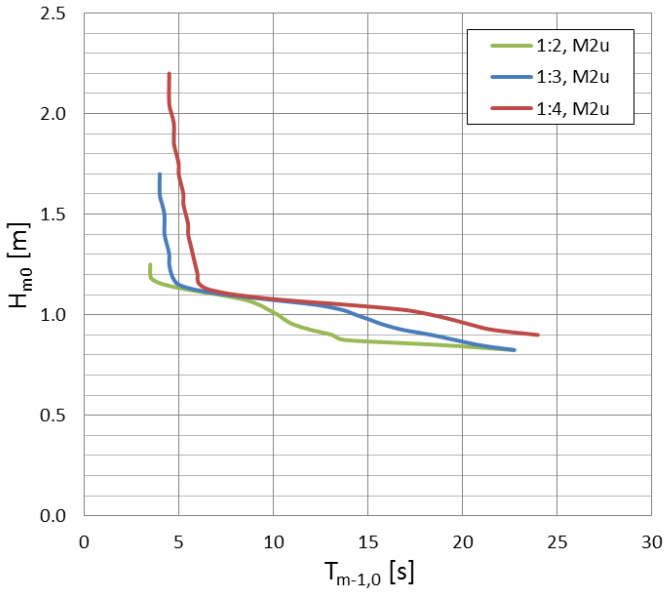


**Figure 5.13:** Risk envelopes for seadike with $R_c$= 3m. and seaward slopes 1:2, 1:3 and 1:4. calculated with M2u.

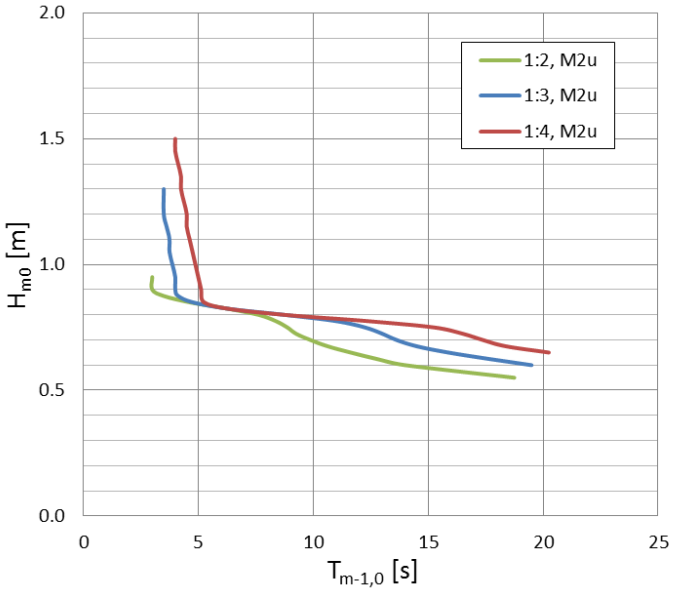


**Figure 5.14:** Risk envelopes for seadike with $R_c$= 2m. and seaward slopes 1:2, 1:3 and 1:4. calculated with M2u.

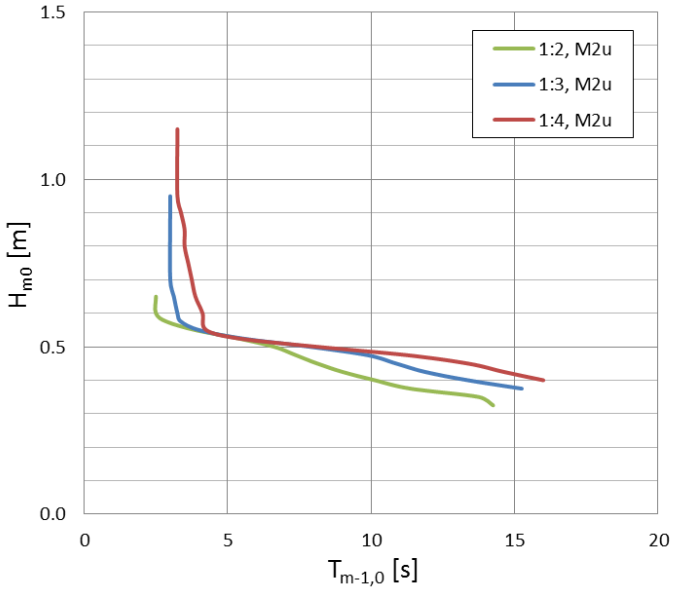


**Figure 5.15:** Risk envelopes for seadike with $R_c$= 1m and seaward slopes 1:2, 1:3 and 1:4, calculated with M2u.

In order to compare the new predictions generated against the general criteria that exist at the present, which use the mean discharge $q$ or the maximum volume $V_{max}$ as indicators of the onset of negative consequences (Table 2.2), the minimum $q$ and $V_{max}$ for each envelope was calculated. Figure 5.16 shows the minimum $q$ for hazard onset. It can be seen that different levels of overtopping are needed in each seadike configuration. Hazardous conditions begin at around 0.35 l/s/m. This discharged is notable higher than the lowest limit in table 2.2, where 0.03 l/s/m is suggested as the threshold for hazard for an unaware and easily frightened pedestrian. Much closer is this limit to 0.1 l/s/m which is the one proposed for an aware pedestrian. It is seen that according a lower crest requires a greater mean discharge to generate a hazardous condition. The graphs also show that the hazardous conditions start with bigger discharges for steeper slopes.

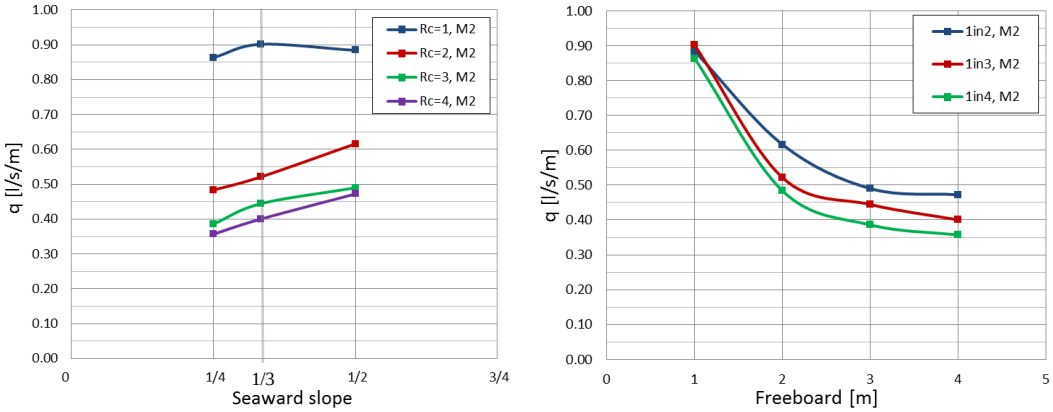


**Figure 5.16:** Minimum mean overtopping discharge required to generate a hazardous condition for personnel at seaside of a seadike.

Figure 5.17 related the onset of hazard to the minimum $V_{max}$ calculated for each seadike configuration. As for the mean discharge, the onset of hazardous conditions in each configuration of the seawall is associated with different $V_{max}$ values. The risk to be knock over begin with $V_{max}$ of around 330 l/m. Table 2.2 gives a volume of 2-5 l/m as a hazardous threshold for an unaware and easily frightened pedestrian, and 20-50 l/m for aware pedestrian with clear view of the situation. These limits are much ower than the value of $V_{max}$ calculated here. It is however more similar to the one corresponding to a person expecting to get wet, given as 500 l/m. The threshold $V_{max}$ decreases with the increase of the slope steepness and $V_{max}$ increases with the increase of the freeboard height.

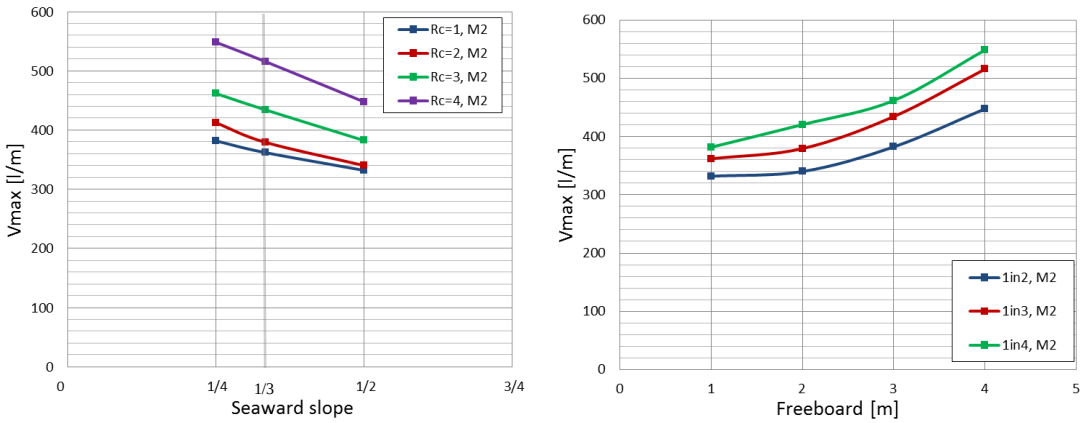


**Figure 5.17:** Minimum overtopping volume to generate a hazardous condition for personnel at seaside of a seadike.

From the comparison of Figures 5.16 and 5.17 with the limits suggested in table 2.3, it can be seen that the current guidelines are more conservative. The results predicted here are however inside the range estimated for previous works. In addition, with the new method it is confirmed that different coastal dike configuration have different admissible $q_{max}$ and $V_{max}$ for onset of hazard, and that it is therefore inadequate to set one admissible discharge for all seawalls.

Figure 5.18 presents the critical ($u_{max}$, $d_{max}$) predicted by the models for the wave conditions for onset of hazard for the seadikes analysed. It can be seen that M1d estimates faster but less deep flow, while on the other hand, M2u predicts deeper but slower flows. Comparing these results with the ones estimated from the overtopping videos, it can be seen that M2u is more similar to these conditions. M1d does not predict an overtopping flow deeper than 0.22m, perhaps a sign of an underestimation of the water depth which in turn produces an overestimation of the velocity. For example the fastest flow predicted was 31 m/s with 0.05 m. depth. On the other hand the maximum depth calculated in M2u is 25.17m for a velocity of 0.04 m/s, a flow condition which is clearly not realistic. Three more conditions with extremely great depth, over 4m, are predicted by M2u. These are generated for long wave condition which generate low run-up but large $V_{max}$, a combination producing a slow but very deep flow. But, even though M2u is generating unrealistic flows the classification as hazardous is agrees with what it would be expected for massive overtopping volumes (over 1,000 l/m). Overall M2u generated more realistic flow condition with the exception of some overestimation of the depth for some wave condition but they do not result in an incorrect hazard classification.

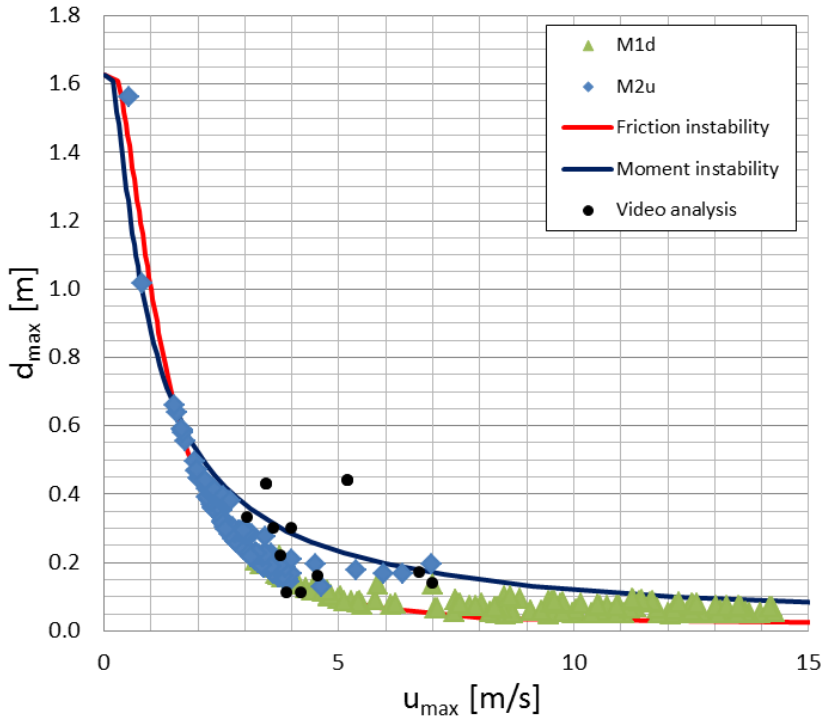


**Figure 5.18:** Critical ($u_{max}$, $d_{max}$) calculated according to Table 5.1.

## 5.4 Sensitivity analysis

All the main parameters used to describe an overtopping flow, to predict the resistance of a person to the flow, and for the subsequent derivation of the hazard matrices and envelopes have uncertainties associated with them. Here, the sensitivity of the hazard predictions to these parameters and associated uncertainty is explored. This information guide priorities for decided future work. For this sensitivity study a seadike with $R_c$=2m and seaward slope 1:2 is used due to this configurations being representative of common cases in urban areas.

### 5.4.1 Human stability

Four parameters will be analysed here, and their influence in the hazard matrix explored. These are person´s height and weight; the friction coefficient, and the drag coefficient.

- **Characteristics of people subject to hazard**

The average features of an adult female were used as a representative person to be exposed to a flow, but it is common that the victims of overtopping accidents are children who are significantly shorter and lighter, and therefore more susceptible to be unbalanced by an overtopping flow.

Figure 5.19 shows the envelopes of risk for a child of 28.1kg and 1.33m tall, representative of a child of around 9 years old. It can be seen that the envelopes get reduced compared with those for an adult (70kg and 1.61m).

The differences can also be examined in the form of hazard matrices (Figure 5.20). Here, the wave conditions of the onset of hazard of Figure 5.8 are highlighted in purple. It can be seen clearly that the hazard matrix for a child will be much more pessimistic than for an adult.

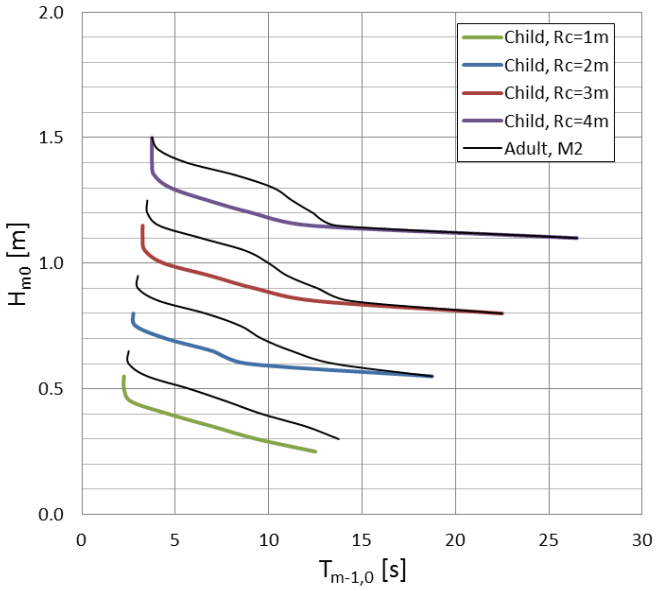


**Figure 5.19:** Risk envelopes for child of $m$=28,1 kg, $h_p$=1.33m (representative for a child of 9 years old) for seadike with seaward slope 1 in 2 and Rc={1,2,3,4} calculated with M2u.

| HM2 | Rc= | 2 | m | slope | 1/2 | | | | |
|---|---|---|---|---|---|---|---|---|---|
| $H_{m0}$ [m] / $T_{m-1,0}$ [s] | 0.50 | 0.65 | 0.80 | 0.95 | 1.10 | 1.25 | 1.40 | 1.55 | 1.70 |
| 3 | R<Rc | R<Rc | H | H | ** | ** | ** | ** | ** |
| 4 | R<Rc | NH | H | H | H | H | H | H | H |
| 5 | R<Rc | NH | H | H | H | H | H | H | H |
| 6 | R<Rc | NH | H | H | H | H | H | H | H |
| 7 | R<Rc | RH | H | H | H | H | H | H | H |
| 8 | R<Rc | H | H | H | H | H | H | H | H |
| 9 | R<Rc | H | H | H | H | H | H | H | H |
| 10 | R<Rc | H | H | H | H | H | H | H | H |
| 11 | R<Rc | H | H | H | H | H | H | H | H |
| 12 | R<Rc | H | H | H | H | H | H | H | H |
| 13 | R<Rc | H | H | H | H | H | H | H | H |
| 14 | R<Rc | H | H | H | H | H | H | H | H |
| 15 | R<Rc | H | H | H | H | H | H | H | H |
| 16 | R<Rc | H | H | H | H | H | H | H | H |
| 17 | R<Rc | H | H | H | H | H | H | H | H |
| 18 | ** | H | H | H | H | H | H | H | H |
| 19 | ** | H | H | H | H | H | H | H | H |

**Figure 5.20: :** Risk Matrix for a child $m$=28.1kg and $h_p$=1.33m at seaside of a seadike crest, $R_c$ = 2 m and seaward slope 1 in 2. Green: No hazard is predicted. Red: Hazardous flow is predicted. Yellow: Relative hazard. Purple: onset of hazard (red) for an adult.

- **Friction coefficient, $\mu$, between person´s feet and ground**

For the derivation of the initial hazard prediction, rubber shoes and a smooth concrete pavement were assumed which, according to Endoh and Takahashi (1995), has a friction coefficient of 0.62. Here, a more pessimistic condition is assumed with leather-soled shoes and a concrete surface covered with seaweed. This situation has a friction coefficient of 0.38, calculated by the same study—a reduction of 39%. Figure 5.21 shows the new prediction. It can be seen that the hazard starts at the same wave height as in the initial prediction. On the other hand the period for onset of hazard change for $H_{m0}$=0.65m and 0.8m, with a reductions of 3s and 5s respectively.

| HM2 | Rc= | 2 | m | slope | 1/2 | μ friction = 0.38 | | | |
|---|---|---|---|---|---|---|---|---|---|
| $H_{m0}$ [m] / $T_{m-1,0}$ [s] | 0.50 | 0.65 | 0.80 | 0.95 | 1.10 | 1.25 | 1.40 | 1.55 | 1.70 |
| 3 | R<Rc | R<Rc | RH | H | ** | ** | ** | ** | ** |
| 4 | R<Rc | NH | H | H | H | H | H | H | H |
| 5 | R<Rc | NH | H | H | H | H | H | H | H |
| 6 | R<Rc | NH | H | H | H | H | H | H | H |
| 7 | R<Rc | NH | H | H | H | H | H | H | H |
| 8 | R<Rc | RH | H | H | H | H | H | H | H |
| 9 | R<Rc | RH | H | H | H | H | H | H | H |
| 10 | R<Rc | H | H | H | H | H | H | H | H |
| 11 | R<Rc | H | H | H | H | H | H | H | H |
| 12 | R<Rc | H | H | H | H | H | H | H | H |
| 13 | R<Rc | H | H | H | H | H | H | H | H |
| 14 | R<Rc | H | H | H | H | H | H | H | H |
| 15 | R<Rc | H | H | H | H | H | H | H | H |
| 16 | R<Rc | H | H | H | H | H | H | H | H |
| 17 | R<Rc | H | H | H | H | H | H | H | H |
| 18 | ** | H | H | H | H | H | H | H | H |
| 19 | ** | H | H | H | H | H | H | H | H |

**Figure 5.21:** Risk Matrix for a person at seaside of a seadike crest, $R_c$ = 2m seaward slope 1:2 and μ=0.38 (Leather shoes and concrete covered with seaweed). Green: No hazard is predicted. Red: Hazardous flow is predicted. Yellow: Relative hazard. Purple: onset of hazard (red) for an adult.

- **Drag coefficient, $C_d$**

The drag coefficient $C_d$ it is needed to estimate the drag force of the flow on the person. Here, it is calculated according to the method proposed by Endoh and Takahashi (1995). This method depends of the position of the person, the separation of the legs and the person´s height. According to the assumption used in this thesis, the value $C_d$ is 0.88, lower value than 1.1 which was proposed in Jonkman and Penning-Rowsell (2008). In order to compare the influence of $C_d$ and $\mu$ in the hazard prediction, an increment of 39% is applied—a percentage corresponding to the reduction of 39% applied to μ. With this increment, the new value for $C_d$ is 1.22—value closer to the one suggested in Jonkman and Penning-Rowsell (2008).

In Figure 5.22, the new prediction is presented. It can be seen that, as expected, that matrix gives a prediction more pessimistic than the initial results. A reductions of 2s and 4s occur for $H_{m0}$=0.65m and 0.80m respectively.

| HM2 | Rc= | 2 | m | slope | 1/2 | Cd = | 1.22 | | |
|---|---|---|---|---|---|---|---|---|---|
| $H_{m0}$ [m] / $T_{m-1,0}$ [s] | 0.50 | 0.65 | 0.80 | 0.95 | 1.10 | 1.25 | 1.40 | 1.55 | 1.70 |
| 3 | R<Rc | R<Rc | RH | H | ** | ** | ** | ** | ** |
| 4 | R<Rc | NH | RH | H | H | H | H | H | H |
| 5 | R<Rc | NH | H | H | H | H | H | H | H |
| 6 | R<Rc | NH | H | H | H | H | H | H | H |
| 7 | R<Rc | NH | H | H | H | H | H | H | H |
| 8 | R<Rc | NH | H | H | H | H | H | H | H |
| 9 | R<Rc | RH | H | H | H | H | H | H | H |
| 10 | R<Rc | RH | H | H | H | H | H | H | H |
| 11 | R<Rc | H | H | H | H | H | H | H | H |
| 12 | R<Rc | H | H | H | H | H | H | H | H |
| 13 | R<Rc | H | H | H | H | H | H | H | H |
| 14 | R<Rc | H | H | H | H | H | H | H | H |
| 15 | R<Rc | H | H | H | H | H | H | H | H |
| 16 | R<Rc | H | H | H | H | H | H | H | H |
| 17 | R<Rc | H | H | H | H | H | H | H | H |
| 18 | ** | H | H | H | H | H | H | H | H |
| 19 | ** | H | H | H | H | H | H | H | H |

**Figure 5.22:** Risk Matrix for a person at seaside of a seadike crest, $R_c$ = 2m, seaward slope 1:2 and $C_d$=1.22. Green: No hazard is predicted. Red: Hazardous flow is predicted. Yellow: Relative hazard. Purple: onset of hazard (red) for an adult.

### 5.4.2 Overtopping flow parameters

Three main parameters are key factors for the derivation of the hazard matrix and envelopes: the overtopping duration ($T_{ovt}$); the maximum depth ($d_{max}$), and the maximum velocity ($u_{max}$). In addition to these parameters, the power curves *d(t)* and *u(t)* also have an influence on the prediction. Here, the influence on the prediction of these parameters is explored.

- **Overtopping duration $T_{ovt}$**

Two possible methodologies were found in the literature to calculate the overtopping duration, Hughes *et al.* (2012), equation 4.16, and Bosman et al. (2008), equation 4.15. Due to the Bosman method predicting longer durations, which could produce an underestimation of the velocity and depth of the flow, the Hughes method was selected for the derivation of the envelopes and matrices of hazard. In this section, the risk matrix is recalculated using the Bosman equation for the duration instead of Hughes equation, with the new result labelled HM2b.

Figure 5.23 shows the new hazard matrix for a seaward slope 1:2 and freeboard 2m. Comparing Figure 5.23 with Figure 5.8, a big difference is seen, with the new predictions being much less pessimistic. This happens because the Bosman equation predicts longer overtopping durations, and therefore the flow is less violent, and $d_{max}$, $u_{max}$ are smaller. With this it is clear that the hazard predictions are very sensitive to $T_{ovt}$. This may present a challenge, as this is perhaps the most poorly researched parameter.

| HM2B Rc= 2 m slope 1/2 | | | | | | | | | |
|---|---|---|---|---|---|---|---|---|---|
| $H_{m0}$ [m] / $T_{m-1,0}$ [s] | 0.50 | 0.65 | 0.80 | 0.95 | 1.10 | 1.25 | 1.40 | 1.55 | 1.70 |
| 3 | R<Rc | R<Rc | NH | H | ** | ** | ** | ** | ** |
| 4 | R<Rc | NH | NH | RH | H | H | H | H | H |
| 5 | R<Rc | NH | NH | RH | H | H | H | H | H |
| 6 | R<Rc | NH | NH | RH | H | H | H | H | H |
| 7 | R<Rc | NH | NH | NH | H | H | H | H | H |
| 8 | R<Rc | NH | NH | NH | H | H | H | H | H |
| 9 | R<Rc | NH | NH | NH | H | H | H | H | H |
| 10 | R<Rc | NH | NH | RH | H | H | H | H | H |
| 11 | R<Rc | NH | NH | RH | H | H | H | H | H |
| 12 | R<Rc | NH | NH | H | H | H | H | H | H |
| 13 | R<Rc | NH | NH | H | H | H | H | H | H |
| 14 | R<Rc | NH | RH | H | H | H | H | H | H |
| 15 | R<Rc | NH | RH | H | H | H | H | H | H |
| 16 | R<Rc | NH | RH | H | H | H | H | H | H |
| 17 | R<Rc | NH | RH | H | H | H | H | H | H |
| 18 | ** | NH | H | H | H | H | H | H | H |
| 19 | ** | RH | H | H | H | H | H | H | H |
| 20 | ** | RH | H | H | H | H | H | H | H |
| 21 | ** | ** | H | H | H | H | H | H | H |
| 22 | ** | ** | H | H | H | H | H | H | H |

**Figure 5.23:** Risk Matrix for a person at seaside of a seadike crest, $R_c$ = 2m, seaward slope 1:2 and $T_{ovt}$ according to Bosman *et al.* (2007). Green: No hazard is predicted. Red: Hazardous flow is predicted. Yellow: Relative hazard. Purple: onset of hazard (red)as predicted by preferred (Hughes *et al*. 2012) method for $T_{ovt}$.

- **Maximum velocity and depth, ($u_{max}$ $d_{max}$)**

Figure 5.21 shows the hazard matrix for a seadike with $R_c$=2m and seaward slope 1:2, but with and increment of the 50% on the calculation of $d_{max}$. This generates a $c_{d,2\%}$=0.35 (equation 4.19), very close to 0.33 which is the value estimated in Schüttrumpf *et al.* (2002) for a large scale model, Figure 4.13. The rise of the depth implies a reduction of $u_{max}$ in order to maintain the volume flow rate. It can be seen

that these new risk prediction is less pessimistic than the previous one (Figure 5.8), reaching the hazardous zone with longer waves.

Figure 5.25 shows the same analysis, but now with an increment of 50% in $u_{max}$ and a reduction of $d_{max}$. The new coefficient $c_{u,2\%}$ is 2.15, 38% greater than the one estimated in Schüttrumpf *et al.* (2002). It can be seen that this new prediction is more pessimistic, compared with figure 5.8, with hazard onset at shorter waves. The periods for the critical conditions are reduced but the $H_{m0}$ which is hazardous for all periods remains the same at 0.95m.

| HM2 | Rc = | 2 m | | slope | 1/2 | 1.5 dmax | | umax/1.5 | |
|---|---|---|---|---|---|---|---|---|---|
| $T_{m-1,0}$ [s] \ $H_{m0}$ [m] | 0.50 | 0.65 | 0.80 | 0.95 | 1.10 | 1.25 | 1.40 | 1.55 | 1.70 |
| 3 | R<Rc | R<Rc | NH | RH | ** | ** | ** | ** | ** |
| 4 | R<Rc | NH | NH | RH | H | H | H | H | H |
| 5 | R<Rc | NH | NH | H | H | H | H | H | H |
| 6 | R<Rc | NH | NH | H | H | H | H | H | H |
| 7 | R<Rc | NH | NH | H | H | H | H | H | H |
| 8 | R<Rc | NH | RH | H | H | H | H | H | H |
| 9 | R<Rc | NH | RH | H | H | H | H | H | H |
| 10 | R<Rc | NH | H | H | H | H | H | H | H |
| 11 | R<Rc | NH | H | H | H | H | H | H | H |
| 12 | R<Rc | RH | H | H | H | H | H | H | H |
| 13 | R<Rc | RH | H | H | H | H | H | H | H |
| 14 | R<Rc | H | H | H | H | H | H | H | H |
| 15 | R<Rc | H | H | H | H | H | H | H | H |
| 16 | R<Rc | H | H | H | H | H | H | H | H |
| 17 | R<Rc | H | H | H | H | H | H | H | H |
| 18 | ** | H | H | H | H | H | H | H | H |
| 19 | ** | H | H | H | H | H | H | H | H |

**Figure 5.24:** Risk Matrix for a person at seaside of a seadike crest, with $R_c$ = 2 m, seaward slope 1:2 and with and increment of 50% on the $d_{max}$. Green: No hazard is predicted. Red: Hazardous flow is predicted. Yellow: Relative hazard. Purple: onset of hazard (red) for an adult.

| HM2 | Rc= | 2 m | | slope | 1/2 | 1.5 umax | | dmax/1.5 | |
|---|---|---|---|---|---|---|---|---|---|
| $H_{m0}$ [m] / $T_{m-1,0}$ [s] | 0.50 | 0.65 | 0.80 | 0.95 | 1.10 | 1.25 | 1.40 | 1.55 | 1.70 |
| 3 | R<Rc | R<Rc | RH | H | ** | ** | ** | ** | ** |
| 4 | R<Rc | NH | RH | H | H | H | H | H | H |
| 5 | R<Rc | NH | H | H | H | H | H | H | H |
| 6 | R<Rc | NH | H | H | H | H | H | H | H |
| 7 | R<Rc | NH | H | H | H | H | H | H | H |
| 8 | R<Rc | NH | H | H | H | H | H | H | H |
| 9 | R<Rc | RH | H | H | H | H | H | H | H |
| 10 | R<Rc | RH | H | H | H | H | H | H | H |
| 11 | R<Rc | H | H | H | H | H | H | H | H |
| 12 | R<Rc | H | H | H | H | H | H | H | H |
| 13 | R<Rc | H | H | H | H | H | H | H | H |
| 14 | R<Rc | H | H | H | H | H | H | H | H |
| 15 | R<Rc | H | H | H | H | H | H | H | H |
| 16 | R<Rc | H | H | H | H | H | H | H | H |
| 17 | R<Rc | H | H | H | H | H | H | H | H |
| 18 | ** | H | H | H | H | H | H | H | H |
| 19 | ** | H | H | H | H | H | H | H | H |

**Figure 5.25:** Risk Matrix for a person at seaside of a seadike crest, with $R_c$ = 2 m, seaward slope 1:2 and with and increment of 50% on the $u_{max}$. Green: No hazard is predicted. Red: Hazardous flow is predicted. Yellow: Relative hazard. Purple: onset of hazard (red) for an adult.

- **Power curves, *d(t)* and *u(t)***

The power curves of the velocity and depth are necessary to do the balance of volume flow rate and in turn, enable the calculation of the maximum parameters upon which it is decide whether the flow has the potential to unbalance a person. The records of *d(t)* and *u(t)* found in the literature offer a convex curve as a good approximation, with a power of 1.5 chosen (equation 4.17 and 4.18, Figure 4.13). There is, however, evidence that in cases of large overtopping volume or violent flows, the form of *d(t)* and *u(t)* can be very convex. On the other hand, has also been suggested in the literature (Bosman 2007) that a linear variation of the velocity and depth can be a good approximation. In this section, the variation of the prediction resulting from the use of a quadratic and a linear variation of the hydraulic parameters, *d(t)* and *u(t)*, is explored.

Figure 5.26 shows that a quadratic function of *h(t)* and *d(t)* generated a more pessimistic risk matrix, as is expected, but the hazard start at the same wave height as in Figure 5.8. On the other hand, a linear variation, Figure 5.27, produces a more

optimistic prediction postponing the beginning of the hazard in 1s and 2s for $H_{m0}$=0.8m and $H_{m0}$=0.65m respectively.

| HM2 | Rc= | 2 m | | slope | 1/2 | Quadratic variation | | | |
|---|---|---|---|---|---|---|---|---|---|
| $H_{m0}$ [m] / $T_{m-1,0}$ [s] | 0.50 | 0.65 | 0.80 | 0.95 | 1.10 | 1.25 | 1.40 | 1.55 | 1.70 |
| 3 | R<Rc | R<Rc | RH | H | ** | ** | ** | ** | ** |
| 4 | R<Rc | NH | RH | H | H | H | H | H | H |
| 5 | R<Rc | NH | RH | H | H | H | H | H | H |
| 6 | R<Rc | NH | H | H | H | H | H | H | H |
| 7 | R<Rc | NH | H | H | H | H | H | H | H |
| 8 | R<Rc | NH | H | H | H | H | H | H | H |
| 9 | R<Rc | RH | H | H | H | H | H | H | H |
| 10 | R<Rc | RH | H | H | H | H | H | H | H |
| 11 | R<Rc | H | H | H | H | H | H | H | H |
| 12 | R<Rc | H | H | H | H | H | H | H | H |
| 13 | R<Rc | H | H | H | H | H | H | H | H |
| 14 | R<Rc | H | H | H | H | H | H | H | H |
| 15 | R<Rc | H | H | H | H | H | H | H | H |
| 16 | R<Rc | H | H | H | H | H | H | H | H |
| 17 | R<Rc | H | H | H | H | H | H | H | H |
| 18 | ** | H | H | H | H | H | H | H | H |
| 19 | ** | H | H | H | H | H | H | H | H |

**Figure 5.26:** Risk Matrix for a person at seaside of a seadike crest, $R_c$ = 2m, seaward slope 1:2 and assuming a quadratic variation of *h(t)* and *u(t)*. Green: No hazard is predicted. Red: Hazardous flow is predicted. Yellow: Relative hazard. Purple: onset of hazard (red) for an adult according to basic model (1.5 power variation in *d(t)* and *u(t)*).

| HM2 | Rc= | 2 m | | slope | 1/2 | Linear variation | | | |
|---|---|---|---|---|---|---|---|---|---|
| $H_{m0}$ [m] / $T_{m-1,0}$ [s] | 0.50 | 0.65 | 0.80 | 0.95 | 1.10 | 1.25 | 1.40 | 1.55 | 1.70 |
| 3 | R<Rc | R<Rc | NH | RH | ** | ** | ** | ** | ** |
| 4 | R<Rc | NH | NH | H | H | H | H | H | H |
| 5 | R<Rc | NH | NH | H | H | H | H | H | H |
| 6 | R<Rc | NH | NH | H | H | H | H | H | H |
| 7 | R<Rc | NH | NH | H | H | H | H | H | H |
| 8 | R<Rc | NH | RH | H | H | H | H | H | H |
| 9 | R<Rc | NH | RH | H | H | H | H | H | H |
| 10 | R<Rc | NH | H | H | H | H | H | H | H |
| 11 | R<Rc | NH | H | H | H | H | H | H | H |
| 12 | R<Rc | RH | H | H | H | H | H | H | H |
| 13 | R<Rc | RH | H | H | H | H | H | H | H |
| 14 | R<Rc | RH | H | H | H | H | H | H | H |
| 15 | R<Rc | H | H | H | H | H | H | H | H |
| 16 | R<Rc | H | H | H | H | H | H | H | H |
| 17 | R<Rc | H | H | H | H | H | H | H | H |
| 18 | ** | H | H | H | H | H | H | H | H |
| 19 | ** | H | H | H | H | H | H | H | H |

**Figure 5.27:** Risk Matrix for a person at seaside of a seadike crest, $R_c$ = 2m, seaward slope 1:2 and assuming a linear variation of *h(t)* and *u(t)*. Green: No hazard is predicted. Red: Hazardous flow is predicted. Yellow: Relative hazard. Purple: onset of hazard (red) for an adult according to basic model (1.5 power variation in *d(t)* and *u(t)*).

## 5.5 Weaknesses and constraints

Due to the near impossibility to predict the actions of a person in the situation of a overtopping flow, a pessimistic posture was used to calculate stability, which was assumed to remain the same during the overtopping event. It was observed in the videos analysed in Chapter 3 that it is common that a person tends to move away from incoming the flow, causing a change in posture and loss contact with the ground during this movement (walking or running). These reactions should have an effect on the stability curves, making it higher if the new posture is more stable or lower if the movement results in a loss of traction and support. These reactions are not being considered here, which could cause an incorrect estimation of the person´s stability.

Due to the limited knowledge of the overtopping flow and the prediction of its main parameters, no well validated methodologies exist at present to calculate the overtopping duration and the velocity and depth of the flow, leaving the prediction of the overtopping flow with a significant uncertainty.

The overtopping duration was calculated with an equation which depends only upon the overtopping volume. It is well-understand that different wave conditions can produce the same volume, but there is no reason to expect that they will have the same duration.

The equation used to calculate $u_{max}$, gives the velocity of the leading edge of the flow, which might be lower than the velocity in the cross section of the flow, which should be used. Sadly no literature on this is known to the author. This could produce and underestimation of the hazard matrix using M2u. This is not a problem in M1d because $u_{max}$ is calculated using $d_{max}$ and $T_{ovt}$, therefore the result corresponds to the velocity needed.

It has been assumed that the parameters $R_{2\%}$, $u_{2\%}$ and $d_{2\%}$ are very close to their maxima. This assumption could generate a small underestimation of the hazard of each wave condition.

The risk predictions derived here are only valid for overtopping composed by mainly green water, where water jets do not present a significant factor in the hazard. In the

derivation of the instability curves, it is only considered that the person will receive the flow at foot level, and impact of water airborne higher up the body are not considered. This situation could be produced in violent overtopping or with the presence of crown walls partially sheltering a person. The effects of the wind on the person´s stability are also not considered here.

## 5.6 Chapter conclusions

Using the findings of Chapter 3 and Chapter 4, a series of risk matrices and envelopes were derived for the crest of a seadike with different freeboard and seaward slopes. For their derivation, an adult with $m$=70 kg and $h_p$=1.61m was assumed, equivalent to the average of adult female. It is assumed that the person is standing at the seaside of the seadike´s crest and standing in front of the flow, as was defined in Chapter 3. For the calculation of the overtopping flow parameters, two different methods, elaborated in Chapter 4, were used resulting two risk predictions, HM1 and HM2. The first one generates the more conservative risk matrices, predicting that shorter wave condition will generate a hazardous flow at the seaside of the crest. In HM1 it was detected the tendency to overestimate the flow velocity which results in unrealistic flows in conditions of very small difference between the run-up and the freeboard, which generated hazardous flows in cases where the overtopping volume is very low—in reality would not present hazard.

The predictions derived were compared with the current guidelines, EurOtop (2007), which use $q$ and $V_{max}$ as indicators of when hazardous situation may occur. The predictions were found to be less pessimistic than these guidelines, with the new method suggesting onset of hazard with greater values of $q$ and $V_{max}$ than the ones suggested for an “unaware and easily frightened pedestrian”. However, the results are much closer to the values related to a “trained staff and expecting to get wet”. This could be explained because the current work neglects the reaction of the person, assuming that the posture will remain throughout the duration of the overtopping flow—an attitude which could be more akin to a trained person´s reaction than for an untrained pedestrian.

It was found that one single value of admissible $q$ or $V_{max}$ is not a good indicator of hazard for all types of seawall. Different seadike configurations will require different level of overtopping to generate a hazardous flow. No clear evidence was found that $V_{max}$ is a better indicator of hazard than $q$, in contrast of what has often been asserted in the literature. This could be related to an overdependence of the overtopping duration with $V_{max}$.

It was found that and increment in the freeboard is much effective to reduce hazard at the crest than change to a gentler slope.

The effect upon the hazard matrix of the inclusion of a child as the subject was explored. A child of 9 years old, m=28.1kg and $h_s$=1.33m was assumed. As was expected, a lower tolerance was found.

A sensitivity analysis of the influence of uncertainties in the friction and drag coefficients was conducted. It was found that of the two, the friction coefficient has a slightly bigger influence on the results, but the uncertainties associated with the estimation of its value are smaller than for the drag coefficient. The definition of a representative $C_d$ for a person standing in different depth of flow has been less studied and validate.

Regarding the overtopping parameters, a large influence of the overtopping duration on the hazard matrix was found. The use of the two methods found in the literature to calculate the overtopping duration—Hughes *et at.* (2012) and Bosman *et al.* (2007)—generated very different hazard matrices, with the one calculated with Bosman method being much less pessimistic. Less influence on the hazard prediction was found for the power curves *d(t)* and *u(t)*. As was expected a quadratic variation—more convex curves—generate a more pessimistic matrix while, on the other hand, a linear variation—less convex curves—generated a less pessimistic matrices.

The influence of a variation in the value of $d_{max}$ and $u_{max}$ in hazard matrices was also explored. It was found that an increment of $d_{max}$ generates a less pessimistic hazard prediction, *i.e.* onset of hazard with bigger waves. On the other hand, an increment of the value of $u_{max}$ generates more pessimistic matrices.

The methodology developed here could generate realistic hazard prediction for seadikes, but more studies are needed in order to verify this.

# Chapter 6

# Conclusions and further work

## 6.1 Conclusions

This research was focused in the study of the human stability in wave overtopping flows, specifically exploring the overtopping flows which can cause people to lose their balance and fall into the flow.

A review of the overtopping process was conducted in Chapter 2, highlighting that it is a very turbulent flow with a diversity of possible scenarios from green waters to a spectaculars splash. It was mentioned that a number of accidents occur due to people being exposed to overtopping flows, producing and average of 2-3 deaths per year in the UK. The definition of the admissible or tolerable overtopping for people has significant uncertainties, as the present recommendations are based upon estimations from a small number of studies. At the present these admissible levels are related to the mean discharge ($q$) and the overtopping maximum volume ($V_{max}$).

The human stability under overtopping flows has little specific literature, so it was necessary to extend the search to other fields of investigation—principally fluvial flows. Four studies were analyse: Abt *et al.* (1989); Endoh and Takahashi (1995); RESCDAM (2001), and Jonkman and Penning-Rowsell (2008). All explored the critical parameters than can cause an unstable condition for a person in running waters. Laboratories and outdoor channels were used to test 31 subjects, males and females, and the critical velocity and depth of the flow at the moment of the instability were recorded. From this, 131 data were generated. Compiling this data together it was found that a wide range of flow conditions can cause unstable situations. Flows with depths between 0.26m to1.2m and velocities between 0.6m/s to 3.6m/s were measured.

In order to verify whether these results can be apply to overtopping flows, an exhaustive internet search was conducted, yielding a dataset of estimates velocity

and depth of the overtopping flows that caused the actual accidents. Hazardous flows with depth between 0.11m to 0.44m and velocities from 3.05m/s to 7m/s were estimated from the overtopping events analysed. Faster and less deep waters were found compared with the data of the previous studies where deeper and slower water were explored. Plotting this two dataset together—literature and video analysis—in a graph $u_{cr}$ v/s $d_{cr}$ demonstrates a clear division of hazardous and non-hazardous flow.

With this enlarged and synthesised dataset of 151 points, the mechanisms of human instability in overtopping flows were studied. The literature identifies two main reasons of instability for persons under flow. The first one—"friction instability"—occurs when the drag force of the flow is bigger than the horizontal resistance of the person given by the friction between their feet and the surface. The second mechanism—"moment instability"—is triggered when the rotational resistance of the person is smaller than the moment generated by the flow. These mechanisms were studied extensively in Endoh and Takahashi (1995) where values for the friction and drag coefficient were elaborated. In the present research the effect of the buoyancy force was included in Endoh´s formulation and an improvement from 35% to 69% was achieved in the accuracy to predict the hazardous zone in a graph $u_{cr}$ v/s $d_{cr}$. The influence of the person´s weight and height was also explored. Considering the minimum weight and height of the sample subjects and separating them by gender, a 90% accuracy was reached for the instability mechanism. According to this method, the resistance of a person is a function of their weight, height, posture, and the friction between surface and feet. On the other hand the hazard of the flow is produced by its depth and velocity.

The video analysis also suggests that the more frequent reason of instability in wave overtopping flows is falling into the flow due to a lack of friction resistance because fast, shallow water are a common combination in this type of flows. Accidents due to moment instability need deeper waters to generate sufficient moment to unbalance a person, but no flow´s depths higher than the person´s knees were estimated in the video analysis.

Another important aspect detected in the video analysis was the range of the human reaction when exposed to the same event. Some people stay still, others walk or run

from the flow. All these different scenarios can change the person´s instability curves, so it is therefore necessary to identify the most pessimistic for input into design and risk assessment.

The calculation of the overtopping flow parameters was studied in Chapter 4 and important literature applicable to seadikes was found. The parameters most studied have been the velocity (u) and the depth (d) of an overtopping flow. From the results of physical models carried it out in Schüttrumpf *et al.* (2002), Van Gent (2002) and Schüttrumpf and Oumeraci (2005), equations to calculate these parameters were developed and calibrated. The equations derived relate the difference between the run-up and the freeboard of the seawall to the overtopping flow depth and the velocity which can be expected during a wave condition. These equations can be used to estimate the maximum overtopping flow depth ($d_{max}$) and maximum overtopping flow velocity ($u_{max}$) which may occur during a storm.

The overtopping duration ($T_{ovt}$) is the other key parameter which has attracted the attention of researchers but it has been much less studied than the velocity and depth. Hughes *et al*. (2012) explored the relation between the overtopping volume of an individual event and the overtopping duration, and developed an equation to predict it. Using the findings for these three parameters ($d_{max}$, $u_{max}$ and $T_{ovt}$), and doing a balance of volume at the crest of a seadike, two methods (M1d and M2u) have been derived here to describe an overtopping flow. Each method gives a combination of $d_{max}$ and $u_{max}$ which may occur during the largest overtopping events under the wave condition.

In Chapter 5 a series of hazard predictions were developed and presented as "matrices" and "envelopes". These predictions are based in the instability mechanisms developed in Chapter 3, and on the two methods now developed for prediction of $u_{max}$ and $d_{max}$ in Chapter 4. It was found that M1d generated less realistic flows due to an over prediction of $u_{max}$ therefore, the prediction calculated with M2u were analysed in deep. For the determination of the onset of instability, an average adult UK female ($m$=70kg and $h$=1.61m) standing in front of the flow at the seaside of the seadike crest was assumed—which was considered as a pessimistic

scenario. Different seadike geometries were explored; $R_c$=1m, 2m, 3m and 4m, and seaward slopes of 1:2, 1:3 and 1:4.

The predictions developed here were compared with the limits $q$ and $V_{max}$ suggested in the EurOtop (2007). With regard to the mean discharge ($q$), the new predictions are in the order of magnitude of those suggested for an "aware pedestrian". It was estimated that hazardous conditions start with a $q$=0.35l/s/m, compared with $q$=0.1 l/s/m suggested for an "aware pedestrian", and 1-10 l/s/m for "trained staff". Comparing instead with the limits expressed in terms of the maximum individual volume, the new predictions are in the order of the one suggested for "trained staff" (500 l/m); $V_{max}$=330l/m. This is significantly higher than the recommendation for an "aware pedestrian" of 20-50 l/m.

The method reflects a significant dependence of the overtopping limits upon the seadike geometry. It is suggest that for higher freeboard, a smaller $q$ is required to generate hazard compared to that needed at lower freeboard. It is also observed that for gently seaward slopes, the $q$ values for unset of hazard are smaller than for a steeper slope. Analysing the maximum volume greater volumes are required for higher freeboard and less steep seaward slope. It is important to notice that different limits were identified for different freeboards, thus the tolerable levels of overtopping if expressed as $q$ or $V_{max}$, actually change during the day together with the tidal fluctuation.

The influence on the hazard prediction of the subject being a child was explored. A nine year old, $m$=28.1kg and $h_s$=1.33m subject was considered instead of an average adult. A considerable reduction in the condition required for hazard onset was observed in the risk matrix, reducing the critical wave height—which cause hazard with any period—from 0.95m to 0.85m.

The sensitivity of the prediction to the friction ($\mu$) and drag ($C_d$) coefficients was also explored. It was found that these parameters had a very similar influence in the results. When the same variation in their values was applied, the wave period at which onset of hazard was predicted was reduced an average of 3s. However important uncertainties exist in the calculation of the $C_d$.

Regarding the calculation of the overtopping parameters ($T_{ovt}$, $u_{max}$ and $d_{max}$), the greatest sensitivity of the outputs was shown to arise from the overtopping duration ($T_{ovt}$), parameter which also have the biggest uncertainties in its calculation. Very different hazard matrices were found depending on which method was used to calculate $T_{ovt}$, Hughes *et al.* (2012) or Bosman *et al.* (2007). The matrix calculated with Bosman´s method were much more optimistic, classifying large overtopping event, over 2,000l/m, as no hazardous, this could be explained for an overestimated $T_{ovt}$.

While methods for the prediction of overtopping discharge and wave-by-wave volumes have become quite advanced, the relationship between this wave overtopping (discharge or volume) and the consequent hazard for people remains a "black box" in the design and assessment of coastal structures, the improvement made during this research aims to whiten this "black box" to reach better and functional coastal defences.

## 6.2 Further work

One of the aims of this project was to include as many of the processes that could influence the prediction of the hazard due to wave overtopping as possible, including human stability and the overtopping flow description. This wide view of the system gave the opportunity to identify areas where improvements are needed due to significant uncertainties or because they have not been deeply studied. Here, the priority areas for further study are proposed in order to improve the hazard prediction developed in this thesis.

- **Related to the human stability:**
    - Previous studies principally motivated by fluvial flow hazard, had generated deeper and slower flows than the ones expected during a wave overtopping flow. A validation of instability mechanism with faster flows is necessary.

- From the video analysis, it was seen that people tend to move away from the flow. This reaction was not considered in the predictions developed here. It is necessary to estimate the influence on the instability curves due to the reaction of the people in order to estimate the more conservative assumption for the human stability.
- The mechanism of instability analysed here only considers flows at ground level and which do not give violent change in velocity and depth. Wave overtopping can result in very violent flows, with water jets which could hit a person's upper body. This situation was not considered in the instability mechanism and requires improvement, especially for the study for hazard at vertical walls were splash and jet waters are very common.
- Great uncertainties exist in the estimation of the drag coefficient $C_d$ which is a critical factor to estimate the overtopping flow force. Its value depends mainly of the shape of the body. This is difficult to define for persons because it depends upon (at least) posture, clothing and leg separation. Endoh and Takahashi (1995) made a significant improvement in this but more tests are needed to validate the method proposed.
- The influences of external factors apart from the overtopping flow were not studied here. The effect of wind and debris are necessary to study.

- **Related to the overtopping flow:**
  - Literature on the calculation of the overtopping flow parameters is restricted to seadikes, but it is necessary to extend the study of overtopping flows at vertical sea walls which are common coastal defence in urban areas. In second place, armoured defences should also be studied from these perspectives.
  - The overtopping duration is shown to have an important influence upon hazard predictions, but is the overtopping flow parameter least studied. Its relation with the overtopping volume and wave steepness

should be studied. In addition, the relation of the overtopping duration with the overtopping volume could give an estimation of the flow violence.

- Significant differences were found between the coefficients used to estimate the overtopping flow depth and velocity, but there have not been new tests which could help to clarify which values describe better the process. New large scale experiments with a seadike are needed in order to reduce these uncertainties.

# References


- Abt. S.R., Wittler R.J., Taylor A. and Love D.J., 1989. Human stability in a high flood hazard zone. Water resources bulletin, Vol. 25, No. 4, pp. 881-890.

- Adams, Matthew (2010). *Massive rogue wave injures crowd at the Maverick's Surf contest on 2/13/10*. [Online Video]. Available from: https://www.youtube.com/watch?v=jV7KhSdUQPU. [Accessed: August 18th 2014].

- BBC (2014). *39 deaths in Scottish coastal waters*. BBC. 24 July 2014. http://www.bbc.co.uk/news/uk-scotland-28451477.

- BBC. *Environment Agency: 7,000 properties to be lost to sea*. 29 December 2014. http://www.bbc.co.uk/news/science-environment-30627285.

- Bosman, G. (2007). *Velocity and flow depth variations during wave overtopping*. Master Thesis. Delft University of Technology, the Netherlands.

- Bosman, G., van der Meer, J.W., Hoffmans G., Schüttrumpf H., and Verhagen H.J., (2008). Individual overtopping events at dikes. ASCE, proc. ICCE 2008, Hamburg, Germany, pp. 2944-2956.

- Bruce, T., Allsop, N. W. H. and Pearson, J. (2001). Violent overtopping of seawall-extended prediction methods. Paper 19 in Proc. Conf. Shorelines, Structures & Breakers, pp 245-255, ICE, London.

- Bruce, T., Allsop, N. W. H. and Pearson, J. (2002). Violent wave overtopping: discharge throw velocities, trajectories an resulting crown deck loading. Proc. Ocean Wave Measurement and Analysis. ASCE, New York. Pp. 1783-1796.

- CLASH. Crest Level Assessment of coastal Structures by full scale monitoring, neural network prediction and Hazard analysis on permissible wave overtopping. Fifth Framework Programme of the EU, Contract n° EVK3-CT-2001-00058.

- De Rouck, J., Verdonck, R., Troch, P., Van Damme, L., Schlütter, F., De Ronde, J. (1998), Wave run-up and overtopping: Prototype versus scale models. In *International coastal engineering conference.* Copenhagen, Denmark, 1998. pp 1039-1052.

- Endoh K. and Takahashi S., 1995. Numerically modeling personnel danger on a promenade breakwater due to overtopping waves. Proceeding of the twenty-fourth international conference on coastal engineering 1994, Vol. 1, ASCE, pp. 1016-1029.

- EurOtop Manual, 2007. *Wave overtopping of Sea Defences and Related Structures – Assessment manual*. UK: Allsop, N.W.H., Pulles, T., Bruce, T. NL: van der Meer, J.W. DE: Schüttrumpf, H., Kortenhaus, A. www.overtopping-manual.com.

- Franco, L., de Gerloni, M. and van der Meer, J.W. (1994). Wave overtopping on vertical and composite breakwaters. Proc. 25th International Conference on coastal engineering. Kobe. Pp. 1030-1044.

- Fox News Chicago (2011). *Dangerous Storm Surge Waves on Lake Michigan!!! Best Footage!!!* [Online Video]. Available from: https://www.youtube.com/watch?v=T9HUwAIFSEo. [Accessed: August 18th 2014].

- Hughes, S.A., and Nadal, N.C. 2009. Laboratory study of combined wave overtopping and storm surge overflow of a levee, Coastal Engineering, Elsevier. Vol. 56. No. 3. Pp 244-259.

- Jonkman S.N. and Penning-Rowsell, 2008. Human instability in flood flows. Journal of the American water resources association, Vol. 44, No. 4.

- Nadal, N.C., Hughes, S.A. (2009), Laboratory study of combined wave overtopping and storm surge overflow of a levee. Coastal Engineering, vol. 56, pp. 244-259.

- National Geographic. *Annual Wave*. [Online Video]. Available from: http://video.nationalgeographic.com/video/annual-wave?source=relatedvideo. [Accessed: August 18th 2014].

- Margaret A. Mcdowell, cheryl D. Fryar, Cybthia L. ogden and Katherine M. Flegal, 2008. Anthropometric reference data for children and adults: United States, 2003-2006, National health statistical reports, number 10.

- Moody, A., 2013, Health Survey for England (HSE) 2012: Vol 1, Chapter 10: Adult Anthropometric Measures, Overweight and Obesity.

- Oumeraci, H., Kortenhaus, A., Allsop, W., de Groot, M., Crough, R., Vrijling, H., Voortman, H. (2001) *Probabilistic design tools for vertical*

*breakwaters* (PROVERBS). Printed by: GPB Gorter bv, Steenwijk, The Netherlands.

- RESCDAM, Helsinki University of Technology, 2001. Co-ordinate by the Finnish Environment Institute. Development of Rescue Actions Based on Dam-Break Flood Analysis. Appendix 2: The use of physical models in dam break flood analysis.

- Schüttrumpf, H. (2001). *Wellenüberlaufströmung bei Seedeichen – experimentelle und ttheoretische Untersuchungen–*. PhD. Thesis. Leichtweiß-Institute (LWI) of the Technical University of Braunschweig, Germany.

- Schüttrumpf, H. and Van Gent M.R.A. (2003). Wave overtopping at seadikes. Proceeding of Coastal Structures 2003. American Society of Civil Engineers, pp. 431-443.

- Schüttrumpf, H. and Oumeraci, H. (2005). Layer thickness and velocities of wave overtopping flow at seadikes. Coastal Engineering, Vol. 52, pp. 473-495.

- Van der Meer, J.W., Bernardini, P., Snejders, W. and Regeling, E. (2006), The wave overtopping simulator. Proc. 30th International Conference on Coastal Engineering, (4654-4666), San Diego, USA.

- Yang X.G., Li YP., Ma G.S., Hu X.Q., Wang J.Z, Cui Z.H., Wanq Z.H., Yu W.T., Yang Z.X., and Zhai F.Y., 2005. Study on weight and height of the Chinese people and the differences between 1992 and 2002.

Appendix A

# Video Analysis

## Video 1: Qiantang River

**Source:** National Geographic. "Annual Wave". 18 August 2014. http://video.nationalgeographic.com/video/annual-wave?source=relatedvideo.


**Figure A.1:** Cars identification video 1.

Assumptions:

- Wide car I: 1.6 m
- Wide car II: 1.66 m.

} Street width: 8.0 m.

- Length car I: 3.92 m.
- Average Chinese male height: $h_s$=1.7 m. (Yang *et al.* 2005)
- High to the knees of the person = 1/4 $h_s$.

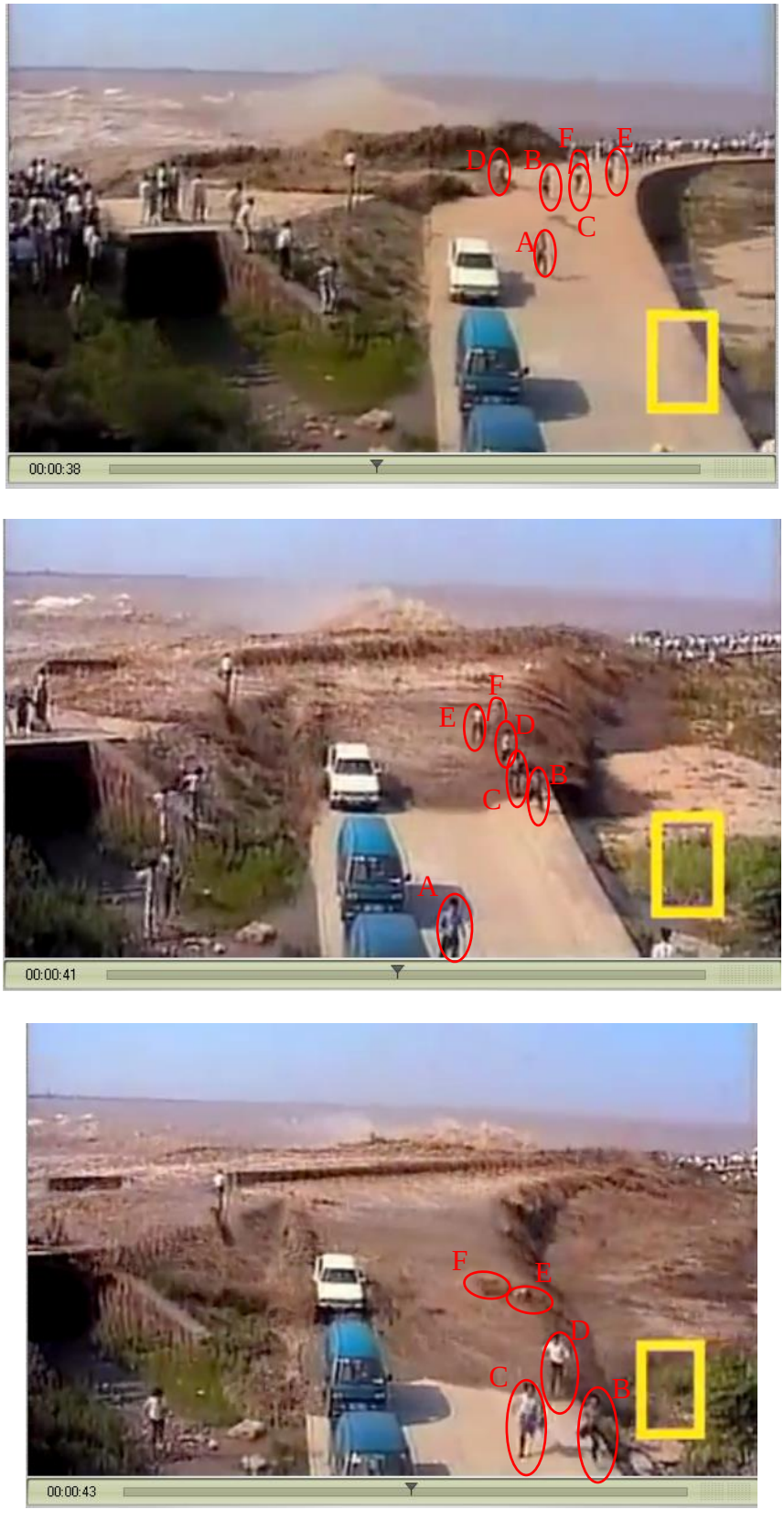


**Figure A.2:** Subjects label**.**

- **Person C:**


**Figure A.3:** Calculation subject C, video 1.

- Velocity front of the flow:

$$\left.\begin{array}{l} a = 4.33m \\ b = 5.3m. \end{array}\right\} h = \sqrt{4.33^2 + 5.3^2} = 6.8m. \qquad \left.\begin{array}{l} t_i = 00:03:16 \\ t_f = 00:04:53 \end{array}\right\} \Delta t = 1.37s$$

$$\left.\begin{array}{l} \\ \\ \end{array}\right\} u = \frac{6.8}{1.37} = 4.96\left[\frac{m}{s}\right] (\text{speed front of the flow})$$

- Depth:

$$d = \frac{1}{4}\cdot\left(\frac{1}{4}\cdot h_s\right) = \frac{1}{4}\cdot\left(\frac{1}{4}\cdot 1.7\right) = 0.11m.$$

- **Person D:**


**Figure A.4:** Calculation subject D, video 1.

- Velocity front of the flow:

$$\left.\begin{array}{l} a = 8m \\ b = 3.19m. \end{array}\right\} h = \sqrt{8^2 + 3.19^2} = 8.61m. \qquad \left.\begin{array}{l} t_i = 00:00:26 \\ t_f = 00:02:70 \end{array}\right\} \Delta t = 2.44s$$

$$\left.\begin{array}{l} \\ \\ \end{array}\right\} u = \frac{8.61}{2.44} = 3.52\left[\frac{m}{s}\right] (\text{speed front of the flow})$$

- Depth:

$$d = \frac{1}{2}\cdot\left(\frac{1}{4}\cdot h_s\right) = \frac{1}{2}\cdot\left(\frac{1}{4}\cdot 1.7\right) = 0.21m.$$

- **Person E and F:**

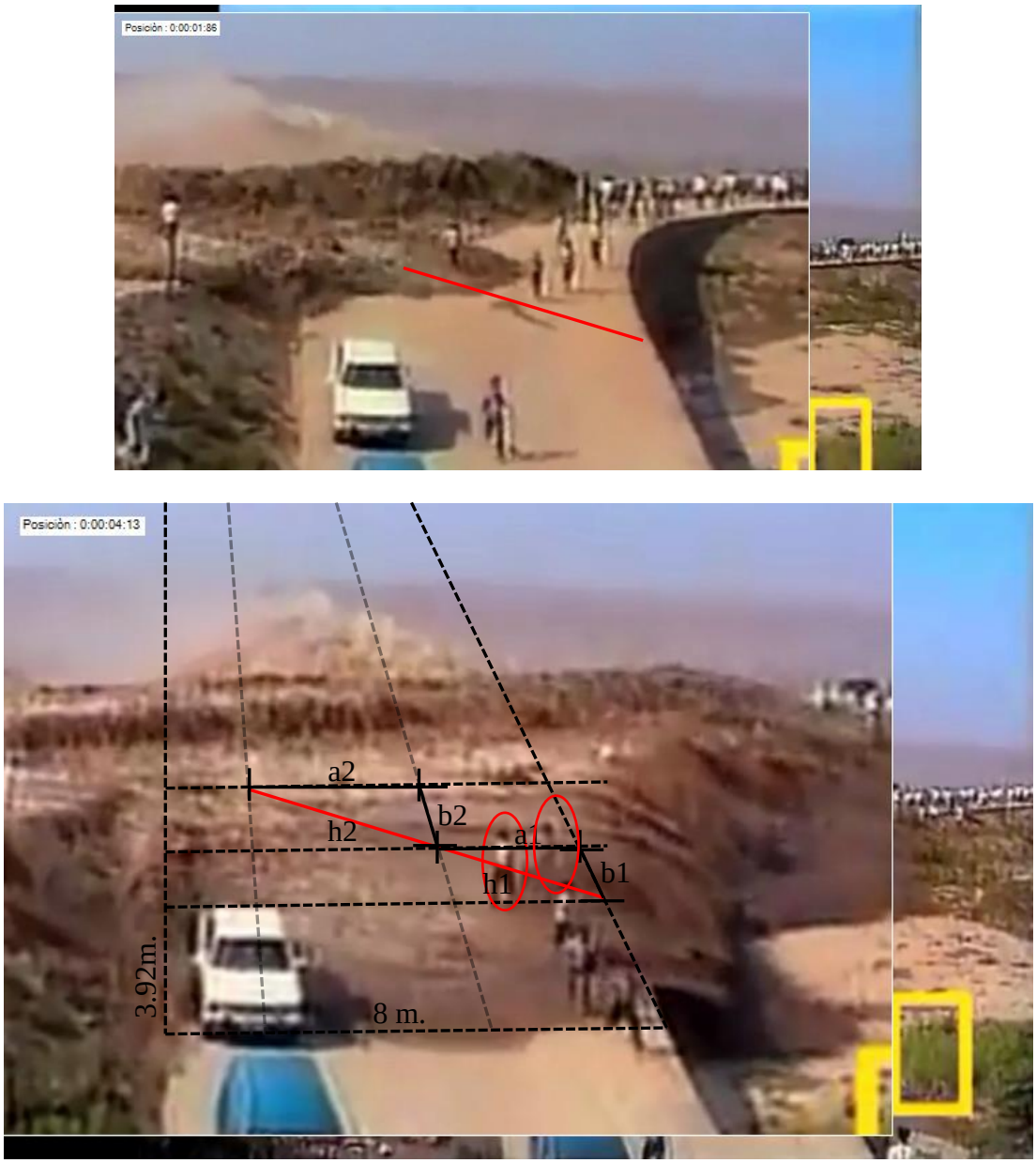


**Figure A.5:** Calculation subject E and F, option1, video 1.

- Velocity front of the flow, option1:

$$\left.\begin{array}{l} \left.\begin{array}{l} a1 = 2.98m \\ b1 = 2.1m. \end{array}\right\} h1 = \sqrt{2.98^2 + 2.1^2} = 3.64m. \\ \left.\begin{array}{l} a2 = 3.53m \\ b2 = 2.5m. \end{array}\right\} h2 = \sqrt{3.53^2 + 2.5^2} = 4.33m. \end{array}\right\} h = 7.97$$

$$\left.\begin{array}{l} t_i = 00:01:86 \\ t_f = 00:04:13 \end{array}\right\} \Delta t = 2.27s$$

$$u1 = \frac{7.97}{2.27} = 3.51\left[\frac{m}{s}\right] \text{(speed front of the flow)}$$


**Figure A.6:** Calculation subjects E and F, option2, video 1.

- Velocity front of the flow, option2:

$$\left.\begin{array}{l} a = 6.45m \\ b = 1.3m. \end{array}\right\} h = \sqrt{6.45^2 + 1.3^2} = 6.58m. \qquad \left.\begin{array}{l} t_i = 00:02:03 \\ t_f = 00:03:97 \end{array}\right\} \Delta t = 1.94s$$

$$\left.\begin{array}{l} \\ \\ \end{array}\right\} u2 = \frac{6.58}{1.94} = 3.39\left[\frac{m}{s}\right] (\text{speed front of the flow})$$

- Velocity front of the flow:

$$u = \frac{u1 + u2}{2} = \frac{3.51 + 3.39}{2} = 3.45\left[\frac{m}{s}\right] (\text{speed front of the flow})$$

- Depth:

$$d = \left(\frac{1}{4} \cdot h_s\right) = \left(\frac{1}{4} \cdot 1.7\right) = 0.43m.$$

Table A.1: **Summary video 1.**

| Subject | Sex | Age | Height* [m] | Surface | $u_f$ [m/s] | $d$ [m] | $T_{ovt}$ [s] | Consequence | Observation |
|---|---|---|---|---|---|---|---|---|---|
| A | male | adult | 1,7 | concrete | -- | -- | -- | No | No reached by overtopping |
| B | male | adult | 1,7 | concrete | -- | -- | -- | No | No reached by overtopping |
| *E* | male | adult | 1,7 | concrete | 3,45 | 0,43 | > 10 | Wash out | Running |
| *F* | male | adult | 1,7 | concrete | 3,45 | 0,43 | > 10 | Wash out | Running |
| *C* | male | adult | 1,7 | concrete | 4,96 | 0,11 | > 10 | No | Running |
| *D* | male | adult | 1,7 | concrete | 3,52 | 0,21 | > 10 | No | Running |

## Video 2: Michigan Lake, United Estates.

**Source:** Fox Chicago. "Dangerous Storm Surge Waves on Lake Michigan!!! Best Footage!!!". YouTube. 18 August 2014. https://www.youtube.com/watch?v=T9HUwAIFSEo.

Assumptions:

- Average USA male height: $h_{sm}$=1.77 m (Margaret A. *et al.* 2008).
- Average USA female height: $h_{sf}$=1.63 m (Margaret A. *et al.* 2008).
- Diameter bike wheel 26", $D_b$= 66cm.
- Referential distances according to Figure A.7.
- High to the knees of the person = 1/4 $h_s$.

**Table A.2:** Subject identification video 2.

| Subject | Sex | Age | Height* [m] | Type | Time in video [s] | Observation |
|---|---|---|---|---|---|---|
| Ach | Male | Adult | 1.77 | Biker | 0:45 to 1:00 | Not reached by overtopping. |
| Bch | Male | Adult | 1.77 | Biker | 1:22 to 2:10 | Reached by overtopping. |
| Cch | Male | Adult | 1.77 | Pedestrian | 2:57 to 3:23 | Not reached by overtopping. |
| Dch | Male | Adult | 1.77 | Pedestrian | 3:23 to 4:04 | Not reached by overtopping. |
| Ech | Female | Adult | 1.63 | Pedestrian | 4:40 to 5:08 | Reached by overtopping. |
| Fch | Male | Adult | 1.77 | Biker | 5:09 to 5:34 | Reached by overtopping. |
| Gch | Male | Adult | 1.77 | Biker | 5:34 to 6:24 | Reached by overtopping. |
| Hch | Male | Adult | 1.77 | Biker | 6:31 to 6:48 | Reached by overtopping. |
| Ich | Male | Adult | 1.77 | Biker | 6:31 to 7:05 | Reached by overtopping. |
| Jch | Male | Adult | 1.77 | Biker | 6:59 to 7:26 | Reached by overtopping. |
| Kch | Male | Adult | 1.77 | Biker | 8:19 to 8:43 | Reached by overtopping. |
| Lch | Male | Adult | 1.77 | Biker | 9:17 to 9:28 | Not reached by overtopping. |

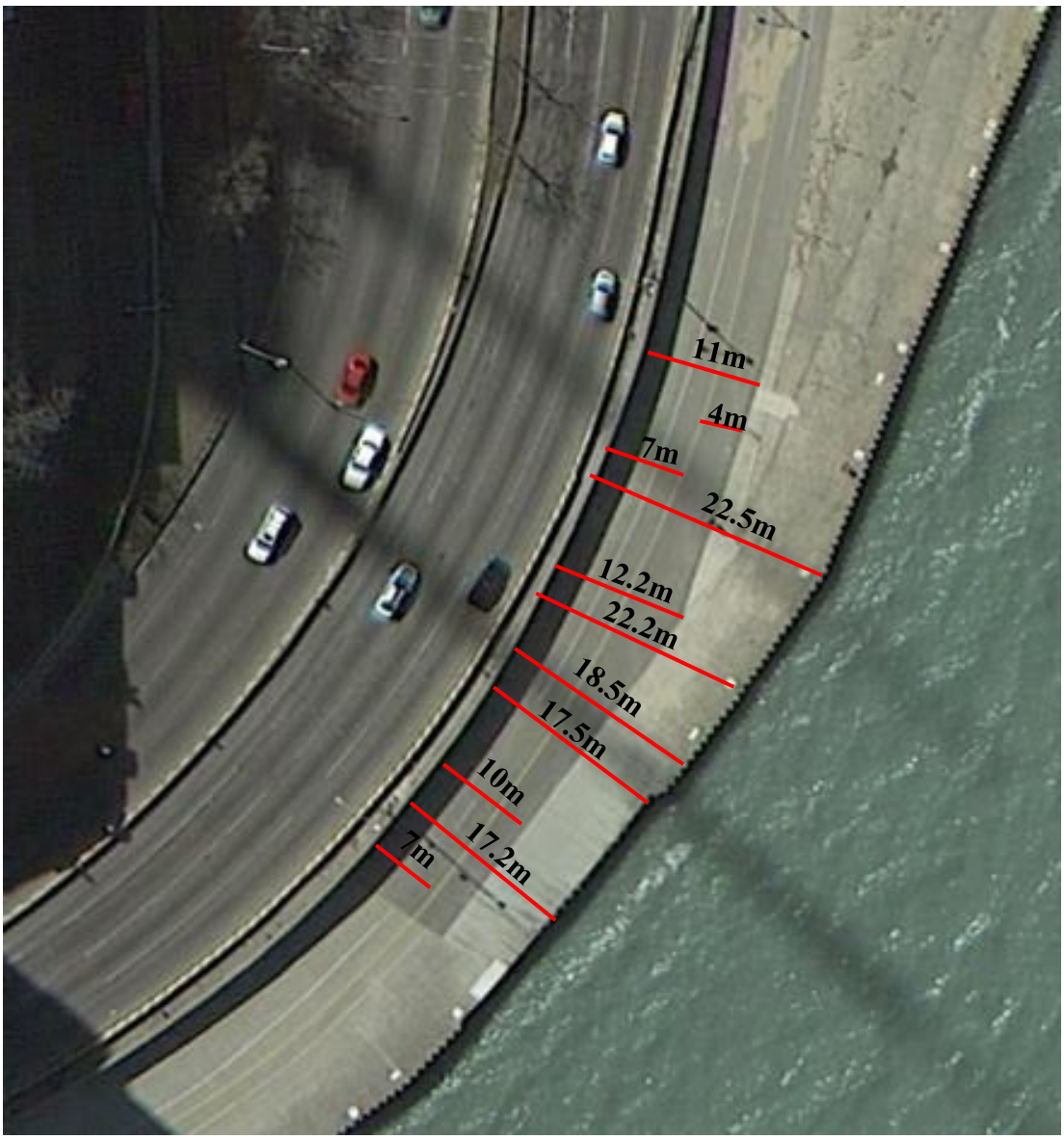


**Figure A.7:** Referential distances used to calculate velocity in video 2. All measurements estimated wit Google earth. Source: Google Earth.

- **Person Bch first flow:**


**Figure A.8:** Calculation first flow speed v1 subject Bch, video2.

$$\left.\begin{array}{l} Dis\tan ce = 7m. \\ t_i = 01:22:53 \\ t_f = 01:24:30 \end{array}\right\} \Delta t = 1.77s \Big\} u1 = \frac{7}{1.77} = 3.95\left[\frac{m}{s}\right]$$

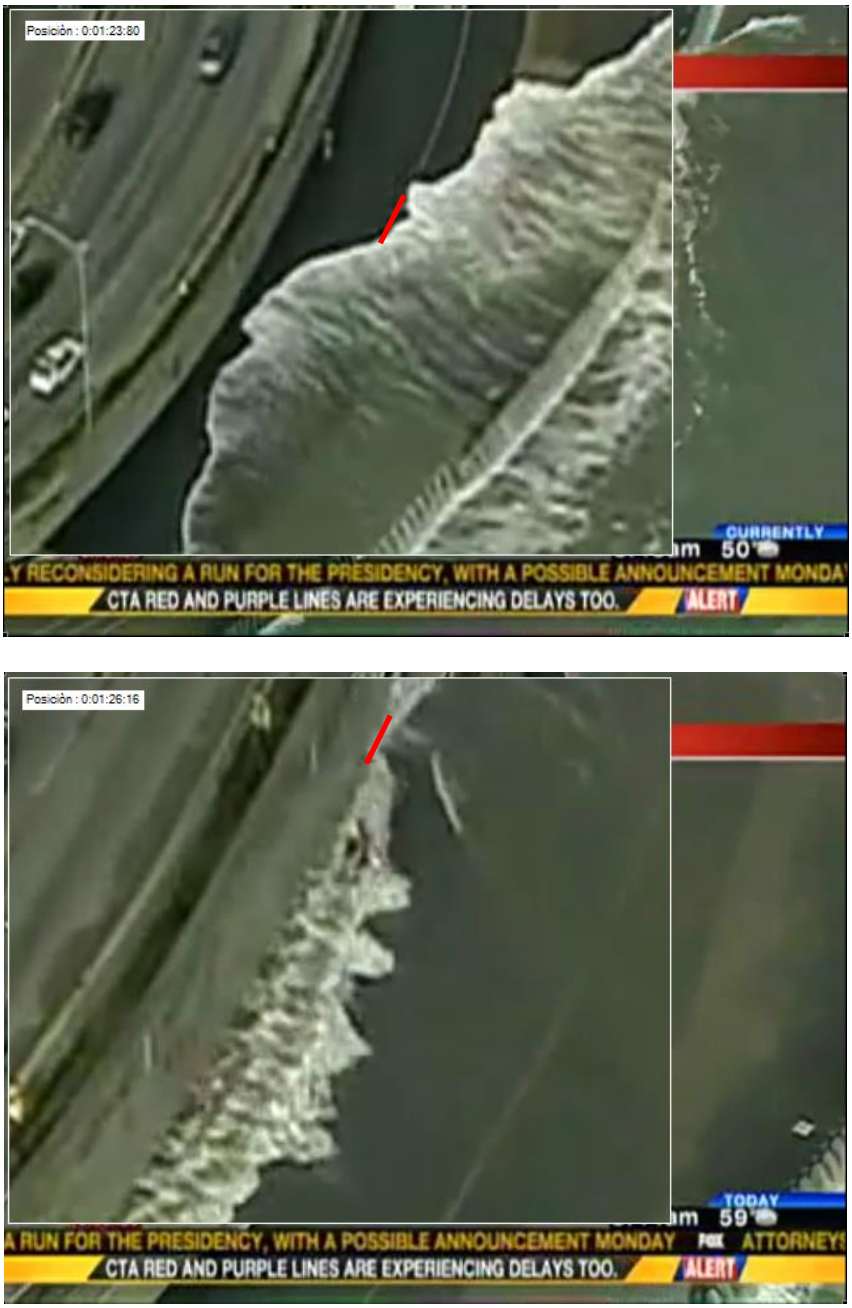


**Figure A.9:** Calculation first flow speed v2 subject Bch, video2.

$$\left.\begin{array}{l} Dis\tan ce = 7m. \\ t_i = 01:23:80 \\ t_f = 01:26:16 \end{array}\right\} \Delta t = 2.36s \Bigg\} u2 = \frac{7}{2.36} = 2.97\left[\frac{m}{s}\right]$$

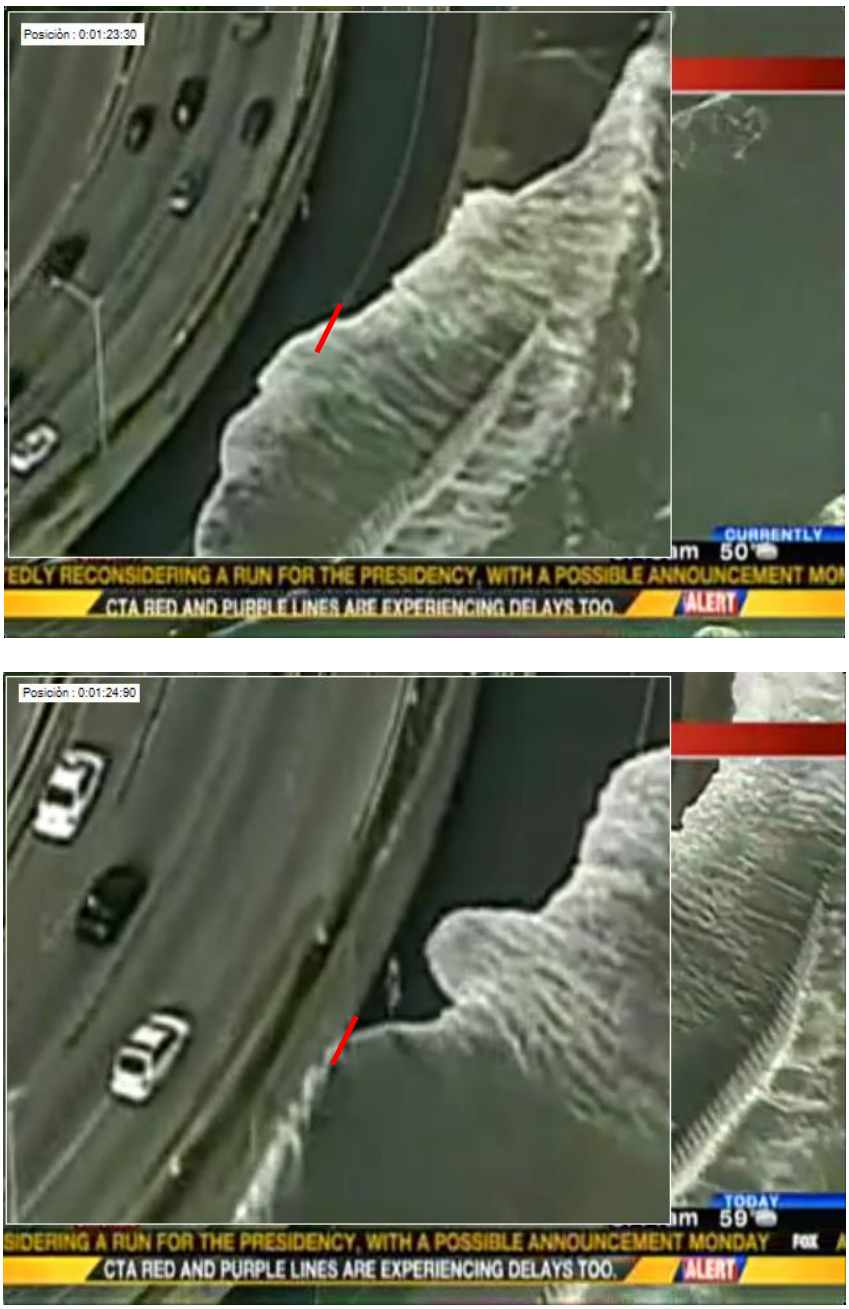


**Figure A.10:** Calculation first flow speed v3 subject Bch, video2.

$$\left.\begin{array}{l} Dis\tan ce = 7m. \\ t_i = 01:23:30 \\ t_f = 01:24:90 \end{array}\right\} \Delta t = 1.6s \Bigg\} u3 = \frac{7}{1.6} = 4.38\left[\frac{m}{s}\right]$$

- Velocity front of the flow:

$$u = \frac{u1+u2+u3}{2} = \frac{3.95+2.97+4.38}{2} = 3.77\left[\frac{m}{s}\right]$$

- Depth:

$$d = \frac{1}{3}\cdot D_b = \frac{1}{3}\cdot 66 = 22m.$$

- **Person Bch second flow:**


**Figure A.11:** Calculation second flow speed subject Bch, video2.

- Velocity front of the flow:

$$\left.\begin{array}{l} Dis\tan ce = 7m. \\ t_i = 01:32:86 \\ t_f = 01:33:90 \end{array}\right\}\Delta t = 1.04s \left.\right\} u2 = \frac{7}{1.04} = 6.73\left[\frac{m}{s}\right]$$

- Depth:

$$d = \frac{1}{4}\cdot D_b = \frac{1}{4}\cdot 0.66 = 0.165m.$$

- **Person Bch third flow:**


**Figure A.12:** Calculation third flow speed subject Bch, video2.

- Velocity front of the flow:

$$\left.\begin{array}{l} Dis\tan ce = 4m. \\ t_i = 01:45:80 \\ t_f = 01:46:86 \end{array}\right\}\Delta t = 1.06s \Bigg\} u = \frac{4}{1.06} = 3.77\left[\frac{m}{s}\right]$$

- Depth:

$$d = \frac{1}{2}\cdot\left(\frac{1}{4}\cdot h_s\right) = \frac{1}{2}\cdot\left(\frac{1}{4}\cdot 1.77\right) = 0.22\,m.$$

- **Person Ech flow:**


**Figure A.13:** Calculation speed subject Ech, video2.

- Velocity front of the flow:

$$\left.\begin{array}{l} Dis\tan ce = 7m. \\ t_i = 04:40:10 \\ t_f = 04:44:60 \end{array}\right\} \Delta t = 4.5s \left\{ u = \frac{7}{4.5} = 1.56\left[\frac{m}{s}\right] \right.$$

- Depth:

$$d = \frac{1}{4}\cdot\left(\frac{1}{4}\cdot h_s\right) = \frac{1}{4}\cdot\left(\frac{1}{4}\cdot 1.63\right) = 0.10\,m.$$

- **Person Fch flow:**



**Figure A.14:** Calculation speed subject Fch, video2.

- Velocity front of the flow:

$$\left.\begin{array}{l} Dis\tan ce = 7m. \\ t_i = 05:11:36 \\ t_f = 05:12:36 \end{array}\right\} \Delta t = 1s \Bigg\} \; u = \frac{7}{1} = 7\left[\frac{m}{s}\right]$$

- Depth:

$$d = \left(\frac{1}{6} \cdot D_b\right) = \left(\frac{1}{6} \cdot 0.66\right) = 0.11 m.$$

- **Person Gch first flow:**


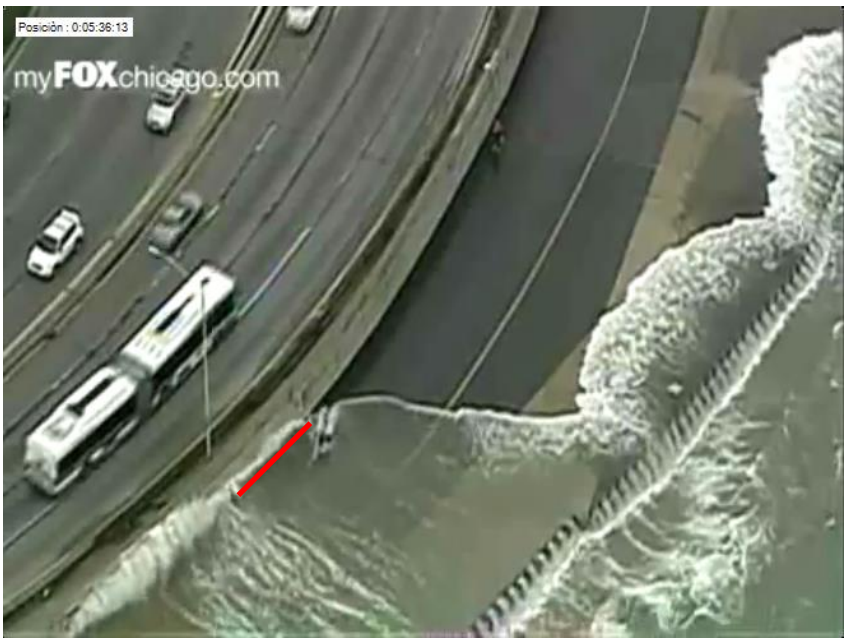


**Figure A.15:** Calculation first flow speed subject Gch, video2.

- Velocity front of the flow:

$$\left.\begin{array}{l} Dis\tan ce = 7m. \\ t_i = 05:34:46 \\ t_f = 05:36:13 \end{array}\right\} \Delta t = 1.67s \left.\right\} \; u = \frac{7}{1.67} = 4.19\left[\frac{m}{s}\right]$$

- Depth:

$$d = \left(\frac{1}{6}\cdot D_b\right) = \left(\frac{1}{6}\cdot 0.66\right) = 0.11m.$$

- **Person Gch second flow:**


**Figure A.16:** Calculation second flow speed subject Gch, video2.

- Velocity front of the flow:

$$\left.\begin{array}{l} Dis\tan ce = 6m. \\ t_i = 05:36:83 \\ t_f = 05:38:80 \end{array}\right\} \Delta t = 1.97s \left.\right\} \; u = \frac{6}{1.97} = 3.05\left[\frac{m}{s}\right]$$

- Depth:

$$d = \left(\frac{1}{2}\cdot D_b\right) = \left(\frac{1}{2}\cdot 0.66\right) = 0.33m.$$

- **Person Gch third flow:**



**Figure A.17:** Calculation third flow speed subject Gch, video2.

- Velocity front of the flow:

$$\left.\begin{array}{l} Dis\tan ce = 7m. \\ t_i = 05:45:00 \\ t_f = 05:46:36 \end{array}\right\} \Delta t = 1.36s \left.\right\} \; u = \frac{7}{1.36} = 5.15\left[\frac{m}{s}\right]$$

- Depth:

$$d = \frac{2}{3}\cdot\left(\frac{1}{4}\cdot h_s\right) = \frac{2}{3}\cdot\left(\frac{1}{4}\cdot 1.77\right) = 0.3m.$$

- **Person Hch:**

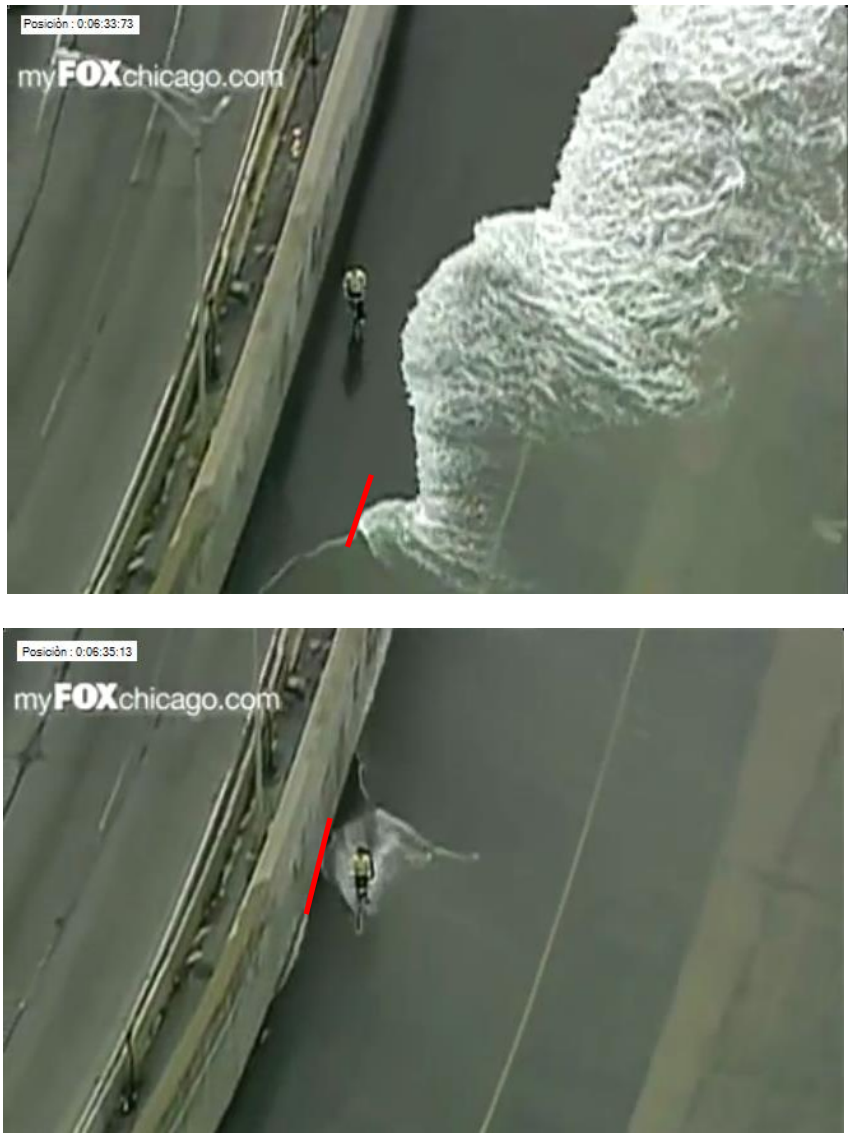


**Figure A.18:** Calculation speed´s flow subject Hch, video2.

- Velocity front of the flow:

$$\left.\begin{array}{l} Dis\tan ce = 3.5m. \\ t_i = 06:33:73 \\ t_f = 06:35:13 \end{array}\right\} \Delta t = 1.4s \Bigg\} \; u = \frac{3.5}{1.4} = 2.5\left[\frac{m}{s}\right]$$

- Depth:

$$d = \left(\frac{1}{8}\cdot D_b\right) = \left(\frac{1}{8}\cdot 0.66\right) = 0.08\,m.$$

- **Person Ich first flow:**


**Figure A.19:** Calculation first speed´s flow subject Ich, video2.

- Velocity front of the flow:

$$\left.\begin{array}{l} Dis\tan ce = 7m. \\ t_i = 06:47:13 \\ t_f = 06:48:66 \end{array}\right\} \Delta t = 1.53s \left.\right\} \; u = \frac{7}{1.53} = 4.56\left[\frac{m}{s}\right]$$

- Depth:

$$d = \left(\frac{1}{4}\cdot D_b\right) = \left(\frac{1}{4}\cdot 0.66\right) = 0.165\,m.$$

- **Person Ich second flow:**



**Figure A.20:** Calculation second speed´s flow subject Ich, video2.

- Velocity front of the flow:

$$\left.\begin{array}{l} Dis\tan ce = 3.5m. \\ t_i = 06:59:13 \\ t_f = 07:00:13 \end{array}\right\} \Delta t = 1.0s \Bigg\} \; u = \frac{3.5}{1.0} = 3.5\left[\frac{m}{s}\right]$$

- Depth:

$$d = \left(\frac{1}{8}\cdot D_b\right) = \left(\frac{1}{8}\cdot 0.66\right) = 0.08\,m.$$

- **Person Kch:**


**Figure A.21:** Calculation speed´s flow subject Kch, video2.

- Velocity front of the flow:

$$\left.\begin{array}{l} Dis\tan ce = 7m. \\ t_i = 08:21:66 \\ t_f = 08:23:46 \end{array}\right\} \Delta t = 1.8s \Bigg\} \; u = \frac{7}{1.8} = 3.89\left[\frac{m}{s}\right]$$

- Depth:

$$d = \left(\frac{1}{6}\cdot D_b\right) = \left(\frac{1}{6}\cdot 0.66\right) = 0.11m.$$

**Table A.3:** Summary video 2.

| Subject | $u$ [m/s] | $d$ [m] | $T_{ovt}$ [s] | Consequence | Observation |
|---|---|---|---|---|---|
| B ch | 3.77 | 0.22 | 4 | Stop | He couldn´t ride the bike more. |
| | 6.73 | 0.17 | -- | Wash out | Fall by the reflected flow. See figure 3.15 |
| | 3.77 | 0.22 | 5 | No | Walk a resist new overtopping flow. Used bike as a third point |
| E ch | 1.56 | 0.1 | 4 | No | |
| F ch | 7 | 0.14 | 4 | Stop | He couldn´t ride the bike more. |
| G ch | 4.19 | 0.11 | -- | Stop | He couldn´t ride the bike more. |
| | 3.05 | 0.33 | -- | Fall | Fall by the reflected flow |
| | 5.15 | 0.3 | -- | No | The person used the bike as a "walking stick". The biker is aware of the risk. |
| H ch | 2.5 | 0.08 | -- | No | |
| I ch | 4.56 | 0.16 | -- | Stop | Stop due to the flow crashing against second wall |
| | 3.5 | 0.08 | -- | No | |
| K ch | 3.89 | 0.11 | -- | Stop | Stop due to the flow crashing against second wall |

## Video 3: Maverick´s coast, United Estate.

**Source:** Adams , Matthew. "Massive rogue wave injures crowd at the Maverick's Surf contest on 2/13/10". YouTube. 18 August 2014. https://www.youtube.com/watch?v=jV7KhSdUQPU.

Assumptions:

- Average USA male height: $h_{sm}$=1.77 m (Margaret A. *et al.* 2008).
- Average USA female height: $h_{sf}$=1.63 m (Margaret A. *et al.* 2008).
- Referential distances according to Figure A.7.
- High to the knees of the person = 1/4 $h_s$.

**Table A.4:** Subject identification video 2.

| Subject | Observation |
|---|---|
| Am | *d*: OK.<br>*u*: Important uncertainties. |
| Bm | *d*: Important uncertainties.<br>*u*: Important uncertainties. |
| Cm | *d*: No shot.<br>*u*: No shot. |
| Dm | *d*: OK.<br>*u*: OK. |
| Em | *d*: Not possible to estimate.<br>*u*: Not possible to estimate. |
| Fm | *d*: OK.<br>*u*: OK. |
| Gm | *d*: Important uncertainties.<br>*u*: Important uncertainties. |
| Hm | No reached by overtopping |
| Im | *d*: Not possible to estimate.<br>*u*: Not possible to estimate. |
| Jm | *d*: Not possible to estimate.<br>*u*: Not possible to estimate. |
| Km | *d*: Not possible to estimate.<br>*u*: Not possible to estimate. |


**Figure A.22:** Subject label video3.


**Figure A.23:** Subject label video3.


Figure A.24: **Subject label video3.**

- **Person Am:**

  Subject reached by the flow on the crown of the wall and wash out. Splash and violent flows occur.


**Figure A.25:** Calculation speed´s flow subject Am, video3.

- Velocity front of the flow:

$$\left.\begin{array}{l} Dis\tan ce = 2.75m\,(\text{Estimated scaffoldin g width}) \\ \left.\begin{array}{l} t_i = 02.23^{**} \\ t_f = 02.76 \end{array}\right\}\Delta t = 0.53s \end{array}\right\} \quad u = \frac{2.75}{0.53} = 5.19\left[\frac{m}{s}\right]$$

** Time estimated when flow reached the seaside of the scaffolding, not clear shot.

- Depth:

$$d = \left(\frac{1}{4}\cdot h_s\right) = \left(\frac{1}{4}\cdot 1.77\right) = 0.44\,m.$$

- **Person Bm:**

  Subject falling from same place than Am. Flow conditions estimated as the one hit Am.


**Figure A.26:** Calculation speed´s flow subject Bm, video3.

- Velocity front of the flow: $u = 5.19\left[\frac{m}{s}\right]$

- Depth: $d = 0.44\,m.$

- **Person Dm:**


**Figure A.27:** Calculation speed´s flow subject Dm, video3.

- Velocity front of the flow:

$$\left.\begin{array}{l} Dis\tan ce = 6.5m \\ \left.\begin{array}{l} t_i = 02.90 \\ t_f = 04.53 \end{array}\right\}\Delta t = 1.63s \end{array}\right\} \; u = \frac{6.5}{1.63} = 3.99\left[\frac{m}{s}\right]$$

- Depth:

$$d = \frac{2}{3}\cdot\left(\frac{1}{4}\cdot h_s\right) = \frac{2}{3}\cdot\left(\frac{1}{4}\cdot 1.77\right) = 0.3m.$$

- **Person Fm:**

  Person reached by a thin layer of water. Problem to calculate velocity no distance reference. Velocity estimated similar as Dm.

**Figure A.28:** Calculation speed´s flow subject Fm, video3.

- Velocity front of the flow: $u = 3.99\left[\frac{m}{s}\right]$
- Depth:

$$d = \frac{1}{3}\cdot\left(\frac{1}{4}\cdot h_s\right) = \frac{1}{3}\cdot\left(\frac{1}{4}\cdot 1.77\right) = 0.14m.$$

- **Person Gm:**

  Person fell and wash out. It is not clear if the person fell because of the flow of was knock over by person Km.

- Velocity front of the flow:

$$\left.\begin{array}{l} Dis\tan ce = 7.5m \\ \left.\begin{array}{l} t_i = 02.83 \\ t_f = 04.90 \end{array}\right\}\Delta t = 2.07s \end{array}\right\} \; u = \frac{7.5}{2.07} = 3.62\left[\frac{m}{s}\right]$$

- Depth:

$$d = \frac{2}{3}\cdot\left(\frac{1}{4}\cdot h_s\right) = \frac{2}{3}\cdot\left(\frac{1}{4}\cdot 1.77\right) = 0.3m.$$


**Figure A.29:** Calculation speed´s flow subject Gm, video3.

**Table A.5:** Summary video 3.

| Subject | $u$ [m/s] | $d$ [m] | $T_{ovt}$ [s] | Consequence | Observation |
|---|---|---|---|---|---|
| Am | 5.19 | 0.44 | 5 to 10 | Wash out | Beaten by the flow |
| Bm | 5.19 | 0.44 | | Wash out | Beaten by the flow |
| Dm | 3.99 | 0.3 | | Wash out | |
| Gm | 3.62 | 0.3 | | Fall | |
| Fm | 3.99 | 0.14 | | No | |

# Appendix B

# Literature Results

**Table B.1:** Results literature studies, Abt et al. (1989), RASCDAM 2001, Jonkman and Penning-Rowsell 2008, Endoh and Takahashi (1995). F=Female, M=Male, C=Concrete, T=Turf, G=Gravel, S=Steel, SG= Steel grating, n/m= not mentioned.

| Study | Subject | Sex | Age | Height [m] | Weight [kg] | slope % | surface | *u* [ m/s] | *d* [m] |
|---|---|---|---|---|---|---|---|---|---|
| Abt et al. 1989 | 2 | F | 27 | 1.727 | 56.6 | 0.5 | C | 1.54 | 0.84 |
| Abt et al. 1989 | 2 | F | 27 | 1.727 | 56.6 | 1.5 | C | 1.42 | 0.59 |
| Abt et al. 1989 | 2 | F | 27 | 1.727 | 56.6 | 1.5 | T | 1.36 | 0.52 |
| Abt et al. 1989 | 2 | F | 27 | 1.727 | 56.6 | 1.5 | G | 1.28 | 0.78 |
| Abt et al. 1989 | 2 | F | 27 | 1.727 | 56.6 | 1.5 | S | 1.4 | 1.01 |
| Abt et al. 1989 | 3 | F | 29 | 1.524 | 40.9 | 0.5 | C | 1.4 | 0.84 |
| Abt et al. 1989 | 3 | F | 29 | 1.524 | 40.9 | 0.5 | T | 1.25 | 0.83 |
| Abt et al. 1989 | 3 | F | 29 | 1.524 | 40.9 | 1.5 | C | 1.42 | 0.69 |
| Abt et al. 1989 | 3 | F | 29 | 1.524 | 40.9 | 1.5 | T | 2.48 | 0.49 |
| Abt et al. 1989 | 3 | F | 29 | 1.524 | 40.9 | 1.5 | G | 1.1 | 0.85 |
| Abt et al. 1989 | 3 | F | 29 | 1.524 | 40.9 | 1.5 | S | 1.07 | 1.04 |
| Abt et al. 1989 | 1 | M | 39 | 1.702 | 73 | 0.5 | C | 1.48 | 0.88 |
| Abt et al. 1989 | 1 | M | 39 | 1.702 | 73 | 0.5 | T | 1.36 | 0.87 |
| Abt et al. 1989 | 1 | M | 39 | 1.702 | 73 | 0.5 | G | 1.24 | 0.95 |
| Abt et al. 1989 | 1 | M | 39 | 1.702 | 73 | 0.5 | S | 0.82 | 1.13 |
| Abt et al. 1989 | 1 | M | 39 | 1.702 | 73 | 1.5 | C | 2.46 | 0.57 |
| Abt et al. 1989 | 1 | M | 39 | 1.702 | 73 | 1.5 | T | 1.72 | 0.70 |
| Abt et al. 1989 | 1 | M | 39 | 1.702 | 73 | 1.5 | G | 1.52 | 0.76 |
| Abt et al. 1989 | 1 | M | 39 | 1.702 | 73 | 1.5 | S | 1.23 | 1.04 |
| Abt et al. 1989 | 4 | M | 29 | 1.778 | 85.9 | 0.5 | T | 1.66 | 0.76 |
| Abt et al. 1989 | 4 | M | 29 | 1.778 | 85.9 | 0.5 | G | 1.27 | 1.01 |
| Abt et al. 1989 | 4 | M | 29 | 1.778 | 85.9 | 0.5 | S | 0.87 | 1.16 |
| Abt et al. 1989 | 4 | M | 29 | 1.778 | 85.9 | 1.5 | C | 2.12 | 0.66 |
| Abt et al. 1989 | 4 | M | 29 | 1.778 | 85.9 | 1.5 | T | 1.81 | 0.64 |
| Abt et al. 1989 | 4 | M | 29 | 1.778 | 85.9 | 1.5 | G | 1.68 | 0.85 |
| Abt et al. 1989 | 4 | M | 29 | 1.778 | 85.9 | 1.5 | S | 1.45 | 1.04 |

| Study | Subject | Sex | Age | Height [m] | Weight [kg] | slope % | surface | *u* [ m/s] | *d* [m] |
|---|---|---|---|---|---|---|---|---|---|
| Abt et al. 1989 | 5 | M | 26 | 1.829 | 59.1 | 0.5 | T | 1.62 | 0.77 |
| Abt et al. 1989 | 5 | M | 26 | 1.829 | 59.1 | 0.5 | G | 1.21 | 1.20 |
| Abt et al. 1989 | 5 | M | 26 | 1.829 | 59.1 | 0.5 | S | 1.23 | 1.07 |
| Abt et al. 1989 | 5 | M | 26 | 1.829 | 59.1 | 1.5 | C | 1.98 | 0.61 |
| Abt et al. 1989 | 5 | M | 26 | 1.829 | 59.1 | 1.5 | T | 2.24 | 0.49 |
| Abt et al. 1989 | 5 | M | 26 | 1.829 | 59.1 | 1.5 | G | 1.46 | 0.82 |
| Abt et al. 1989 | 5 | M | 26 | 1.829 | 59.1 | 1.5 | S | 1.22 | 1.04 |
| Abt et al. 1989 | 6 | M | 30 | 1.803 | 91.4 | 0.5 | C | 2.99 | 0.71 |
| Abt et al. 1989 | 6 | M | 30 | 1.803 | 91.4 | 0.5 | T | 2.91 | 0.73 |
| Abt et al. 1989 | 6 | M | 30 | 1.803 | 91.4 | 0.5 | G | 1.39 | 0.98 |
| Abt et al. 1989 | 6 | M | 30 | 1.803 | 91.4 | 0.5 | S | 1.34 | 1.07 |
| Abt et al. 1989 | 7 | M | 31 | 1.727 | 73.2 | 1.5 | C | 3.05 | 0.43 |
| Abt et al. 1989 | 7 | M | 31 | 1.727 | 73.2 | 1.5 | T | 2.89 | 0.55 |
| Abt et al. 1989 | 7 | M | 31 | 1.727 | 73.2 | 1.5 | G | 1.59 | 0.84 |
| Abt et al. 1989 | 7 | M | 31 | 1.727 | 73.2 | 1.5 | S | 1.28 | 1.04 |
| Abt et al. 1989 | 8 | M | 43 | 1.829 | 90.1 | 0.5 | S | 1.77 | 1.07 |
| Abt et al. 1989 | 9 | M | 54 | 1.829 | 72.8 | 0.5 | S | 1.68 | 1.04 |
| Abt et al. 1989 | 10 | M | 41 | 1.778 | 85.2 | 0.5 | S | 1.68 | 1.07 |
| Abt et al. 1989 | 11 | M | 36 | 1.765 | 85.2 | 0.5 | S | 1.74 | 1.07 |
| Abt et al. 1989 | 12 | M | 30 | 1.829 | 74.1 | 0.5 | S | 1.53 | 1.04 |
| Abt et al. 1989 | 13 | M | 21 | 1.791 | 70.2 | 1.5 | C | 2.07 | 0.73 |
| Abt et al. 1989 | 13 | M | 21 | 1.791 | 70.2 | 1.5 | S | 1.55 | 1.06 |
| Abt et al. 1989 | 14 | M | 22 | 1.778 | 78.9 | 1.5 | C | 2.04 | 0.73 |
| Abt et al. 1989 | 14 | M | 22 | 1.778 | 78.9 | 1.5 | S | 1.69 | 1.05 |
| Abt et al. 1989 | 15 | M | 21 | 1.867 | 84.4 | 1.5 | C | 1.79 | 0.72 |
| Abt et al. 1989 | 15 | M | 21 | 1.867 | 84.4 | 1.5 | G | 1.44 | 0.94 |
| Abt et al. 1989 | 15 | M | 21 | 1.867 | 84.4 | 1.5 | S | 1.83 | 1.06 |
| Abt et al. 1989 | 16 | M | 20 | 1.905 | 90.7 | 1.5 | C | 2.3 | 0.72 |
| Abt et al. 1989 | 16 | M | 20 | 1.905 | 90.7 | 1.5 | S | 1.66 | 1.05 |
| Abt et al. 1989 | 17 | M | 20 | 1.753 | 75.4 | 1.5 | C | 1.82 | 0.72 |
| Abt et al. 1989 | 17 | M | 20 | 1.753 | 75.4 | 1.5 | G | 0.98 | 1.11 |
| Abt et al. 1989 | 17 | M | 20 | 1.753 | 75.4 | 1.5 | S | 1.61 | 1.04 |
| Abt et al. 1989 | 18 | M | 22 | 1.778 | 69.7 | 1.5 | C | 2.01 | 0.73 |

| Study | Subject | Sex | Age | Height [m] | Weight [kg] | slope % | surface | *u* [ m/s] | *d* [m] |
|---|---|---|---|---|---|---|---|---|---|
| Abt et al. 1989 | 18 | M | 22 | 1.778 | 69.7 | 1.5 | S | 1.26 | 1.09 |
| Abt et al. 1989 | 19 | M | 19 | 1.803 | 83.3 | 1.5 | C | 2.13 | 0.72 |
| Abt et al. 1989 | 19 | M | 19 | 1.803 | 83.3 | 1.5 | G | 1.59 | 0.91 |
| Abt et al. 1989 | 19 | M | 19 | 1.803 | 83.3 | 1.5 | S | 1.68 | 1.05 |
| Abt et al. 1989 | 20 | M | 28 | 1.803 | 79.8 | 1.5 | C | 1.81 | 0.82 |
| Abt et al. 1989 | 20 | M | 28 | 1.803 | 79.8 | 1.5 | S | 1.51 | 1.07 |
| Abt et al. 1989 | 21 | Mo | -- | 1.524 | 53.4 | 0.5 | C | 0.66 | 0.59 |
| Abt et al. 1989 | 21 | Mo | -- | 1.524 | 53.4 | 0.5 | T | 0.52 | 0.57 |
| Abt et al. 1989 | 21 | Mo | -- | 1.524 | 53.4 | 0.5 | G | 0.36 | 0.61 |
| Abt et al. 1989 | 21 | Mo | -- | 1.524 | 53.4 | 1.5 | C | 0.43 | 0.64 |
| Abt et al. 1989 | 21 | Mo | -- | 1.524 | 53.4 | 1.5 | T | 0.48 | 0.61 |
| Abt et al. 1989 | 21 | Mo | -- | 1.524 | 53.4 | 1.5 | G | 0.44 | 0.66 |
| RASCDAM 2001 | 4 | F | 32 | 1.62 | 57 | 0 | SG | 0.7 | 1.00 |
| RASCDAM 2001 | 4 | F | 32 | 1.62 | 57 | 0 | SG | 0.8 | 1.00 |
| RASCDAM 2001 | 4 | F | 32 | 1.62 | 57 | 0 | SG | 1.1 | 0.80 |
| RASCDAM 2001 | 4 | F | 32 | 1.62 | 57 | 0 | SG | 1.4 | 0.60 |
| RASCDAM 2001 | 6 | F | 17 | 1.6 | 48 | 0 | SG | 0.6 | 1.05 |
| RASCDAM 2001 | 6 | F | 17 | 1.6 | 48 | 0 | SG | 0.7 | 1.05 |
| RASCDAM 2001 | 6 | F | 17 | 1.6 | 48 | 0 | SG | 0.85 | 0.90 |
| RASCDAM 2001 | 6 | F | 17 | 1.6 | 48 | 0 | SG | 0.95 | 0.90 |
| RASCDAM 2001 | 6 | F | 17 | 1.6 | 48 | 0 | SG | 1.5 | 0.60 |
| RASCDAM 2001 | 1 | M | 28 | 1.7 | 69 | 0 | SG | 0.7 | 1.05 |
| RASCDAM 2001 | 1 | M | 28 | 1.7 | 69 | 0 | SG | 0.8 | 1.05 |
| RASCDAM 2001 | 1 | M | 28 | 1.7 | 69 | 0 | SG | 0.9 | 0.90 |
| RASCDAM 2001 | 1 | M | 28 | 1.7 | 69 | 0 | SG | 1 | 0.90 |
| RASCDAM 2001 | 1 | M | 28 | 1.7 | 69 | 0 | SG | 1 | 0.80 |
| RASCDAM 2001 | 1 | M | 28 | 1.7 | 69 | 0 | SG | 1.1 | 0.80 |
| RASCDAM 2001 | 1 | M | 28 | 1.7 | 69 | 0 | SG | 1.4 | 0.60 |
| RASCDAM 2001 | 2 | M | 31 | 1.95 | 100 | 0 | SG | 1.1 | 1.00 |
| RASCDAM 2001 | 2 | M | 31 | 1.95 | 100 | 0 | SG | 1.2 | 1.00 |
| RASCDAM 2001 | 2 | M | 31 | 1.95 | 100 | 0 | SG | 1.4 | 0.90 |
| RASCDAM 2001 | 2 | M | 31 | 1.95 | 100 | 0 | SG | 1.6 | 0.80 |
| RASCDAM 2001 | 2 | M | 31 | 1.95 | 100 | 0 | SG | 2 | 0.60 |
| RASCDAM 2001 | 2 | M | 31 | 1.95 | 100 | 0 | SG | 2.4 | 0.50 |

| Study | Subject | Sex | Age | Height [m] | Weight [kg] | slope % | surface | *u* [ m/s] | *d* [m] |
|---|---|---|---|---|---|---|---|---|---|
| RASCDAM 2001 | 2 | M | 31 | 1.95 | 100 | 0 | SG | 2.6 | 0.40 |
| RASCDAM 2001 | 3 | M | 28 | 1.79 | 76 | 0 | SG | 0.85 | 1.10 |
| RASCDAM 2001 | 3 | M | 28 | 1.79 | 76 | 0 | SG | 1 | 1.00 |
| RASCDAM 2001 | 3 | M | 28 | 1.79 | 76 | 0 | SG | 1.2 | 0.80 |
| RASCDAM 2001 | 3 | M | 28 | 1.79 | 76 | 0 | SG | 1.3 | 0.80 |
| RASCDAM 2001 | 3 | M | 28 | 1.79 | 76 | 0 | SG | 1.5 | 0.60 |
| RASCDAM 2001 | 3 | M | 28 | 1.79 | 76 | 0 | SG | 2.5 | 0.40 |
| RASCDAM 2001 | 5 | M | 60 | 1.82 | 94 | 0 | SG | 1 | 1.05 |
| RASCDAM 2001 | 5 | M | 60 | 1.82 | 94 | 0 | SG | 1.4 | 0.80 |
| RASCDAM 2001 | 5 | M | 60 | 1.82 | 94 | 0 | SG | 1.9 | 0.60 |
| RASCDAM 2001 | 5 | M | 60 | 1.82 | 94 | 0 | SG | 2.5 | 0.40 |
| RASCDAM 2001 | 7 | M | 19 | 1.74 | 71 | 0 | SG | 0.85 | 1.05 |
| RASCDAM 2001 | 7 | M | 19 | 1.74 | 71 | 0 | SG | 1.2 | 0.90 |
| RASCDAM 2001 | 7 | M | 19 | 1.74 | 71 | 0 | SG | 1.5 | 0.70 |
| RASCDAM 2001 | 7 | M | 19 | 1.74 | 71 | 0 | SG | 2 | 0.50 |
| Jonkman and Penning-Rowsell 2008 | 1 | M | n/m | 1.7 | 68.25 | 1 | C | 2.6 | 0.35 |
| Jonkman and Penning-Rowsell 2008 | 1 | M | n/m | 1.7 | 68.25 | 1 | C | 2.4 | 0.35 |
| Jonkman and Penning-Rowsell 2008 | 1 | M | n/m | 1.7 | 68.25 | 1 | C | 3.1 | 0.26 |
| Jonkman and Penning-Rowsell 2008 | 1 | M | n/m | 1.7 | 68.25 | 1 | C | 3 | 0.26 |
| Endoh and Takahashi 1995 | B | M | n/m | 1.64 | 65 | 0 | C | 2 | 0.52 |
| Endoh and Takahashi 1995 | B | M | n/m | 1.64 | 65 | 0 | C | 1.7 | 0.52 |
| Endoh and Takahashi 1995 | B | M | n/m | 1.64 | 65 | 0 | C | 1.7 | 0.63 |
| Endoh and Takahashi 1995 | B | M | n/m | 1.64 | 65 | 0 | C | 1.5 | 0.63 |
| Endoh and Takahashi 1995 | B | M | n/m | 1.64 | 65 | 0 | C | 1.5 | 0.55 |
| Endoh and Takahashi 1995 | B | M | n/m | 1.64 | 65 | 0 | C | 1.25 | 0.82 |
| Endoh and Takahashi 1995 | B | M | n/m | 1.64 | 65 | 0 | C | 1.25 | 0.67 |
| Endoh and Takahashi 1995 | B | M | n/m | 1.64 | 65 | 0 | C | 1 | 0.85 |

| Study | Subject | Sex | Age | Height [m] | Weight [kg] | slope % | surface | *u* [ m/s] | *d* [m] |
|---|---|---|---|---|---|---|---|---|---|
| Endoh and Takahashi 1995 | A | M | n/m | 1.83 | 73 | 0 | C | 1.5 | 0.45 |
| Endoh and Takahashi 1995 | A | M | n/m | 1.83 | 73 | 0 | C | 1.75 | 0.50 |
| Endoh and Takahashi 1995 | A | M | n/m | 1.83 | 73 | 0 | C | 2 | 0.52 |
| Endoh and Takahashi 1995 | A | M | n/m | 1.83 | 73 | 0 | C | 1.75 | 0.52 |
| Endoh and Takahashi 1995 | A | M | n/m | 1.83 | 73 | 0 | C | 1.5 | 0.55 |
| Endoh and Takahashi 1995 | A | M | n/m | 1.83 | 73 | 0 | C | 1.25 | 0.57 |
| Endoh and Takahashi 1995 | A | M | n/m | 1.83 | 73 | 0 | C | 1.75 | 0.63 |
| Endoh and Takahashi 1995 | A | M | n/m | 1.83 | 73 | 0 | C | 1.5 | 0.63 |
| Endoh and Takahashi 1995 | A | M | n/m | 1.83 | 73 | 0 | C | 1.25 | 0.66 |
| Endoh and Takahashi 1995 | A | M | n/m | 1.83 | 73 | 0 | C | 1 | 0.68 |
| Endoh and Takahashi 1995 | A | M | n/m | 1.83 | 73 | 0 | C | 1.25 | 0.83 |
| Endoh and Takahashi 1995 | A | M | n/m | 1.83 | 73 | 0 | C | 1 | 0.84 |
| Endoh and Takahashi 2008 | A | M | n/m | 1.83 | 73 | 0 | C | 1.75 | 0.50 |
| Endoh and Takahashi 1995 | A | M | n/m | 1.83 | 73 | 0 | C | 2 | 0.52 |
| Endoh and Takahashi 1995 | A | M | n/m | 1.83 | 73 | 0 | C | 1.75 | 0.52 |
| Endoh and Takahashi 1995 | A | M | n/m | 1.83 | 73 | 0 | C | 1.75 | 0.62 |
| Endoh and Takahashi 1995 | A | M | n/m | 1.83 | 73 | 0 | C | 1.5 | 0.62 |

F=Female, M=Male, C=Concrete, T=Turf, G=Gravel, S=Steel, SG= Steel grating, n/m= not mentioned.

**Table B.2:** Height and weight average.

| | Height [m] | Weight [kg] |
|---|---|---|
| Average | 1.76 | 72.54 |
| Female average | 1.61 | 49.82 |
| Male average | 1.78 | 76.63 |
| Minimum | 1.52 | 40.90 |
| Male minimum | 1.64 | 59.10 |
| Female minimum | 1.52 | 40.90 |

Appendix C

# Risk predictions calculated with M1d

| HM1 | Rc = 4 m | | | | slope = 1/4 | | | | | | | | | | | |
|---|---|---|---|---|---|---|---|---|---|---|---|---|---|---|---|---|
| $T_{m-1,0}$ [s] \ $H_{m0}$ [m] | 0.50 | 0.65 | 0.80 | 0.95 | 1.10 | 1.25 | 1.40 | 1.55 | 1.70 | 1.85 | 2.00 | 2.15 | 2.30 | 2.45 | 2.60 | 2.75 |
| 3 | R<Rc | R<Rc | R<Rc | R<Rc | ** | ** | ** | ** | ** | ** | ** | ** | ** | ** | ** | ** |
| 4 | R<Rc | R<Rc | R<Rc | R<Rc | R<Rc | R<Rc | R<Rc | R<Rc | R<Rc | ** | ** | ** | ** | ** | ** | ** |
| 5 | R<Rc | R<Rc | R<Rc | R<Rc | R<Rc | R<Rc | R<Rc | R<Rc | R<Rc | R<Rc | R<Rc | R<Rc | R<Rc | NH | NH | ** |
| 6 | R<Rc | R<Rc | R<Rc | R<Rc | R<Rc | R<Rc | R<Rc | R<Rc | NH | NH | H | H | H | H | H | H |
| 7 | R<Rc | R<Rc | R<Rc | R<Rc | R<Rc | R<Rc | NH | H | H | H | H | H | H | H | H | H |
| 8 | R<Rc | R<Rc | R<Rc | R<Rc | R<Rc | R<Rc | NH | H | H | H | H | H | H | H | H | H |
| 9 | R<Rc | R<Rc | R<Rc | R<Rc | R<Rc | R<Rc | H | H | H | H | H | H | H | H | H | H |
| 10 | R<Rc | R<Rc | R<Rc | R<Rc | R<Rc | R<Rc | H | H | H | H | H | H | H | H | H | H |
| 11 | R<Rc | R<Rc | R<Rc | R<Rc | R<Rc | R<Rc | H | H | H | H | H | H | H | H | H | H |
| 12 | R<Rc | R<Rc | R<Rc | R<Rc | R<Rc | R<Rc | H | H | H | H | H | H | H | H | H | H |
| 13 | R<Rc | R<Rc | R<Rc | R<Rc | R<Rc | NH | H | H | H | H | H | H | H | H | H | H |
| 14 | R<Rc | R<Rc | R<Rc | R<Rc | R<Rc | NH | H | H | H | H | H | H | H | H | H | H |
| 15 | R<Rc | R<Rc | R<Rc | R<Rc | R<Rc | NH | H | H | H | H | H | H | H | H | H | H |
| 16 | R<Rc | R<Rc | R<Rc | R<Rc | R<Rc | NH | H | H | H | H | H | H | H | H | H | H |
| 17 | R<Rc | R<Rc | R<Rc | R<Rc | R<Rc | NH | H | H | H | H | H | H | H | H | H | H |
| 18 | ** | R<Rc | R<Rc | R<Rc | R<Rc | NH | H | H | H | H | H | H | H | H | H | H |
| 19 | ** | R<Rc | R<Rc | R<Rc | R<Rc | NH | H | H | H | H | H | H | H | H | H | H |
| 20 | ** | R<Rc | R<Rc | R<Rc | R<Rc | NH | H | H | H | H | H | H | H | H | H | H |
| 21 | ** | ** | R<Rc | R<Rc | R<Rc | H | H | H | H | H | H | H | H | H | H | H |
| 22 | ** | ** | R<Rc | R<Rc | R<Rc | H | H | H | H | H | H | H | H | H | H | H |
| 23 | ** | ** | ** | R<Rc | R<Rc | H | H | H | H | H | H | H | H | H | H | H |
| 24 | ** | ** | ** | R<Rc | R<Rc | H | H | H | H | H | H | H | H | H | H | H |
| 25 | ** | ** | ** | ** | R<Rc | H | H | H | H | H | H | H | H | H | H | H |

**Figure C.1:** HM1 for person at seaside of a seadike crest, $R_c$ = 4m, seaward slope 1:4, and $d_s$<5cm. Green: No hazard is predicted. Red: Hazardous flow is predicted.

| HM1 | Rc = 2 m | | | | slope = 1/4 | | | | |
|---|---|---|---|---|---|---|---|---|---|
| $H_{m0}$ [m] / $T_{m-1,0}$ [s] | 0.50 | 0.65 | 0.80 | 0.95 | 1.10 | 1.25 | 1.40 | 1.55 | 1.70 |
| 3 | R<Rc | R<Rc | R<Rc | R<Rc | ** | ** | ** | ** | ** |
| 4 | R<Rc | R<Rc | R<Rc | NH | NH | H | H | H | H |
| 5 | R<Rc | R<Rc | H | H | H | H | H | H | H |
| 6 | R<Rc | R<Rc | H | H | H | H | H | H | H |
| 7 | R<Rc | NH | H | H | H | H | H | H | H |
| 8 | R<Rc | NH | H | H | H | H | H | H | H |
| 9 | R<Rc | NH | H | H | H | H | H | H | H |
| 10 | R<Rc | NH | H | H | H | H | H | H | H |
| 11 | R<Rc | NH | H | H | H | H | H | H | H |
| 12 | R<Rc | NH | H | H | H | H | H | H | H |
| 13 | R<Rc | NH | H | H | H | H | H | H | H |
| 14 | R<Rc | NH | H | H | H | H | H | H | H |
| 15 | R<Rc | NH | H | H | H | H | H | H | H |
| 16 | R<Rc | NH | H | H | H | H | H | H | H |
| 17 | R<Rc | H | H | H | H | H | H | H | H |
| 18 | ** | H | H | H | H | H | H | H | H |
| 19 | ** | H | H | H | H | H | H | H | H |
| 20 | ** | H | H | H | H | H | H | H | H |
| 21 | ** | ** | H | H | H | H | H | H | H |

| HM1 | Rc = 4 m | | | | slope = 1/2 | | | | |
|---|---|---|---|---|---|---|---|---|---|
| $H_{m0}$ [m] / $T_{m-1,0}$ [s] | 0.50 | 0.65 | 0.80 | 0.95 | 1.10 | 1.25 | 1.40 | 1.55 | 1.70 |
| 3 | R<Rc | R<Rc | R<Rc | R<Rc | ** | ** | ** | ** | ** |
| 4 | R<Rc | R<Rc | R<Rc | R<Rc | R<Rc | R<Rc | NH | H | H |
| 5 | R<Rc | R<Rc | R<Rc | R<Rc | R<Rc | R<Rc | H | H | H |
| 6 | R<Rc | R<Rc | R<Rc | R<Rc | R<Rc | R<Rc | H | H | H |
| 7 | R<Rc | R<Rc | R<Rc | R<Rc | R<Rc | NH | H | H | H |
| 8 | R<Rc | R<Rc | R<Rc | R<Rc | R<Rc | NH | H | H | H |
| 9 | R<Rc | R<Rc | R<Rc | R<Rc | R<Rc | NH | H | H | H |
| 10 | R<Rc | R<Rc | R<Rc | R<Rc | R<Rc | NH | H | H | H |
| 11 | R<Rc | R<Rc | R<Rc | R<Rc | R<Rc | H | H | H | H |
| 12 | R<Rc | R<Rc | R<Rc | R<Rc | R<Rc | H | H | H | H |
| 13 | R<Rc | R<Rc | R<Rc | R<Rc | R<Rc | H | H | H | H |
| 14 | R<Rc | R<Rc | R<Rc | R<Rc | R<Rc | H | H | H | H |
| 15 | R<Rc | R<Rc | R<Rc | R<Rc | R<Rc | H | H | H | H |
| 16 | R<Rc | R<Rc | R<Rc | R<Rc | R<Rc | H | H | H | H |
| 17 | R<Rc | R<Rc | R<Rc | R<Rc | R<Rc | H | H | H | H |
| 18 | ** | R<Rc | R<Rc | R<Rc | R<Rc | H | H | H | H |
| 19 | ** | R<Rc | R<Rc | R<Rc | R<Rc | H | H | H | H |

| HM1 | Rc = 2 m | | | | slope = 1/2 | | | |
|---|---|---|---|---|---|---|---|---|
| $H_{m0}$ [m] / $T_{m-1,0}$ [s] | 0.50 | 0.65 | 0.80 | 0.95 | 1.10 | 1.25 | 1.40 | 1.55 |
| 3 | R<Rc | R<Rc | H | H | ** | ** | ** | ** |
| 4 | R<Rc | NH | NH | H | H | H | H | H |
| 5 | R<Rc | NH | NH | H | H | H | H | H |
| 6 | R<Rc | NH | NH | H | H | H | H | H |
| 7 | R<Rc | NH | NH | H | H | H | H | H |
| 8 | R<Rc | NH | NH | H | H | H | H | H |
| 9 | R<Rc | H | H | H | H | H | H | H |
| 10 | R<Rc | H | H | H | H | H | H | H |
| 11 | R<Rc | H | H | H | H | H | H | H |
| 12 | R<Rc | H | H | H | H | H | H | H |
| 13 | R<Rc | H | H | H | H | H | H | H |
| 14 | R<Rc | H | H | H | H | H | H | H |
| 15 | R<Rc | H | H | H | H | H | H | H |
| 16 | R<Rc | H | H | H | H | H | H | H |
| 17 | R<Rc | H | H | H | H | H | H | H |
| 18 | ** | H | H | H | H | H | H | H |
| 19 | ** | H | H | H | H | H | H | H |

**Figure C.2:** Risk matrices for person at seaside of a seadike crest calculated with M1d. Green: No hazard is predicted. Red: Hazardous flow is predicted.

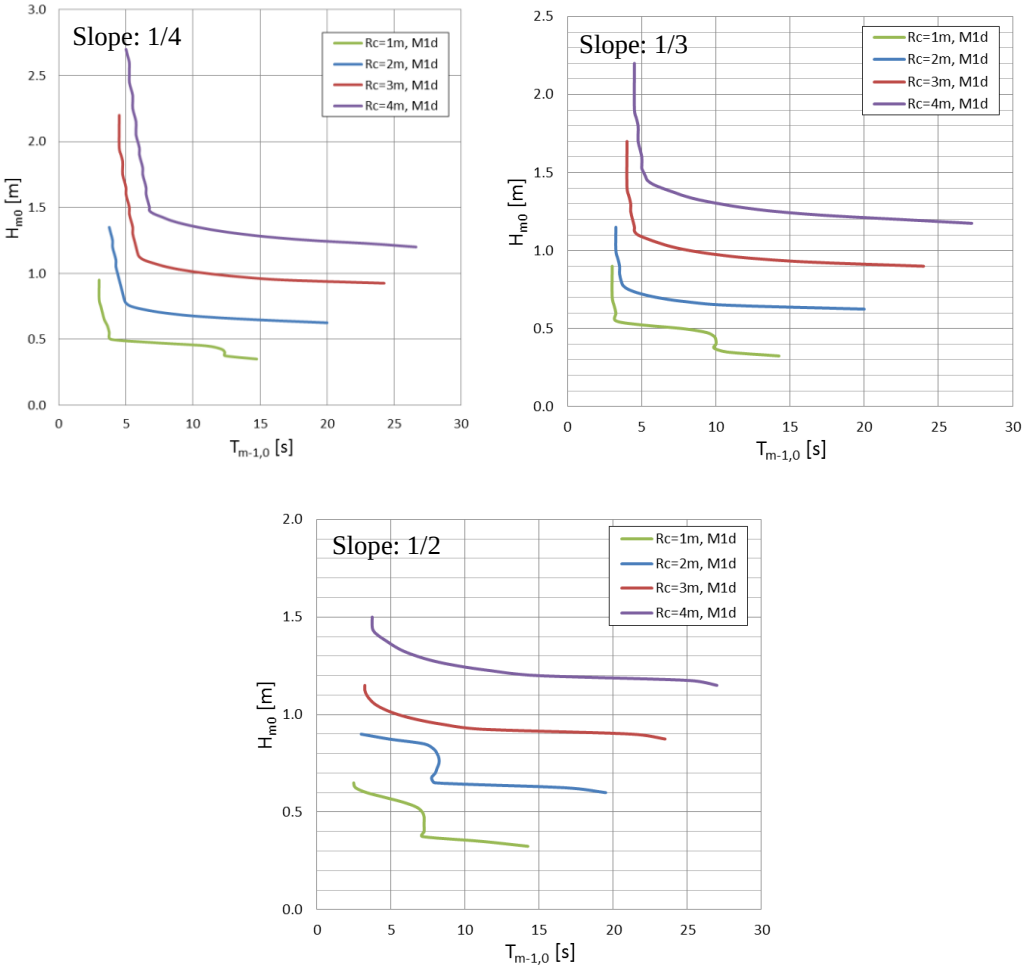


**Figure C.3:** Risk envelopes for seadike calculated with M1d.

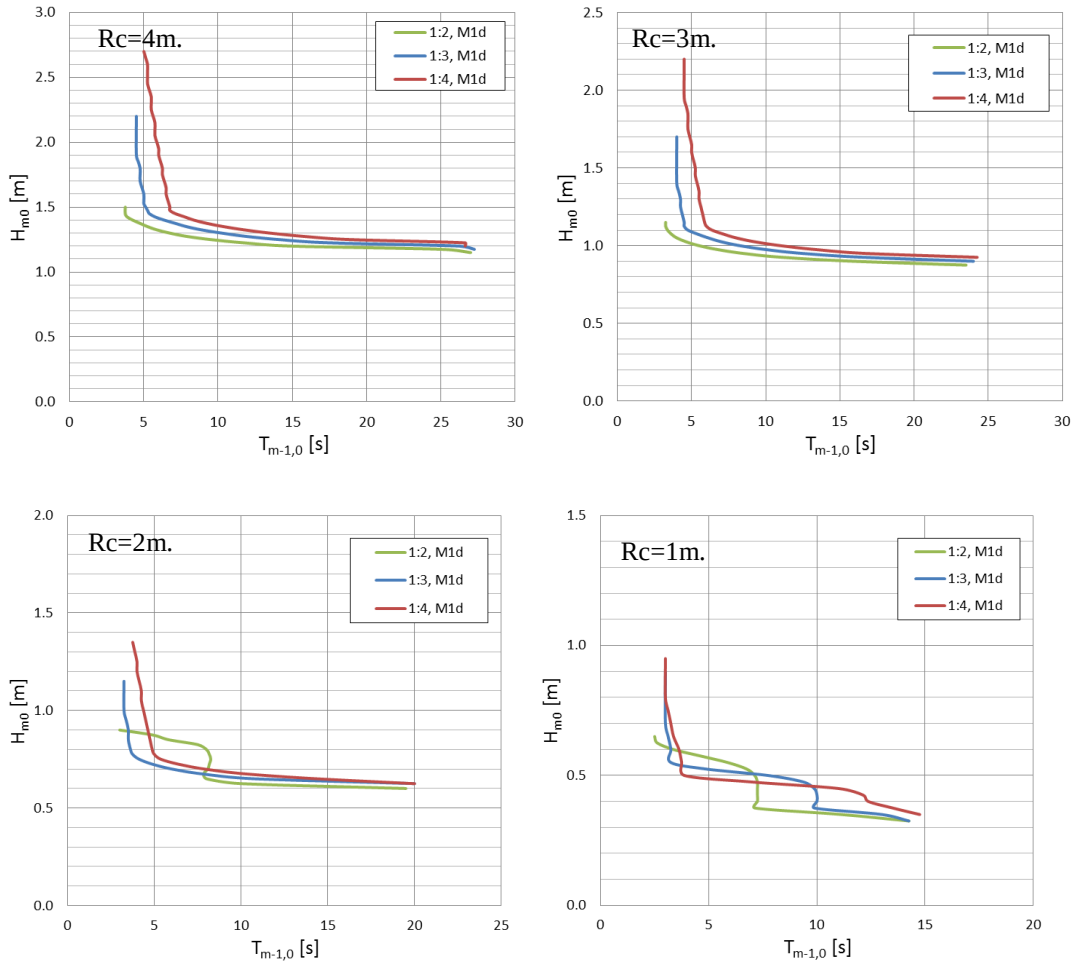


**Figure C.4:** Risk envelopes for seadike with $R_c$= 4m. and seaward slopes 1:2, 1:3 and 1:4. calculated with M1d.